**IMT School for Advanced Studies, Lucca**
Lucca, Italy

# A multi-site image-based data sharing initiative to assess structural brain changes in large cohorts of early and late blind individuals

PhD Program in Cognitive, Computational and Social Neurosciences

XXXIII Cycle

**By**

**Cemal Koba**

**2022**

**The dissertation of Cemal Koba is approved.**

PhD Program Coordinator: Prof. Emiliano Ricciardi, IMT School for Advanced Studies Lucca

Advisor: Prof. Emiliano Ricciardi, IMT School for Advanced Studies Lucca

The dissertation of Cemal Koba has been reviewed by:

Assoc. Prof. Ryo Kitada, Kobe University

Prof. Maurice Ptito, Université de Montreal

IMT School for Advanced Studies Lucca
2022

# Contents

# List of Figures

# List of Tables

# Acknowledgements

I want to thank my supervisor Prof. Emiliano Ricciardi, who helped and guided me during my Ph.D. He made this work possible by starting and leading the data-sharing initiative in blindness research. I had the chance to work on this special dataset that was built thanks to the efforts of the contributor groups: Université Catholique de Louvain - Belgium; Copenhagen University – Denmark; University of Oxford - United Kingdom; National Institute for Physiological Science, Japan; Massachusetts Eye and Ear Infirmary – Harvard Medical School, USA; University of Montreal – Canada; IMT School for Advanced Studies Lucca - Italy; University of Turin – Italy; Brainnetome Center and Beijing Normal University – China.

I want to thank Dr. Luca Cecchetti, Dr. Davide Bottari, and Dr. Andrea Leo for their valuable suggestions and help with the conceptual and methodological aspects of this work.

I thank my friends for their patience while listening to repetitive talks on the status of my project. I wish my colleagues from IMT Lucca the best of luck with their career, and hope to meet them again to remember the good times we shared. I thank my distant friends, Seyf and Emre, who were in touch with me all the time, especially during the Covid pandemic. I am grateful for my mother, Meryem, who motivated me for studying and learning since I was a child, and for her efforts to ensure that I receive proper education.

Finally, I want to thank my beloved wife, Beste, whom I met during the final months of my Ph.D. journey, and who inspired me to make the last push to finish my dissertation. I cannot wait for starting the next chapter in our lives.

# Vita

| | |
|---|---|
| **May 7, 1991** | Born in Mersin, Turkey |
| **2009-2015** | Bachelor's degree in Psychology<br>Bilkent University, Ankara, Turkey |
| **2014** | Research Assistant<br>National Magnetic Resonance Imaging Center<br>Ankara, Turkey |
| **2015-2017** | Master's Degree in Cognitive Neuroscience<br>University of Trento, Trento, Italy |
| **2017-2022** | Ph.D. in Cognitive, Computational and Social Neurosciences<br>IMT School for Advanced Studies Lucca, Lucca, Italy |
| **2022 -** | Research Fellow<br>Sano Center For Computational Medicine<br>Krakow, Poland |

# Publications

1. Koba, C., Notaro, G., Tamm, S., Nilsonne, G., Hasson, U. (2021). *Spontaneous eye movements during eyes-open rest reduce resting-state-network modularity by increasing visual-sensorimotor connectivity*. Network Neuroscience, 5(2), 451-476.
2. Botvinik-Nezer, R., Holzmeister, F., Camerer, C. F., Dreber, A., Huber, J., Johannesson, M., ... Rieck, J. R. (2020). *Variability in the analysis of a single neuroimaging dataset by many teams*. Nature, 582(7810), 84-88..

# Acronyms

**AC-PC** Anterior Commissure-Posterior Commissure. 38

**ALE** Activation Likelihood Estimation. 28–30

**aMTG** anterior Middle Temporal Gyrus. 70

**AN-CB** anophthalmic. x, 13, 16, 17, 19, 45, 59, 60

**BI** Blindness Index. xi, 77–79, 84, 87, 90

**BO** Blindness Onset. 9, 19, 20, 23, 25, 74–79, 84, 87, 90, 92, 96

**CB** Congenital blind. ix, x, 9, 13, 16–21, 25, 37, 38, 43, 44, 46, 47, 49, 51–54, 56, 58–60, 62, 65, 66, 68–70, 72, 76, 84, 94, 95

**CSF** cerebro-spinal fluid. 7, 39, 42

**DBM** Deformation-based Morphometry. 18

**DTI** Diffusion Tensor Imaging. 13, 72, 99

**EB/CB** early blind. 13, 18, 20–23, 25, 27, 29, 30, 69, 96

**FA** Fractional Anisotropy. 8, 13, 16, 21–25, 32, 72

**FDR** False Discovery Rate. 52, 53, 58–60, 80, 81, 92

**FWE** Family-wise Error Rate. 30

**GLM** Generalized Linear Model. 38

**GM** Gray Matter. 25, 27, 41, 42, 46, 47, 79, 80, 87, 96

**ILF** inferior longitudinal fasciculus. 21, 22, 32

**LB** late blind. xi, xvi, 9, 16, 17, 19–23, 25, 27, 29, 74–77, 79–84, 87, 90, 92, 94–97

**LGN** Lateral Geniculate Nucleus. 4, 5, 13, 16, 25, 32, 67, 98

**MA** Modeled activation. 30

**MGN** Medial Geniculate Nucleus. 17, 67

**RLP** Residual light perception. 10, 24, 46, 59, 60, 62, 72, 76, 77, 92

**ROI** Region of Interest. 29, 40, 41, 43, 44, 52, 53

**RoP** Retinopathy of Prematurity. 26, 27, 45, 46, 59, 60, 62, 70, 71

**SC** sighted control. ix–xi, xvi, 13, 16–21, 23, 29, 30, 37, 38, 43, 44, 46, 47, 49, 51, 53, 54, 56, 58, 60, 62, 66, 69, 70, 74–76, 80–84, 92, 95

**STG** superior temporal gyrus. 21, 24, 32

**TSAB** Time Spent as Blind. 25, 75, 77–79, 84, 87, 90, 92, 96

**V1** Primary Visual Cortex. 4, 5, 9, 18, 19, 25

**V2** Secondary Visual Cortex. 5

**VBM** Voxel-based Morphometry. 13, 18, 19, 25–27, 40, 41, 44, 47, 60, 67, 72, 76, 77, 80, 81, 94, 99

**WHO** World Health Organization. 2, 29

**WM** White Matter. 24, 27, 41, 42, 46, 47, 79, 80

# Abstract

Blindness is a widely studied phenomena in order to understand the neuroplasticity in case of sensory deprivation. Number of studies focusing on the structural plasticity during visual deprivation is fewer compared to the functional plasticity. In addition, samples and the results of those studies are heterogeneous. This dissertation utilized the largest dataset of MRI of blind subjects, that is gathered by the efforts of 10 different research labs. The aim was to overcome the previous challenges, and identify pre- and post-natal factors that are confounding the results. In the first chapter, an extensive literature review revealing the current status of the field and identifying the problems is presented. The review is completed with a systematic meta-analysis. Structural plasticity in case of congenital blindness was examined in chapter 3. This chapter focused on between (congenital blind participants versus sighted controls) and within group (effect of the causes of blindness, residual light perception, Braille literacy) differences via utilizing voxel- and surface-based morphometry. In chapter 4, participants with late blindness was examined. In addition to the analyses conducted on the congenital blind subjects, effect of time spent as blind and blindness onset on neuroplasticity was examined. The results indicate a consistent atrophy on the visual pathway, and a critical period for vulnerability. In addition, the effect of premature birth, residual light perception, Braille literacy on the structural plasticity and limited sample sizes on the results were revealed.

# Chapter 1

# Introduction

## 1.1 Epidemiology of Blindness

Vision is the sensory modality that people rely on most. The world we live in is built in such a way that most of the inventions that make daily life easier utilize visual perception (e.g., traffic lights and signs, monitors and screens, etc.). However, blind people cannot make use of such tools, and have to rely on other sensory modalities to interact with the surrounding world. According to Bourne et al. (2021), 43.3 million people suffer from a form of blindness. From a medical perspective, blindness is defined as having less than 3/60 visual acuity in the better eye (WHO, 2019). Visual acuity, described as the ability to see details clearly (WHO, 2019), is measured via the Snellen scale (Perera et al., 2015; Figure 1), a chart containing letters ordered from top to bottom, from larger to smaller font sizes. A person with normal eyesight can see the slightest line from 6 meters away (6/6 vision). 3/60 visual acuity means that a person has to come 3 meters close to see the top letter of the Snellen scale that can be read from 60 meters away by a person with regular eyesight.

The prevalence of blindness increases with age. Seventy-eight percent of the blind population is older than 50 years (Bourne et al., 2021). That being said, losing sight at any age impacts the quality of life and represents an economic burden. As reported in the World Report on Vi-


**Figure 1:** Snellen chart as taken from Perera et al. (2015).

sion published by the World Health Organization in 2019 (WHO, 2019), blindness has different effects on daily life depending on the age of onset. Children suffer from delayed motor or cognitive development and lower in-school achievements (Kestenberg, 1979; C. C. Peterson, J. L. Peterson, and Webb, 2000; Tobin, 1998). At the same time, adults experience isolated social life and a higher risk of unemployment (K. D. Frick et al., 2015; Naidoo et al., 2019). Finally, elders face a higher probability of entering nursing homes earlier (Friedman et al., 2004; Mitchell, Hayes, and J. J. Wang, 1997).

According to the World Health Organization (WHO, 2019), the most common causes of blindness are cataracts, uncorrected refractive errors, glaucoma, and age-related macular degeneration (Figure 2). These causes affect different eye parts or the optic nerve. Cataract impairs the cloudiness in the lens, glaucoma is the 'build-up of fluid' in the lens, refractive errors (e.g., myopia, presbyopia) are related to the abnormal shape or length of the eyeball, and two types of retinopathy, one caused by diabetes, one caused by premature birth, cause damage to the blood vessels in the retina.

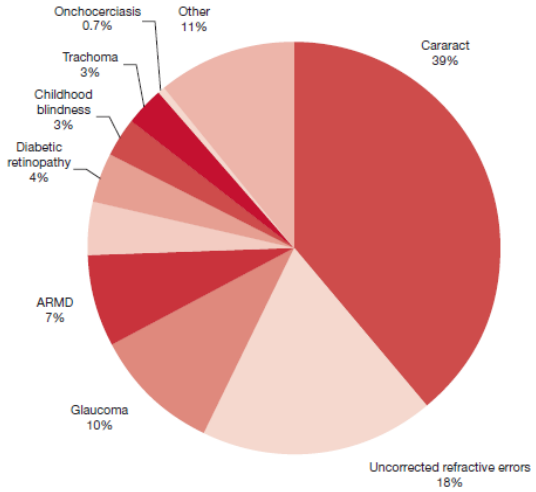


**Figure 2:** Global causes of blindness due to eye diseases (WHO, 2019)

## 1.2 Why study blindness to study the brain?

Blindness has offered an unprecedented opportunity to understand to what extent sight and visual experience - and the lack of it - may be fundamental to shape the development of the brain functional organization and to observe neurophysiological changes related to plastic reorganization following the absence of a sensory input (Ricciardi, Bottari, et al., 2020; Voss, 2019; Fine and J.-M. Park, 2018). Brain regions related to vision are primarily affected because of lack of input, and the brain compensates by focusing on the remaining and preserved sensory modalities. Furthermore, if the age onset of the losing vision is known, the interaction between typical neurodevelopment and compensatory plastic phenomena can be explored and characterized. In other words, whether the structural and functional plasticity occurs in the same way on the mature and immature brains can be studied.

With the advances in the non-invasive neuroimaging technology, especially f/mri since mid-90s, the model offered by the sensory loss has

been exploited. The interest in the visually deprived brain has been gradually increasing (Ricciardi, Bottari, et al., 2020). Earlier studies showed that visual cortex give cross-modal responses to other tasks ( Voss (2019) for a review of cross-modal functional responses in visual cortex). Indication of these studies were already exciting in terms of figuring out how the brain makes use of the regions whose main task is not functioning anymore. Of course, this approach has the assumption that brain regions, at least the primary sensory regions are unimodal. However, later studies revealed that sensory deprived visual cortex, along with other regions in the brain, give response to a specific type of task, rather than a specific modality (see Ricciardi, Bonino, et al. (2014) for a review of supramodality). For example, visual cortex of both blind and sighted people is activated to "direction" whether it is perceived visually or auditory. Therefore, brain works in a "supramodal" way rather than unimodal or crossmodal. The sensory deprived brain is important for further understanding how supramodality works, hence how the brain works.

### 1.2.1 Phsyiology of the visual system

In order to understand how the human brain reacts to blindness, it is essential to know how it processes visual input (Figure 3). As explained in Tovée (2008), after the light enters the eyes, the retina collects, transduces and sends the input to optic nerves. The information collected with nasal and temporal retinas is exchanged at optic chiasm, so that each hemisphere receives information from the opposite side of the visual field. After the exchange, the information arrives at the lateral geniculate nucleus (LGN). LGN is a subnucleus of the thalamus that receives input directly from the eyes and feedbacks from cortical areas. It has six layers and every layer takes input from one eye. LGN is primarily responsible for sending the information to the visual cortex via optic radiations. The primary visual cortex, also known as striate cortex, calcarine cortex, or V1, receives input from optic radiations and relays the information coded in the retina on the cortex. Its function is to detect relatively sim-

ple orientation, edge, and salience features. Secondary visual cortex (V2) is modulated by both simple properties like V1 and more complex properties, like color and disparity. From V2, there are two interacting pathways for visual information processing: dorsal and ventral, also known as where and what pathways, respectively. The dorsal pathway goes through the parietal lobe and is primarily related to the spatial and sensorimotor processing. On the other hand, the ventral pathway extends to the temporal lobe after V2 and is related to object identification and characterization. Third visual cortex (V3), in accordance with the dorsal and ventral streams, has dorsal and ventral parts. Dorsal V3 takes input from the V2 and conveys the information to the parietal cortex. This part is related to global and coherent motion. Ventral V3, on the other hand, is connected to inferior temporal cortex and takes less input from V1. Ventral V3 also has color-selective cells, as it is connected to V4, that is associated with the color perception. Lesions to this region resulted in impaired color constancy and pattern discrimination. Lastly, visual area 5 (V5), also known as middle temporal visual area (MT). This region takes part in perception of direction of the motion of an object rather than its sub-parts. When V5 is lesioned, impaired eye-pursuit was reported, and subjects perceived the world in form of frames rather than a continuous way. This region takes input from V1, V2, and LGN. The visual system starts developing during gestation. Formation of the retina starts around the seventh week of gestation and takes its relatively mature shape around 160 days (Workman et al., 2013). Thalamus and LGN start forming around 43 days, and axons from the retina reach LGN around 60 days (Clancy, Darlington, and Finlay, 2001). Optic radiations start their myelinization around 200 days and connect with the cortex at 60 days. Around day 156, the retina starts a spontaneous activity that stimulates the whole pathway and helps its maturation (Workman et al., 2013). However, this prenatal development is not enough for complete maturation. After birth, both gray matter and white matter structures continue to develop. Gray matter in V1 goes through a rapid expansion and grows until 17 months, then shrinks via synaptic pruning until its adult refinement. On the other hand, white matter tracts continue to

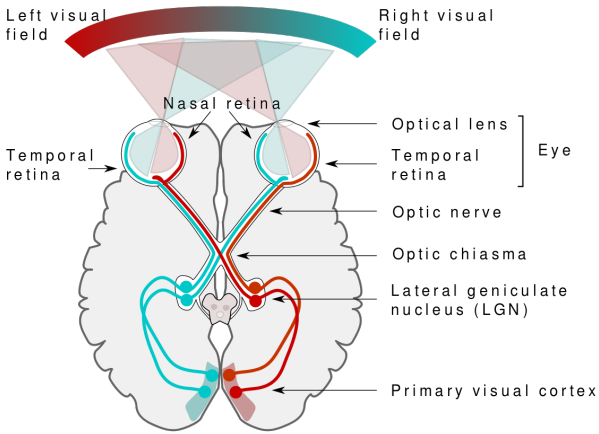


**Figure 3:** A visual representation of the human visual system. Image: Miquel Perello Nieto [CC BY-SA 4.0]

maturate until 22 years of age (Paus et al., 1999; Workman et al., 2013; Siu and Kathryn M Murphy, 2018).

## 1.3 Exploring the brain and blindness with magnetic resonance imaging

Thanks to the advances in non-invasive imaging techniques, it is possible to measure and describe brain anatomy and function with different methods. One of those approach, magnetic resonance imaging (MRI), takes advantage of the magnetization of the atoms, mostly in water. (M. A. Brown and Semelka, 2011; Huettel, A. Song, and McCarthy, 2009). MRI devices are designed to create a homogeneous static magnetic field that is strong enough to align nuclei in human body. This magnetic field is transmitted to body through radiofrequency coils that resonate with atomic nuclei at the times of interest. The resonation excites the atomci nuclei, making them absorb the radiofrequency pulse. After the excitation, the nuclei return to their equlibirium state with the static mag-

netic field. MRI signal is generated from this relaxation process of the nuclei. The most common magnetization technique for structural MRI, T1, which is the magnetization in the same direction as the static magnetic field, generates images in which the gray matter is dark gray, white matter is light gray, and CSF is black. This modality is used to quantify morphological features of the brain such as cortical/subcortical volumes, surface area, cortical thickness. In general, these features are categorized based on the technique used to generate them: voxel-based and surface-based morphometry (Goto et al., 2022). T1 images, already in the voxel-dimension, can be used for segmentation of different cortical (gray and white matter) and subcortical (thalamus, hippocampus, amygdala...) structures, and calculate their total volume as a factor of voxel dimension and total number of voxels in the mask-segmented image. This technique is useful to perform analyses on the whole of the segmented tissue. To study the morphology on the regional level, concentration of the segmented tissues in each voxel can be calculated. This technique, generally known as "voxel-based morphometry", is applied by creating deformation fields of the tissues via normalizing them into a group template with non-linear registration (Ashburner, 2010). The normalized images are modulated with the amount of the deformation needed to for each voxel to match their place in the group template. Lastly, the images are spatially smoothed. In the final output, each voxel contains the probability of the given tissue, which can be also interpreted as "concentration".

Although being useful for tracking the morphological differences between different populations, tissue concentration is difficult to interpret and to tell what it represents (e.g. whether it is surface area, cortical thickness, curvature). Surface-based morphometry, on the other hand, is more specific and more interpretable (Dahnke, Yotter, and Gaser, 2013). The T1 image is sent to the surface domain from the voxel domain by calculating the distance between white matter pia mater/CSF. This step creates a model of the cortex, which is built by "vertices" instead of voxels. Each vertex consists of three points on the cortical model. Each triplet has a face (area between the points) and each point has a geometric coordination on space. Thanks to these specific information, surface area

of a region (via the are a of the triplets), cortical thickness (the distance between white and pial surface), and curvature (or gyrification, the ratio of length between pial surface and the cortex) could be measured. Once generated, the images are ready for statistical analyses after preprocessing. In short, images are aligned to a standard template to perform group-level analyses. Then, any statistical test of choice can be applied to make group-level inferences.

Another imaging technique to study brain structure using MRI is diffusion-weighted imaging (DWI) (Alexander et al., 2007). This technique quantifies the water diffusion from one point to another, hence reveals the pathway that water follows. The resulting image has a contrast between white matter and gray matter, therefore useful to investigate white matter integrity at macro scale. With the introduction of the tensors, that can recognize the direction of the molecules, distinction of the white matter fibres became possible (Basser, Mattiello, and LeBihan, 1994). Most common methods to quantify the integrity of the white matter bundles are fractional anisotropy FA and radial diffusivity (RD). FA shows the myelin integrity (Baliyan et al., 2016).

Results from functional studies consistently indicate that most of the large-scale architecture of the human brain develops and functions also in the congenital blind model as well, while certainly undergoing functional reorganization and long-range connectivity changes. For instance, previous functional studies of blind individuals revealed that visual cortex of blind individuals is still active during a wide range of tasks such as auditory spatial processing (Collignon et al., 2011), tactile object recognition (Amedi et al., 2010), Braille reading (Burton et al., 2002), linguistic stimuli (Roeder et al., 2002), attentional tasks (Weaver and Stevens, 2007). In addition, earlier PET studies showed that congenital blind people have more glucose consumption and higher cerebral blood flow in occipital cortex (Wanet-Defalque et al., 1988; Uhl et al., 1993; De Volder et al., 1997). Whether there is a structural correspondence of this functional adaptation is a question mark. Structural observations are necessary to determine how the brain adapts itself to deprivation of a sensory modality, the structural foundations of the functional changes, and the

relationship between regular neurodevelopment and structural plasticity. Structural MRI studies of blindness point to a general clean result (significant changes in optic radiations and V1) (Noppeney et al., 2005; Pan et al., 2007; Jiang et al., 2009; Nina L Reislev et al., 2016; H. J. Park et al., 2009) and various results on non-vision related regions (Q. Li et al., 2017; Inuggi et al., 2020; Zikou et al., 2012; Chebat et al., 2007).

This work introduces a neuroimaging data-sharing initative of structural T1 brain data of congenital and late blind individuals acquired by different research groups. Launched during the 'Blind Brain Workshop' that was held in Lucca, Italy on October 11th-13th, 2018 (Ricciardi, Bottari, et al., 2020), this action provided an unprecedentedly large sample of 156 CB and 153 LB ((blindness onset - BO $>$ 0 year of age)) individuals. This joint effort will allow on the one hand to replicate previous fragmented observations in a more reliable sample size, and, on the other hand, to exploit the possibility to investigate directly the effects on neuroimaging metrics of individual characteristics relative to the etiology and features of blindness, and with environmental factors. Importantly, we limited a large part of the methodological noise between individual studies by unifying pre-processing and data analysis. In addition, we also aimed at confirming the higher reliability of our multiple sites image-based data sharing initiative as compared to a coordinate-based meta-analytic approach to structural brain data, particularly when the state-of-the-art is represented by observational studies with small size samples and that have often been focusing on specific structural targets, or limited structural-functional correlations

In summary, in this thesis, I aim to:

- Show the current state of the literature on structural reorganization and adaptation in the case of blindness and identify what is currently missing in this characterization of blindness-related changes in brain anatomy

- Gather a large blind sample that has enough statistical power to reveal the anatomical differences between congenital/early/late blind and sighted samples

- Identify the effect of the secondary pre- and post-natal factors (e.g., residual light perception - RLP, causes, Braille) on brain structural reorganization
- Compare the results of coordinate-based meta-analysis and meta-analysis based on real data
- Identify the effects of blindness onset on reorganization phenomena occurring in a late loss of visual input

# Chapter 2

# Literature Review and Meta-analysis

The brain undergoes a set of changes after losing visual perception. Previous studies claim that these differences are observed across the whole brain, thus in the neocortex, subcortical structures, and midbrain (Figures 4 and 5).

As seen in Figures 4 and 5, there is a large body of research on morphological changes in the blind brain. Although there are many common and reliable findings, a complete understanding of structural plasticity in visual impairment has not been achieved yet. Inconsistencies among the findings and heterogeneity among the sample characteristics can be easily observed (Figures 4 and 5). The significant heterogeneity across studies could be related to various factors. First, analyses have been so far performed on limited samples of congenital or late blind individuals and matched sighted controls. In high-income countries, people lacking vision since birth are luckily becoming rarer, as reversible causes of blindness can be treated timely (WHO, 2019). In addition, the exclusion of all participants whose medical characteristics could confound result interpretations, such as neurological or psychiatric disorders, led most studies assessing structural differences in congenital and late blind individuals to samples that do not exceed 30 participants. Then, these

limited, exceptional samples of congenital blind people show different sociodemographic and clinical variables (e.g., residual light perception, causes of blindness, premat(Anurova, Carlson, and Rauschecker, 2019; Maller et al., 2016; C. M. Bauer, Hirsch, et al., 2017). Thus, individuals whose nature of visual loss and lifelong characteristics may play a different role on brain development and (re)organization, are often merged into unique samples. For instance, how could even a minimal perception of light and shadows affect the development of those cortical and subcortical regions that receive retinal inputs? Equally, to what extent does visual deprivation differentially influence the maturation of preterm born cerebral structures, as compared to term born brains? Or which may be the relevance of postnatal, environmental factors, such as Braille literacy, that affect the blind brain for variable time lengths? Accordingly, studies have tried to isolate the effects of diverse causes of blindness (e.g., anophthalmia in Bridge, Cowey, et al. (2009), prematurity in Wan et al. (2013), or open-angle glaucoma; Zikou et al. (2012)), to comprehend the impact of age onset on brain structural development (Andelin et al., 2019), to understand the role of residual light perception (Zhou et al., 2019), or to correlate neuroanatomical metrics with individual behavioral performances, with compensatory perceptual adaptations or with the impact of specific clinical variables (e.g., Voss and Zatorre (2012), Voss and Zatorre (2015) Zhou et al. (2019)). Furthermore, the two most common experimental designs in the literature compare sighted controls and a blind group consisting of both late and congenital blind sample or compare a sighted group and congenital blind sample only (Chebat et al., 2007; Pan et al., 2007; Leporé, Y. Shi, et al., 2009). However, in the first case, the anatomical differences reflect the effect of losing sight at some point in life. In contrast, in the second case, the results show the effect of not having visual perception from birth. The brain may reshape itself differently in those two scenarios. Therefore, individual results alone would not be sufficient to make general statements about the effect of blindness on brain anatomy. Finally, if limited samples directly impinge on (i.e., overestimate) the effect size, and thus raise concerns on the replicability and generalizability of the results Ioannidis et al. (2014), method-based

factors, such as heterogeneity in data acquisition, processing, and analysis protocols, also may affect the observations reported across different studies.

Naturally, structures that are most frequently reported as affected by the lack of sight in the literature are the elements of the visual pathway. In this review, I will cover the anatomical changes in visual pathways and some other structures in the brain that are frequently observed to be altered by blindness. The differences among the sample characteristics will be highlighted throughout the review, and potential confounding will be discussed at the end.

As this thesis aims to explore neuroplasticity in the typically developed brain, I restricted this review's scope to studies involving ocular blindness. For a review on cerebral/cortical blindness, please see Hirsch, C. M. Bauer, and Merabet (2015).

## 2.1 Visual Pathways

### 2.1.1 Optic Nerves, Chiasm, Tract and Radiation

Optic nerves take input from the retina and carry the information to the LGN or superior colliculi through optic chiasm. After the information is processed in LGN, optic radiation carries it to the visual cortex. All those components are white matter fibers. Myelination of white matter almost reaches its adult level around 12-24 months of age but keeps developing until 17 years (Paus et al., 1999).

Different methodologies were used to study the integration of white matter in the visual pathway. The most basic method, examining the MRI images by visual inspection, revealed that that visual white matter fibers are atrophied in congenital blind (CB) and anophthalmic (AN-CB, a special group of congenital blind subjects who are born without eyes) subjects (Breitenseher et al., 1998; Bridge, Cowey, et al., 2009). Voxel-based morphometry (VBM) and diffusion tensor imaging (DTI) results showed reduced volume and fractional anisotropy (FA) in early blind (EB/CB) sample compared to sighted controls (SC) (Noppeney et al., 2005; Pan

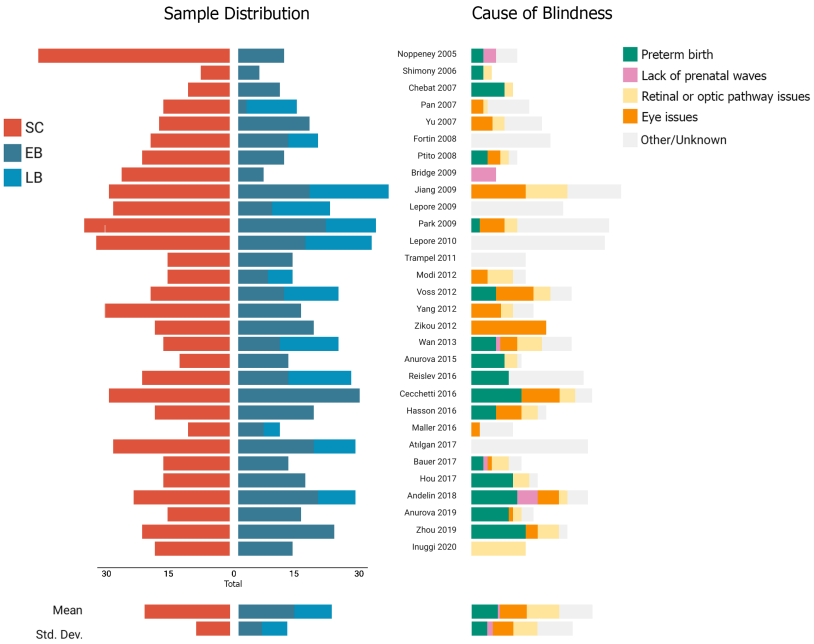


**Figure 4:** This figure offers a synthetic perspective of previous brain structural studies on congenital/late blind samples, their sample sizes, the characteristics of the blind samples relative to the causes of blindness. Each line represents a study. On the left side, under "Sample Distribution", number of sighted, early and late blind participants can be seen. On the right side, under "Causes of Blindness", there is the number of blind subjects falling into four categories of blindness. The categorization was decided based on the description of ICD10 WHO (2004): causes related to premature birth (retinopathy of prematurity), causes related to lack of prenatal waves (anophthalmia/microphthalmia), causes related to eye problems (e.g. glaucoma, cataract), causes related to retina and optic pathway (e.g. retinal detachment, optic pathway atrophy).

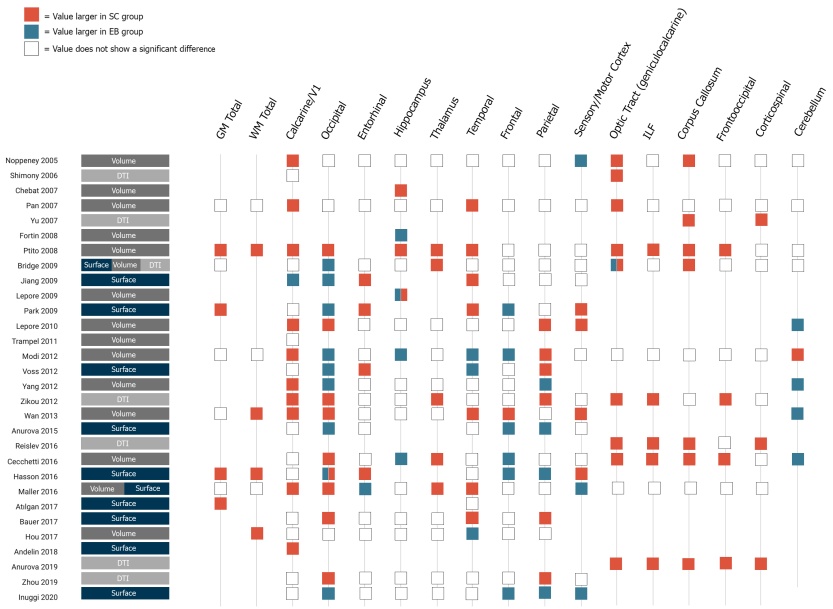


**Figure 5:** Results of the studies listed in Figure 4. Each line represents a study. On the middle column, the method of the study is listed. "Volume" is for volumetric approaches (total volume of the tissues of subcortical structures, or voxel-based morphometry), "Surface" indicates a surface-based metric is used (such as thickness or gyrification), "DTI" refers to diffusion tensor imaging and related metrics such as fraction al anisotropy or radial diffusivity. On the right side, there is the list of most commonly reported structures in those studies and the direction of the result for the relevant structure is represented by a color.

et al., 2007; Ptito, F. C. G. Schneider, et al., 2008; Shu, Liu, et al., 2009). In late blind group (LB), FA was even lower compared to the congenital blind group (Wan et al., 2013), but this was falsified by Tregillus and Likova (2020) that found lower FA in optic radiations of CB. For AN-CB subjects, through, a reduction in the optic tract was observed in the right occipital lobe (Bridge, Cowey, et al., 2009). One interesting finding is that in optic radiation of AN-CB, a secondary fiber was detected and could account for the lack of volume difference. Decreased FA was reported for optic radiation (Yu et al., 2007; Shu, Liu, et al., 2009; Bridge, Cowey, et al., 2009; Bridge, Coullon, et al., 2021), indicating that the consistency of white matter is reduced in those areas.

The only study that reports null results is (Schoth et al., 2006): no difference in relative anisotropy or pyramidal tract, when exploring DTI to check differences between LB and SC. There are two possible explanations for this null finding. First, the metrics used for measuring the difference are different from other studies (i.e., relative anisotropy and pyramidal tract): those metrics may be specifically detecting an aspect that is not different between LB and . Second, blindness onset of the sample is much higher than other studies (older than 12 years of age, none of them had residual light perception) and it may be possible that LB does not show any anisotropic difference.

### 2.1.2 Thalamus

The information sent from the optic tract is sent to the thalamus, specifically LGN. In AN-CB, ventral thalamus (Bridge, Cowey, et al., 2009), and in CB, both thalami are smaller (Cecchetti et al., 2016; Ptito, F. C. G. Schneider, et al., 2008; Maller et al., 2016). Specifically, LGN, temporal, prefrontal, occipital, and right premotor nuclei of the thalamus showed volume reductions (Cecchetti et al., 2016). FA of the whole thalamus was lower in CB (N. H. Reislev et al., 2017), and FA of pulvinar was in LB (Dietrich et al., 2015).

Animal studies showed that if the visual pathway is damaged, the retina can relay the visual input to the auditory thalamus, and the au-

ditory cortex responds to visual stimuli (Sur, Garraghty, and Roe, 1988; Frost et al., 2000). However, auditory thalamic nuclei and medial geniculate nucleus (MGN) did not show any volume differences in CB humans (Cecchetti et al., 2016).

### 2.1.3 Corpus Callosum

The corpus callosum is the structure that connects white matter fibers between two hemispheres. Splenium is the part that connects optical fibers. This part was intact in AN-CB (Bridge, Cowey, et al., 2009), but had reduced volume and surface area (Tomaiuolo et al., 2014; Ptito, F. C. G. Schneider, et al., 2008; Cavaliere et al., 2020), and reduced anisotropy (Shimony et al., 2006; Ashtari et al., 2015) in CB but not in LB (J. Shi et al., 2015). Leporé, Voss, et al. (2010) reproduced similar results using tensor-based morphometry and added that this difference is observable only in CB, but not LB. On the other hand, using the same dataset of anophthalmic subjects from (Bridge, Cowey, et al., 2009), reported that there is no difference in splenium volume or diffusivity among the three groups (AN-CB, CB, SC). These findings contrast with results of papers that feature animal studies. Visual callosal neurons (splenium of corpus callosum) were intact in AN-CB mice (Bola et al., 2017) but atrophied in bilaterally enucleated mice within 12 hours after birth (Bock et al., 2013).

Another part of the corpus callosum, the isthmus, also carries visual information. Leporé, Voss, et al. (2010) found that the isthmus is also defective in CBs, while, Tomaiuolo et al. (2014) stated that the isthmus is larger. The first study relied on tensor-based morphometry, the latter one compared volumetric information across groups. One can say that the difference in the direction of the findings is due to the methods used. However, different methods give similar results about the splenium of the corpus callosum, thus the inconsistency about the isthmus must be due to another factor.

Lastly, body of the corpus callosum is often reported as the same between blind and sighted groups (Ptito, F. C. G. Schneider, et al., 2008; Leporé, Voss, et al., 2010; Pan et al., 2007; Cavaliere et al., 2020) except

in a couple of studies. Posterior mid-body (region next to isthmus) was found larger in CB (Tomaiuolo et al., 2014), but had less anatomical connectivity (Nina Linde Reislev et al., 2016). The anterior body and the genu was not reported as different between blind and sighted samples in any of the studies.

### 2.1.4 Visual Cortex

Development of the visual cortex starts in the prenatal period and its volume expands rapidly within the first few postnatal months (Peter R. Huttenlocher, 1990), almost as big as its maximum size. It reaches its peak around 2-3 years of age and then shrinks gradually until late childhood (Rice and Jr, 2000; Peter R. Huttenlocher, 1990). This pattern is also observed in other animal species, such as cats, macaque monkeys, and rats (Duffy, Kathryn M. Murphy, and Jones, 1998).

From the literature, it can be inferred that the brain has different ways to reshape the visual cortex in congenital and late blindness. VBM analyses showed gray matter in the visual cortex of CB and EB/CB (Noppeney et al., 2005; Pan et al., 2007; Ptito, F. C. G. Schneider, et al., 2008). These studies were followed by cortical thickness studies, which showed that the visual cortex of CB is thicker than SC (Jiang et al., 2009; H. J. Park et al., 2009). Even though results from the two methods seem to be contradictory at first, H. J. Park et al. (2009) tried to find the bridge between them. In addition to cortical thickness, the surface area was also calculated and V1 surface area resulted to be smaller in CB, matching with the results of VBM. This finding indicates that VBM indirectly 'measures' also the surface area. Overall, the CB visual cortex has a smaller surface but is thicker. In a deformation-based morphometry DBM analysis, Yang et al. (2014) found that the visual cortex is contracted, which is in line with results about surface area, while Aguirre et al. (2016) also found that thickness is independent of surface area. The only study that shows a different result from the other studies is C. M. Bauer, Hirsch, et al. (2017). They found a significant decrease in volume, whereas null results in thickness.

Inuggi et al. (2020) found that a thicker cortex is already present in CB children younger than 12 years. However, this effect was only seen on the right cuneus, whereas the common finding in adults covers the lingual gyrus and precuneus bilaterally. Ankeeta et al. (2021) compared the children and adolescent VBM. The difference in the occipital cortex was the most prominent in children who lost sight at an earlier age.

The excess thickness in the visual cortex was permanent even after recovering sight (Guerreiro et al., 2015). Six subjects born with congenital cataracts and recovered their sight at a relatively early period (between 5 and 24 months) have a thicker visual cortex than normally sighted subjects. Hölig et al. (2022) confirmed this phenomena and added that surface area of visual cortex in the sight-restored participants was still smaller compared to sighted participants. These studies suggest that incidents that occur during critical period leave permanent damage visual cortex and differences are irreversible even after the visual cortex starts functioning.

Two studies (Büchel et al., 1998; Bridge, Cowey, et al., 2009), after visual inspection of MRI images, concluded that the visual cortex of CB and AN-CB is no different from SC. It is possible that they missed the slight differences in surface area by visual inspection. Büchel et al. (1998), on the other hand, used a simpler version of VBM, which may be the reason why they could not get significant results.

The difference between LB and SC has a different pattern than CB and SC. While Jiang et al. (2009) reported no difference in cortical thickness for this contrast, H. J. Park et al. (2009) and Voss and Zatorre (2012) found a thinner visual cortex in LB. Andelin et al. (2019) showed that the ratio of surface area of the visual cortex to surface of the whole-brain changes with blindness onset. According to their model, earlier blindness onset is associated with a smaller visual cortex surface area. However, after a critical period, blindness onset does not affect V1. This critical period is roughly post-natal day 116.

Metabolic changes in the occipital lobe are also in favor of the above findings. More glucose consumption and higher cerebral blood flow were reported in early blind subjects (blindness onset - BO $<$3 years),(Wanet-

Defalque et al., 1988; Uhl et al., 1993; De Volder et al., 1997), but not in late blind subjects (BO 13 years, Veraart et al., 1990).

From the above findings, it is possible to conclude that an early loss of sight before the critical period leaves the visual cortex thicker and smaller than the typically developed brain. This critical period is the beginning of synaptic pruning, which depends on visual experience (Andelin et al., 2019). In case of lack of visual experience, the visual cortex cannot eliminate the synapses and results as thicker. In the studies that feature LB with a very late onset, development of the visual cortex is completed, so the difference between LB and SC reported in the studies must be due to blindness per se, not development. Cortical thickness is generally attributed to increasing age or correlated with the performance of the respective brain region (Squeglia et al., 2013; Kharitonova et al., 2013; Salat et al., 2004).

The thickness of the occipital cortex has been also associated to task performance. Thickness was negatively correlated with performance in sound localization and pitch identification tasks in EB/CB (BO $<$2 years, Anurova, Renier, et al., 2015) and pitch discrimination (Voss and Zatorre, 2012), but positively with melody discrimination task (Voss and Zatorre, 2012), in a mixed group of CB and LB subjects. Those findings show that even after developmental plasticity (thicker occipital cortex) occurs, experience-dependent plasticity may still affect the brain in the same direction for both CB and LB groups.

Another approach to deciding the effect of blindness on brain morphometry is to check the covariance of different metrics of anatomical regions. This is often achieved by correlating cortical thickness values among different brain regions. Structural covariance networks can predict anatomical white matter connectivity and reproduce structural networks (Mitelman et al., 2005; Lerch et al., 2006). Reduced anatomical covariance between the right cuneus and the rest of the brain has been reported in CB (Voss, Pike, and Zatorre, 2014). The cuneus was selected as a seed region because its thickness correlates with auditory task performance. Hasson et al. (2016), instead, showed that in SC, lingual and visual regions form a separate cluster: In CB, they tend to merge with

the rest of the network. Anurova, Carlson, and Rauschecker (2019) used a different method and correlated FA with performance during auditory spatial tasks, and showed that FA of inferior longitudinal fasciculus (ILF) correlates with activity in visual and auditory areas in CB, whereas in SC, correlation with auditory areas is negative. Shu, Jun Li, et al. (2009) compared the anatomical networks of two groups using graph theory and network metrics: EB/CB had disrupted network characteristics, such as lower connectivity and longer path length. The region with the most disrupted network characteristic was the visual cortex. In a similar study, Jiajia Li et al. (2013) replicated the same findings and showed that the disruption is correlated with age onset of blindness. Those findings suggest that blindness also changes communication among the different brain regions. In other words, structural connections between different regions of the brain seem to be affected by loss of vision.

## 2.2 Brain structures beyond visual pathways

In addition to vision, studies reported changes in other sensory or motor areas, such as increased white matter in primary and sensorimotor cortices (Noppeney et al., 2005), thinning on the inferior temporal areas for CB and LB, thinner visual, auditory, and sensory cortex (H. J. Park et al., 2009; Hasson et al., 2016). Thinner cortices have been often related to increased performance in other cognitive functions. One example of this phenomenon is reported by H. J. Park et al. (2009). The thickness of the superior temporal gyrus (STG) is negatively correlated with the years of Braille reading, suggesting that post-natal experience may contribute shaping STG (for a review of cross-modal plasticity in the blind brain, see Ricciardi, Bonino, et al., 2014). One contradictory finding is reported in Atilgan, Collignon, and Hasson, 2017 with no difference in thickness in the superior temporal plane. However, the surface area was smaller in CB.

In several cortical thickness studies, entorhinal cortices and temporal poles were thinner in CB (Jiang et al., 2009; H. J. Park et al., 2009; Q. Li et al., 2017; Inuggi et al., 2020). This region is related to the spatial mem-

ory and gives direct input to the hippocampus (Strange et al., 2014). The right hippocampus of the blind sample has a larger anterior and smaller posterior part (Chebat et al., 2007; Fortin et al., 2008; Leporé, Y. Shi, et al., 2009). Additionally, Chebat et al. (2007) showed that the anterior hippocampus volume is positively correlated with spatial-navigation task performance. The experiments consisted of mixed groups of EB/CB and LB. In terms of functional activation, it was reported that hippocampus and parahippocampal area show higher BOLD activity in blind sample during a tactile maze task (Gagnon et al., 2012) compared to sighted controls.

The caudate was found to have decreased volume and less FA in blind sample (Zikou et al., 2012). However, in an extensive study, Voss, Pike, and Zatorre (2014) found no volumetric difference in caudate between blind and sighted individuals. Fortin et al. (2008) exploited the same dataset from the 'hippocampus study' and found no correlation between spatial navigation tasks and caudate performance.

The cerebellum is related, among other functions, to the initiation of eye movements and some studies managed to detect the differences in cerebellum between blind and sighted individuals. Modi et al. (2012) detected a large area in the cerebellum that shows a decrease in gray matter volume. Kosif, Sahin, and Gürel (2013) made a volumetric comparison and found that total volume of cerebellum was smaller in congenitally blind females. Yang et al. (2014) and Wan et al. (2013) reported expansion and increases in cerebellar gray matter. However, in additional analysis, it is revealed that some of this increase can be attributed to preterm birth (Wan et al., 2013). Interpreting those results is challenging since they do not have a common pattern.

If we focus on the white matter pathways, the inferior longitudinal fasciculus (ILF), which connects auditory and visual cortices, results atrophied in some studies (Ptito, F. C. G. Schneider, et al., 2008; Nina L Reislev et al., 2016; Nina Linde Reislev et al., 2016). Nina Linde Reislev et al. (2016) also reported that time spent as blind has a positive correlation with fractional anisotropy of left ILF. It maybe suggested that even though ILF is defective compared to sighted, it recovers its integrity as

time passes.

The corticospinal tract connects motor cortices to the spine. Since blind people need to increase their finer finger skills for Braille reading, an anatomical difference in this population can be expected. Yu et al. (2007) showed an increased FA in the corticospinal tract of early blind (BO<1) male individuals, but not female individuals. Author speculated that this results can be attributed to the fact that number of males who have a profession related to finger use (guitarist, pianist, massaguse) were more than the number of females who have the same profession in the sample. Therefore, this difference can be explained with the expertise rather than the sex difference. Lao et al. (2015) also found an increase in corticospinal tract but without gender difference. Tregillus and Likova (2020) found the same effect for LB.

The uncinate fasciculus, the white matter bundle that connects the frontal lobe to the temporal lobe, is larger in EB/CB on the left hemisphere (C. M. Bauer, Cattaneo, and Merabet, 2018) and has higher FA in and LB than SC (Tregillus and Likova, 2020). Uncinate is related to higher cognitive functions such as verbal memory, working memory, and name retrieval (Cited in Tregillus and Likova, 2020). These are the functions in which blind subjects show higher performance than sighted (Tregillus and Likova, 2020).

Unlike the visual pathway, effect of blindness on other regions have inconsistent results. This can be caused by a small effect size of the true effect. The sample of the studies (in terms of characteristics and size) may not be suitable to detect a difference with a small effect size. Alternatively, the reported findings may not be reflecting the truth they can be sourced from the variability in the samples and methods used in the studies.

## 2.3 Blindness-related variables that could affect structural changes in the brain

Some variables may appear to affect the results but are often overlooked by researchers. Taking a close look at those may help to improve the

quality of research protocols and to better interpret the experimental observations.

### 2.3.1 Braille Literacy

Being a skill that is learned by blind subjects only, Braille literacy can be considered a potential confounding for blindness research. Even though many studies have shown that the visual cortex is recruited for the Braille reading (Sadato, 2005, for a review), structural changes related to this activity are not extensively explored. The only direct evidence, as reported above, is from Park's study in 2009. They showed a negative correlation between thickness on STG and years of Braille reading. The effect was still strong (Pearson r=-0.56 and -0.49 for right and left hemispheres) after correction the data for age. Age correction is important because years of Braille reading increases with age, creating collinearity between the two factors. Using only sighted subjects, Bola et al. (2017) and Matuszewski et al. (2021) showed increased volume in early visual gray matter and increased FA in white matter in the early visual cortex after nine months of blindfolded Braille training. These changes were still present after nine months of no training.

### 2.3.2 Residual Light Perception

Some blind people can still perceive light and can detect if it is day or night or the lights are on. This may be an essential parameter that, beyond affecting the individual circadian rhythms, may impact also brain structural changes. Atrophy in the optic nerves, chiasm and tracts, and superior frontal gyrus were less severe for the RLP subjects Shimony et al. (2006) and Zhou et al. (2019). In terms of cortical thickness, there was no difference found between RLP and non-RLP groups Qin et al. (2013).

Comparing subjects with and without RLP can tell us how much of the atrophy is due to blindness or how much of the integrity of WM is due to residual light perception.

### 2.3.3 Time Spent as Blind - Blindness Onset

Studies listed in this review give solid evidence for the effect of blindness on the visual cortex. Together with the critical period, blindness onset could affect the thickness of the visual cortex. However, it is not entirely clear how intrinsic brain organization and experience-dependent plasticity do interact, or how blindness alone affects the brain over time. If there is a fixed effect of time, it must be accounted for in future studies.

There are some attempts to clarify this relationship. For example, earlier BO (Noppeney et al., 2005; Voss, Pike, and Zatorre, 2014) and time spent as blind (TSAB, Pan et al. (2007)) were associated with decreased gray and white matter density in optic radiations in the EB/CB. The association between GM and TSAB was only valid for different small regions (Pan et al., 2007). Authors commented that this might be due to the fact that the visual cortex is atrophic but is invaded by other modalities. So the effect of atrophy can be interrupted by compensatory, cross-modal plastic phenomena. If we consider VBM results as an indicator of surface area, which is independent of the critical period, the results complete each other.

As for cortical thickness, H. J. Park et al. (2009) found no correlation between cortical thickness and any metrics, whereas Voss and Zatorre (2012) reported that thickness of lingual gyrus correlated positively with BO and cuneus thickness correlated negatively with TSAB as blind in a mixed sample of CB and LB. Since there is a clear distinction between CB and LB in terms of thickness, the two samples must be studied separately to have more accurate estimates and acquire more consistent results.Q. Li et al. (2017) found that earlier BO is related to thicker V1, and this relationship is significant for the BO that occurred in childhood and adolescence.

In LB, optic nerve volume is correlated negatively with the TSAB. No such correlation was found for optic chiasm, optic tract, and LGN (Ptito, Paré, et al., 2021). D. Wang et al. (2013), on the other hand, reported no correlation between FA of white matter and BO or TSAB neither in CB nor in LB.

To study the effect of blindness independently from development, there must be data showing the effect of blindness in different periods, before and after the cortex completes its maturation. That would enable us to detect how much time blindness needs to leave a permanent effect on brain structure. In other words, a critical period for structural plasticity. Time spent as blind is a useful parameter for this purpose, but cannot be manipulated in an experimental setting. Blindfolding studies enable us to specify the duration of visual impairment, so it is possible to detect plastic changes quickly. The occipital cortex starts responding for other modalities after a short period of blindfolding (2 hours, reviewed in Lazzouni and Lepore, 2014). However, there is no evidence for a critical period for structural plasticity.

### 2.3.4 Causes of Blindness

Every study has a unique distribution of causes of blindness. If one type of disorder is dominant in the sample, the results of that study may be biased. For example, one of the most common types of blindness, retinopathy of prematurity (RoP), is related to preterm birth.

It has been shown that preterm birth has a systematic effect on brain anatomy. Smaller total gray and white matter volumes (D. K. Thompson et al., 2008), and smaller subcortical structure volumes (Boardman et al., 2006; B. S. Peterson, Vohr, Staib, Cannistraci, B. A. Dolberg, et al., n.d.) were observed in RoP. These effects correlate with gestational age (Boardman et al., 2006; B. S. Peterson, Vohr, Staib, Cannistraci, B. A. Dolberg, et al., n.d.). Deformation in white matter is stronger in the more immature RoP. Therefore, including many RoP subjects in the sample could impact the results. Since there is a unique effect of RoP subjects, and they are only included in the blind group, it is impossible to tell if differences between the sighted and the blind groups are due to blindness or to prematurity. There have been some attempts to clarify this relationship. After removing RoP subjects from their VBM analysis, Wan et al. (2013) found that differences in temporal and frontal regions disappear. Ptito, F. C. G. Schneider, et al. (2008) also limited their analysis to preterm

birth subjects and observed that total GM and WM decreases were larger in those subjects. However, even without RoP subjects, the difference between other blind groups and sighted people was still significant. This may explain the variation in the results, especially in findings that are not on the visual pathway.

Studies investigating the effect of one specific disorder usually involve participants who are not completely blind yet. This must be due to the difficulty of finding enough subjects that are both blind and have the same cause of blindness. Partial visual impairment caused by open-angle glaucoma (Zikou et al., 2012; Chen et al., 2013), amblyopia (Mendola et al., 2005), retinitis pigmentosa (Ohno et al., 2015; Machado et al., 2017), Leber's hereditary optic neuropathy (Barcella et al., 2010) showed very similar patterns of structural differences to those of EB/CB and LB. Their occipital lobe has reduced volume, optic radiations have reduced volume, and fractional anisotropy weaker. Those studies show that atrophy in the visual pathway starts before losing sight completely.

### 2.3.5 Statistical Power

As shown in the Figure 4, the number of blind subjects in listed studies is not more than 36 (mean=18.6±8.2). Studies with low sample sizes tend to miss the detection of true effects (if any) and report inflated false positives (Yarkoni, 2009). It has been suggested that to detect large and medium effects, the sample size must be around 80. However, even if the sample size is 100, it is difficult to detect small effects (Geuter et al., 2018). A more recent study, Marek et al. (2022), highlighted that brain-wide association studies need thousands of subjects in order for the results to be reproducible. Therefore, the inconsistencies among the previous studies can be attributed to the low power of the studies. For example, Zikou et al. (2012) and Chen et al. (2013) applied VBM on patients with primary open-angle glaucoma and sighted controls. Both studies used the same analytical tool (SPM, versions were different). However, their results were quite dissimilar. One study reported gray matter reductions in caudate and putamen, the other reported in superior and inferior pari-

etal gyri. The only common area between the two results was the left calcarine sulcus. Moreover, Zikou et al. (2012) did not report any gray matter increase in glaucoma patients, whereas Chen et al. (2013) did. What can be the source of the difference? The cause of blindness, methodology, and software are identical and sample sizes are similar 15 and 18 (for only the experimental group). This is a clear example of how studies with small samples could suffer from overestimation of results, as discussed below.

## 2.4 Meta-Analysis

### 2.4.1 Methods

Our multiple sites image-based data sharing initiative to structural brain data was compared to a coordinate-based meta-analytic approach, such as the activation-likelihood estimation (ALE) that gathers MNI coordinates of peak locations to integrate published findings of observational studies with small size samples (Turkeltaub et al., 2002). Critically, this quantitative approach overcomes the typical limitations inherent in single neuroimaging studies (e.g., sensitivity to analytic procedures, lack of replication studies, as well as small sample size - (Carp, 2012; Salimi-Khorshidi et al., 2009) and was aimed to identify the brain regions consistently associated with structural changes in congenital blindness.

The literature search was started by searching for "congenital blind MRI morphometry" and "early blind MRI morphometry" on Pubmed (https://www.ncbi.nlm.nih.gov/pubmed/). The preliminary pool of 29 studies, after duplicates were removed, was first screened by title and then abstract. Studies fulfilling the following criteria were retained:

- Studies written in English language;
- Empirical structural MRI studies, while excluding review and meta-analysis articles, single case reports and those employing other techniques;

- Studies reporting any neurometric (voxel or surface-based morphometry, white matter integrity) comparison between EB/CB/LB (otherwise healthy subjects) vs. SC in whole-brain activation coordinates (results must be corrected via multiple comparison correction), rather than results limited to region of interest (ROI) or using small volume corrected (SVC) analyses (Müller et al., 2018). The direction of the results (blind <sighted or sighted <blind) is ignored;
- Studies dealing with blindness due to non-ocular causes (i.e., cortical visual impairment) are excluded.
- In case of studies dealing with partial visual impairment (e.g. studies about one causes of blindness - glaucoma, Leber's amaurosis etc...), if the participants have visual acuity below the WHO's criteria of blindness (less than 6/60), they were considered as blind and included in the study.

This selection phase resulted in 10 studies fulfilling our criteria. When an article fit our criteria but lacked MNI coordinates of the results, we tried to directly contact the corresponding or the first author of the studies to have the necessary information regarding MNI coordinates of the whole-brain results, so that we can include the experiment in our analyses.

The studies cited by or citing these papers were checked as a next step. This step highlighted nine further studies fitting our search criteria. This procedure included the main ALE meta-analysis on blind participants in 19 previously published studies (see Table 1), resulting from 19 experiments (individual comparisons reported) with 675 subjects and 178 foci. This number of contrasts is in line with minimum requirements for ALE meta-analyses (Eickhoff, T. E. Nichols, et al., 2016; Müller et al., 2018) and allows achieving sufficient power for moderate effects ensures that results will not be driven by single experiments.

Importantly, combining multiple contrasts from the same set of subjects can lead to dependence across experiment maps, lowering the validity of the results. To avoid this, we accounted for within-group effects

by combining the coordinates from all of a paper's relevant contrasts into a single experiment (Turkeltaub et al., 2002).

Using the GingerALE software, an ALE analysis was performed to identify consistently altered brain structures in EB/CB compared to SC (Eickhoff, Laird, et al., 2009). Activation foci were initially interpreted as the centers of three-dimensional Gaussian probability distributions to capture the spatial uncertainty associated with each coordinate. All coordinates were reported or converted into MNI space, using the automatic routine implemented in GingerALE. The three-dimensional probabilities of all activation foci in a given experiment were then combined for each voxel, resulting in a modeled activation (MA) map. The union of these maps produces ALE scores describing the convergence of results at each brain voxel (Turkeltaub et al., 2002). To distinguish "true" convergence across studies from random convergence (i.e., noise), the ALE scores are compared with an empirically defined null distribution (Turkeltaub et al., 2002). The latter reflects a random spatial association between experiments, with the within-experiment distribution of foci being treated as a fixed property. A random-effects inference is thus invoked by focusing on the above-chance convergence between different experiments and not on the clustering of foci within a specific experiment. From a computational standpoint, deriving this null hypothesis involved sampling a voxel at random from each MA map and taking the union of the resulting values. The ALE score obtained under this assumption of spatial independence was recorded, and the permutation procedure was iterated 100 times to obtain a sufficient sample of the ALE null distribution. The "true" ALE scores were tested against the ALE scores obtained under the null distribution and thresholded at $p < 0.05$, corrected for voxel-level family-wise error rate (FWE) (Eickhoff, Bzdok, et al., 2012).

### 2.4.2 Results

The coordinate-based meta-analysis consisted of 19 studies, 675 subjects, and 178 foci. From the distribution of the foci included in the analyses (Figure 7), it can be seen that the foci are primarily distributed along

| Study | Number of Subjects | Number of Foci |
|---|---|---|
| Noppeney et al., 2005 | 57 | 6 |
| Pan et al., 2007 | 30 | 13 |
| Ptito, F. C. G. Schneider, et al., 2008 | 32 | 14 |
| Shu, Liu, et al., 2009 | 34 | 4 |
| Voss and Zatorre, 2012 | 32 | 1 |
| Modi et al., 2012 | 28 | 13 |
| Wan et al., 2013 | 40 | 32 |
| Voss, Pike, and Zatorre, 2014 | 40 | 2 |
| Anurova, Renier, et al., 2015 | 40 | 14 |
| Ashtari et al., 2015 | 22 | 6 |
| Dietrich et al., 2015 | 29 | 5 |
| Cecchetti et al., 2016 | 58 | 32 |
| Nina L Reislev et al., 2016 | 42 | 6 |
| C. M. Bauer, Hirsch, et al., 2017 | 28 | 1 |
| Hou et al., 2017 | 32 | 2 |
| Zhou et al., 2019 | 36 | 3 |
| Inuggi et al., 2020 | 31 | 10 |
| Ankeeta et al., 2021 | 35 | 8 |
| Bridge, Coullon, et al., 2021 | 29 | 1 |
| **Total** | **675** | **173** |

**Table 1:** List of the studies included in meta-analysis and number of the foci extracted from them.

| Coordinates | Label |
|---|---|
| 0 -76 4 | Interhemispheric Lingual Gyrus |
| 24 -16 -10 | Right Globus Pallidus |
| 0 -88 4 | Lingual Gyrus |
| -26 -68 16 | White Matter |
| -24 -70 18 | Cuneus |
| -12 -66 22 | Precuneus |

**Table 2:** Cluster locations identified by meta-analysis in MNI space.

the visual pathway, but also expand uniformly all over the brain. The meta-analysis identified significant clusters on the lingual gyrus, cuneus, precuneus, white matter region on optic radiations, and a subcortical region close to LGN (Figure 6, Table 2). Those regions are on the main visual pathway and represent the most consistent findings across structural brain studies in blindness. Regions that are discussed in the literature but not on the visual pathway (such as STG, ILF, sensorimotor regions) are not found as significantly affected by blindness in by the meta-analysis.

## 2.5 Conclusions

Brain reorganization following visual deprivation is differentially affected by blindness onset (Figure 8). Compared to physiological development, losing eyes and retina before light perception leads atrophy in the white matter tracts of visual pathway, smaller LGN, less FA and an additional fibre in optic radiation (Bridge, Cowey, et al., 2009) and smaller (Andelin et al., 2019) and thicker (Jiang et al., 2009) visual cortex. In addition to this list, losing sight during perinatal period but before critical time (17th postnatal week - Andelin et al., 2019) defects splenium of corpus callosum (Tomaiuolo et al., 2014; Leporé, Voss, et al., 2010; Shimony et al., 2006; Ptito, F. C. G. Schneider, et al., 2008). Even though there is a trend for increase in visual cortex surface area in early blind subjects compared to anophthalmic subjects, it is not significant (Andelin et al., 2019).

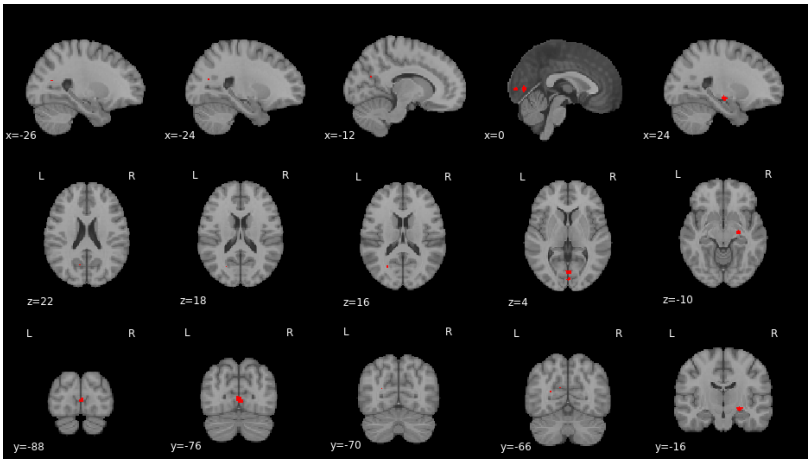


**Figure 6:** Results of the ALE meta-analysis showing clusters with significant ALE maxima ($p<0.05$). Top row: saggital view, middle row: axial view, bottom row: coronal view.

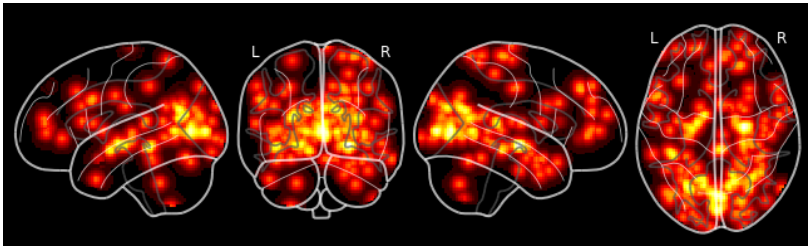


**Figure 7:** All foci that are included in the meta-analysis. It can be seen that there is a high concentration of the foci on the optic radiations and visual cortex (shown in yellow) and lower concentration throughout the rest of the brain (shown in red).

Losing sight after the critical period thins visual cortex and the surface area stays statistically similar to the sighted control. There was no difference in the integrity of the splenium of corpus callosum (Leporé, Voss, et al., 2010). The rest of the reported differences, mainly on the non-visual brain, results to be inconsistent across studies and would need further investigation. This is also confirmed by the meta-analysis results.

Tracing the neuroplastic changes in the brain depending on the age onset of visual deprivation (including blindfolding studies), may allow us to differentiate the effect of development from the effect of blindness. As long as the effects of natural development is known to us, it is possible to place blindness onset on any point on the scale (as in Figure 8). For example, a researcher who wants to study solely the effect of visual deprivation, must choose the subjects whose blindness onset is very close to the right side of the scale, staying away from critical periods. Naturally, it is not possible to apply blindfolding for a long time in order to study the critical period for structural plasticity. In this case, subjects whose blindness onset is close to current day must be chosen. Time spent as partially blind is another crucial factor in this equation, as the brain starts reshaping itself when there is partial visual loss.

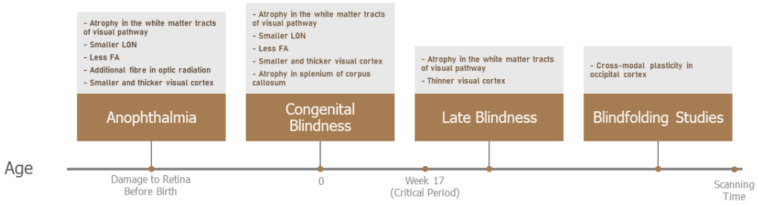


**Figure 8:** A visual summary of the effects of blindness on brain anatomy.

In the light of the topics discussed in the literature review and the results of the meta-analysis, it can be said that samples that are used for blindness research have to properly take into account all factors that are shown to or may have an effect on brain anatomy. For example, to ac-

count for the effect of residual light perception, only the subjects without light perception should be included in the study. If this is not possible, at least it can be included as a regressor in the statistical model, even though this model will not completely rule out the effect. Likely, different causes of blindness, if they are shown that they have a unique affect on brain anatomy, can be treated differently. Retinopathy of prematurity and anophthalmia are good examples for this case. Studies that can point the effect of different causes will help improve the literature. Lastly, sample size must be as large as possible. Otherwise, even though the characteristics of the samples are arranged perfectly, we may not be confident of the results.

# Chapter 3

# Structural Changes in the Congenitally Blind Brain

## 3.1 Methods

### 3.1.1 Data Collection and Contributing Sites

Research groups that have been previously working on structural brain changes in visual deprivation were invited to share their 3D structural T1 MRI scans of congenital or early blind samples and their matched sighted individuals. Ten research groups from different international institutions: Université Catholique de Louvain - Belgium; Copenhagen University – Denmark; University of Oxford - United Kingdom; National Institute for Physiological Science, Japan; Massachusetts Eye and Ear Infirmary – Harvard Medical School, USA; University of Montreal – Canada; IMT School for Advanced Studies Lucca - Italy; University of Turin – Italy; Brainnetome Center and Beijing Normal University – China participated in the study and shared their structural images and supplementary metadata (e.g., blindness onset, cause of blindness, presence of residual light perception, visual acuity, Braille literacy, etc.) after obtaining approval for data sharing from their local institutional review boards. Members from all contributing groups also signed an online

agreement for sharing their data with the IMT School members and a nondisclosure form. Data has been collected and analyzed on the IMT School servers. Detailed information of the samples supplied by each research group can be seen in online supplementary table. Across different laboratories, MRI data were acquired using 1.5, 3T or 4T scanners, T1/3D-TFE/MPRAGE/FSGPR sequences, 3/4 B0 strength, TR changing between 1120-8100, TE changing between 2.19-4.7.

### 3.1.2 MRI dataset and Samples

The research groups gathered 156 T1 images of congenital participants and sighted controls for the study. After data processing and a quality check procedure (see below), 127 CB (blindness onset=0 years of age, 34.17 ± 11.3 years old, 53 female) and 127 SC (34.15 ± 12.2 years old, 49 female) were used to create two samples that were balanced in terms of age, gender and scanning site (online supplementary table). Apart from three left-handed (one CB), four ambidextrous (two CB), and 64 not reported (26 CB), all participants were right-handed. All sighted and blind subjects received a medical interview or examination to exclude any disorder that could affect brain function and metabolism other than blindness in the blind group. All participants provided written consent before the MRI examinations according to the approved protocols of each contributing site.

Causes of blindness included retinopathy of prematurity, optic nerve atrophy/dystrophy/damage, congenital cataract, congenital glaucoma, anophthalmia, microphthalmia or eye dysplasia (e.g., eyeball, retinal, fundus, etc.), Leber's congenital amaurosis, congenital retinitis pigmentosa, infection, tumor, and others. Details on demographic and clinical information of the contributing samples are reported in Supplementary Table 2. Furthermore, according to the shared individual metadata, eighty-eight CB individuals of our sample were able to read Braille language (average 27.6 ± 14.1 years of Braille reading experience).

### 3.1.3 Data Preprocessing and Hypothesis Testing

The preprocessing of the structural T1-weighted MRI images of the CB and SC samples acquired at the various contributing sites included two steps: anterior commisure-posterior commissure (AC-PC) alignment (done via FSL, Jenkinson et al., 2012 and skull-stripping/tissue segmentation (done via Advanced Normalization Tools package (ANTs - Avants, Tustison, and G. Song, 2011). To achieve AC-PC alignment (normalizing the orientation of the images), affine transformation matrices to MNI template (from FSL's library) were first created. Then, the scaling factor was removed from these matrices, leaving only transformation and rotation parameters. This step generated the transformation matrices to MNI space but keeping the original size of brains. Since the MNI template is already on the AC-PC plane, the transformation matrices hold the information for AC-PC alignment for the raw images in one step. The alignment was completed by applying the matrices on the raw images. Next, skull-stripping and tissue segmentation - gray matter (GM), white matter (WM), and cerebro-spinal fluid (CSF)- was applied with ANTs. ANTs has a template that has priors for skull-stripping and tissue segmentation (2012 MICCAI Multi-Atlas Labeling Challenge Data, B. Landman, S. Warfield, MICCAI 2012). The procedure is as follows: the input image is non-linearly registered to ANTs' template, skull-stripping and tissue segmentation is applied within the template space, and the skull-stripped and segmented files are sent back to the subject's space. The quality of segmentation and brain extraction were explored visually for each subject. Low-quality images and images with low-quality segmentation were removed from the dataset. Then, the remaining SC and CB samples were matched in terms of blindness, age, gender, and scanner site, resulting in the final sample of 127 subjects in both groups.

An alternative way to account for the confounding effect of the different scanning sites is the ComBat method, offered by Johnson, C. Li, and Rabinovic, 2007. The difference between ComBat and generalized linear model (GLM) is that ComBat adjusts the parameter estimate of the data from the different batches via empirical priors whereas the param-

eters are left untouched. In this paper, ComBat was implemented on the volumetric comparison of subcortical structures. Instead of adding the scanning site as a regressor to remove the site effects, ComBat algorithm was used via GenePattern (Reich et al., 2006) and residuals are saved. Adjusting the site effects with ComBat did not change the significance of the results. The resulting list was still the same. The F-scores of the group regressor almost overlapped. The very limited difference did not justify the use of ComBat for the rest of the analyses; thus, the site effects were removed within the GLM approach.

The main aim of this study was to investigate differences in cortical and subcortical morphometry related to the congenital lack of visual input. Individual segmentation of cortical and subcortical volumes, cortical thickness and the other neuromorphic indices were merged for participants across all sites into one comprehensive model.

The following multiple linear regression model was used to explain the variance in the sample:

*Y=Intercept+Parenchyma+Age+Gender+Group+ScannerSite+errorterm*

Parenchymal volume (sum of gray and white matter volumes), age and gender were included in the model in order to account for individual differences, whereas scanning sites were included to account for confounds that can be caused by different scanners and acquisition sites. CSF volume was not included in the calculation of whole-brain volume because ANTs segment the tissues within a mask that does not cover the whole cranium. Complete calculation of CSF volume is not possible within that mask. Therefore, adding CSF volume into account would only introduce a confound in our analysis.

For each participant, left and right cerebral and subcortical volumes, voxel-based concentration of the gray and white matter, cortical thickness, and gyrification were calculated.

For the cortical thickness and gyrification analyses, the parenchymal volume was not included in the model, because, before the calculation of the surface values, surface models were already normalized to a template and their size differences were accounted for. See the relevant section for further details. The regressors of the model are orthogonal except from

parenchymal volume, that is not collinear, but also not orthogonal, with age and gender.

The model was tested with a non-parametric permutation test with 10,000 permutations. Considering the fact that permuting a model with one regressor would be faster than a model with many regressors, the main model was first applied on the data without the "Group" regressor and the residuals were saved. Those residuals were used as dependent variables and explained by the group regressor. For each iteration, the group labels were shuffled and the largest F-stat of the whole brain was saved to create an F-stat distribution The value at the 95th percentile of this distribution was used as the significance threshold. The original F-stats were considered as significant if they are larger than the threshold value. This procedure was repeated for each voxel/vertex/structure (depending on the type of the analysis). This non-parametric significance test also corrects for the family-wise error rate (T. Nichols and Hayasaka, 2003) and has a strict threshold. Although this is the preferred method of this work to correct for multiple comparisons, FDR correction was also applied for the sake of the comparison between correction methods. The results of the FDR correction are either presented along with the permutation corrected results, or in the supplementary materials.

In a different model, to check the potential difference of the effect of age between groups, residuals of the following model were acquired:

$Y = Intercept + Parenchyma + Gender + Group + ScannerSite + errorterm$

The only difference between this model and the previous one described above is the Age regressor. The data was not cleaned from te effect of age on purpose. The residuals were fed into another regression model where the independent variables were age, group, and an interaction term between age and group. The permutation procedure described above was applied on the coefficients of this interaction term. Instead of F-stat of the whole model, for each iteration, the maximum absolute value of the interaction coefficient in the whole brain was saved to create a permutation distribution. This test was done on whole-brain and region-of-interest-based (ROI-based) cortical thickness, gyrification, VBM and volumetric comparison of subcortical structures (see below for

the details of the analyses).

### 3.1.4 Comparisons Between Congenitally Blind and Sighted Group

**Voxel-based Analyses**

VBM was applied via the SPM toolbox (Ashburner, 2010). GM and WM masks were first created for each subject. Then, a study-specific template is created to calculate the deformation fields to that template for each subject. Lastly, the group template is transformed into MNI space and the generated transformation matrix is combined with the deformation fields of each image. The combined matrices are used to send smoothed (we used 4mm Gaussian kernel) and Jacobian modulated images to MNI. For the complete process, please see the tutorial (Ashburner, 2010). The resulting files are used to compare the volumetric concentration of GM and WM at the whole-brain level. After generating the VBM results for both GM and WM, Talairach-Tournoux atlas (Talairach, 1988) and Tractotron software (Foulon et al., 2018; http://www.toolkit.bcblab.com) were used to decompose the significant GM and WM clusters. The whole procedure is as follows. First, the mean VBM image (created by addition of mean GM and mean WM images) was non-linearly registered to the MNI152 template from FSL's library space. This is because the MNI template that SPM uses (DARTEL) is larger than MNI152 template, which is utilized by the atlases and the tools that are used to decompose the brain regions. Then, significant clusters of GM and WM results were binarized and saved as masks. The transformation matrices and warp fields that are generated during Dartel to MNI registration were used to send the cluster masks to the MNI template. Lastly, GM results were decomposed via AFNI's whereami function (Cox, 1996). This function returns the corresponding ROI name from the available atlases in AFNI's library based on the coordinates of the cluster. Talairach-Tournoux atlas (Talairach, 1988) was the atlas of choice.

WM results were decomposed with Tractotron, which is a software using FMRIB software library (FSL) as well as previously published white

matter tract atlases (Rojkova et al., 2016) in the MNI152 referential to. For a given lesion, Tractotron provides a probability and the severity of disconnection for almost all known tracts. In other words, Tractotron takes a lesion mask (mask of the significant results in our case) and outputs the proportion of overlap between the mask's volume and the WM tracts' volume. FSL's run-first-all function was used to segment the caudate nucleus, hippocampus, thalamus, amygdala, putamen and globus pallidus for both hemispheres. In addition, segmentation of cerebellum was acquired via ANTs. From the binarized segmentation masks, volumetric information of the mentioned structures was extracted. Along with subcortical structures, parenchymal, gray and white matter volumes were also calculated through the segmentations acquired from this function. Parenchymal volume was removed from the regression model for the comparison of these three volumes. The volumetric information of the abovementioned structures compared between CB and SC groups. Hippocampus masks generated by FSL were segmented into three regions - head, body and tail – using AFNI . As previously defined by Chebat et al. (2007) a segmentation procedure was followed to divide the hippocampus into four parts on the y-axis. This procedure defines the anterior quartile as the head and posterior quartile as the tail. These masks are used to compare the volume of the three segments of the hippocampi between groups.

**Surface-based Analyses**

Surface-based cortical thickness analysis was estimated using an automated Computational Anatomy Toolbox (CAT12, Gaser, Dahnke, et al., 2016), an extension of the SPM toolbox available in MATLAB (MathWorks, Natick, MA, USA). CAT12 is considerably faster, and the thickness estimates are still highly correlated to FreeSurfer performance (Seiger et al., 2018). CAT12 uses projection-based thickness to measure thickness and create surface meshes. To achieve that, the software first relies on tissue segmentation (GM, WM and CSF) of the images to estimate the distance from WM to CSF and projects the local maxima (equivalent to cortical thickness) to a surface. Then, CAT12 corrects the topological

defects and registers all the surfaces to a sphere. Here, all meshes are resampled to 32k (average vertex spacing is around 2mm) and a smoothing with a given 15 mm-FWHM Gaussian kernel was applied. Fitting all the meshes to the same template (the sphere) accounts for the size differences in the brain. Therefore, parenchymal volume is not included in the regression model for the surface-based measures (thickness and gyrification), since the inter-subject variability in the brain size is already dealt with. SC-CB contrast was tested for each vertex on the surface mesh, using the model described in section 3.1.3. The whole brain vertex-wise comparison was followed by a whole-brain ROI-based analysis. Mean thickness values for 68 brain regions defined by Desikan-Killiany atlas (Desikan et al., 2006) were compared between SC and CB. The same procedure was repeated with a different parcellation, the HCP-MM1 atlas (Glasser et al., 2016), that defines the cortical regions based on the functional dynamics rather than structural properties. The aim was to see the distribution of the structural differences in the functional areas.

Since occipital areas have been reliably reported as altered by congenital blindness, to specifically confirm the lack of difference within the calcarine sulcus in the whole brain comparison, the SC-CB comparison was repeated within an occipital ROI that was generated by choosing the vertices with a $p<0.05$ for the SC-CB comparison. The same analysis was repeated and corrected for multiple comparisons within this mask. The only difference between the whole-brain comparison and within-ROI comparison is that instead of saving the maximum F-score in the whole brain, maximum F-score in the occipital ROI was saved in each permutation. Since the area of interest is much smaller, the significance threshold might change. A possible change in the significant result may indicate the null result on the calcarine sulcus is due to a thresholding issue.

SC-CB analysis was repeated with small random subsamples to identify potential findings due to a small number of subjects. Number of participants in the subsamples was set to 34 participants (17 each group) because the mean sample size in the literature review table is 33.9 (mean SC=20.5, mean CB=13.3). The procedure is as follows: first, random sub-

samples of 17 subjects from each group was chosen. Then a regression analysis was applied, and F-stat for each vertex was saved. Lastly, if the F-stat of a vertex is larger than 18 (the critical F-value for the analysis with the whole sample), the final value of that vertex was increased by 1. This procedure was repeated 100 times.

Mean thickness values in 68 ROIs (Desikan-Killiany atlas parcellation, Desikan et al., 2006) were also used to create covariance matrices for CB and SC groups. Pearson's correlation coefficient was used to calculate the relationship between ROIs, and these values were standardized via Fisher's Z transformation. Difference between matrices of the CB and SC samples was calculated via node-wise subtraction of the Z-scores. Significance test of the differences was done with the permutation procedure explained above. After shuffling the labels of the subjects, covariance matrices were created, and difference matrices were calculated. This procedure was repeated 10,000 times. For each repetition, the maximum absolute value of the largest difference is saved. The 95th percentile value of the random distribution was used as the critical value.

In addition, by using the CAT12 toolbox, the gyrification index was also derived. The method described in Luders et al. (2006) is adopted to calculate this metric. This metric is used to quantify the cortical folding, and to run a between-groups comparison. Gyrifcation index (also known as cortical folding) is described as the ratio of "amount of cortex buried within the sulcal folds as compared with the amount of visible cortex" (Schaer et al., 2012). Luders et al. (2006) adopted this metric and calculated the relevant value for each vertex.

### 3.1.5 Within-blind Group Comparisons

The comparisons that resulted in significant differences (whole-brain and ROI-based cortical thickness, gyrification, VBM on both gray and white matter, volumetric comparisons of the subcortical structures and total gray matter, white matter, and parenchyma) were selected to make further investigations within the CB group, and assess the effects on neuroimaging metrics of individual characteristics relative to the etiology

and features of blindness, limiting to those variables that were available in the sample metadata for each site. Importantly, we limited a large part of the methodological noise between individual studies by unifying pre-processing and data analysis.

After cleaning the data from age, gender, site, and parenchymal volume (not included in the surface-based analyses), residuals of the blind sample were used in additional within-group comparisons to investigate the extent to which distinct causes of blindness, residual light perception, or common postnatal experiences (i.e., Braille reading) might have influenced the main effect of the congenital lack of vision on morphometric measures.

To explain the contribution of the selected variables on the differences between groups, the CB sample was further examined by taking potentially important factors into consideration. These factors are causes of blindness, residual light perception and Braille literacy.

Available causes of blindness were sent into four main categories in order to create a more homogenized distribution: causes related to preterm birth (retinopathy of prematurity - RoP), causes related to lack of perinatal waves (anophthalmia/microphthalmia - AN-CB), causes related to eye issues (glaucoma, cataracts), causes related to retinal or optic-pathway issues (optic nerve atrophy, Leber's amaurosis, retinoblastoma, retinal dysplasia). Classification of the causes were decided based on their description on ICD10, classification of mental and behavioral disorders (WHO, 2004). Main categories and the original causes (as sent by the contributors) can be seen in the online supplementary table. At the end, 33 participants were labeled with causes related to preterm birth, 22 participants with causes related to lack of perinatal waves, 19 participants with causes related to eye issues, 41 participants with causes related to retinal and optic pathway issues.

Premature birth affects the anatomy of the brain regardless of vision (Hasler, T. T. Brown, and Akshoomoff, 2020). Therefore, in the following analyses, RoP is treated separately then the rest of the causes. To identify the differences between RoP and the rest of the causes of blindness, a linear regression model with where RoP blind individuals were compared

with the rest of the blind sample. An additional model was run in which an interaction term between age and RoP regressor was added. Lastly, main comparison (SC-CB) was repeated without RoP blind individuals and their matched sighted controls (remaining number of participants in each group = 93).

Causes related to lack of perinatal waves, eye issues or retinal/optic pathway issues were included in a separate one-way model together in order to see if any of the causes captures more variance than others.

Effects of Braille literacy and RLP were examined in separate regression models. Braille literacy was included as a numerical regressor (age onset instead of categorical) because of the imbalanced distribution of the participants (88 Braille literate vs. 6 Braille illiterate). Subjects whose age of Braille onset is unknown were discarded from the analysis, leaving 68 of them (correlation between Braille onset and age=0.2, p0.05). Effect of RLP, on the other hand, was coded as a dummy variable (number of subjects with RLP=46 vs. number of subjects without RLP=67) to explain the variance in the structural measures. Both analyses were repeated with a model additional regressor that tells if the cause of the blindness of the subject is RoP or not, and an interaction term between the two regressors.

The results of all models were corrected with permutation procedure in both whole-brain and within the significant regions/structures revealed by the main (SC-CB) comparison.

## 3.2 Results

### 3.2.1 Sighted vs. Congenital Blind Groups

#### Demographics

There were no significant age (two-way t-test, t=.016, p=.987, Cohen's d=.002) or gender-related ($X^2$ =0.262, p=.609) differences between groups.

#### Quantitative comparison of brain volumes

When assessing the differences in the overall brain parenchymal volume, GM and WM were significantly decreased in CB subjects as compared to

| | Difference in cm^3 | Percent decrease | Cohen's d | P-value |
|---|---|---|---|---|
| **Parenchymal** | 62.91 | 5.21 | 0.55 | **<0.05** |
| **Gray Matter** | 32.27 | 5.11 | 0.48 | **<0.05** |
| **White Matter** | 30.63 | 5.32 | 0.44 | **<0.05** |

**Table 3:** Difference between parenchyma, gray and white matter volumes between groups.

SC (differences in $cm^3$ were 62.9±150.6, 32.3±79.4 and 30.6±89.4, respectively, Table 3). Percent volume losses related to blindness since birth ranged around 5% (specifically, 5.2%, Cohen's d=.55 for parenchymal volume; 5.1%, d=.48 for GM; 5.3%, d=.44 for WM). A preliminary multidimensional scaling was applied based on GM and WM volumes using Euclidean distance metric in order to see if the subject form different clusters (Figure 9). However, both SC and CB groups and subclasses of CB group were close to eachother and did not show clear seperation.

This was confirmed by a whole-brain VBM analysis showing patterns of gray and white matter atrophy primarily affecting vision-related cortical and subcortical structures, or pathways. Specifically, the results of VBM analysis for GM and WM are presented in Tables 5- 4, and Figures 10- 11 .

For the GM, when compared to the SC group, the CB group had significantly lower VBM only in primary and extrastriate visual cortices. These brain areas included the bilateral calcarine and lingual cortices, cuneus, posterior parahippocampal gyri, medial dorsal nuclei. Moreover, bilateral anterior parahippocampal gyri only showed increases in gray matter in the CB group when compared with SC.

For the WM, when compared to the SC group, the CB group had significantly lower VBM in optic radiations, inferior longitudinal, left inferior fronto-occipital, posterior part of the corpus callosum whereas CB group had higher VBM in right pons, right corticospinal tract, and right frontostriatal circuit.

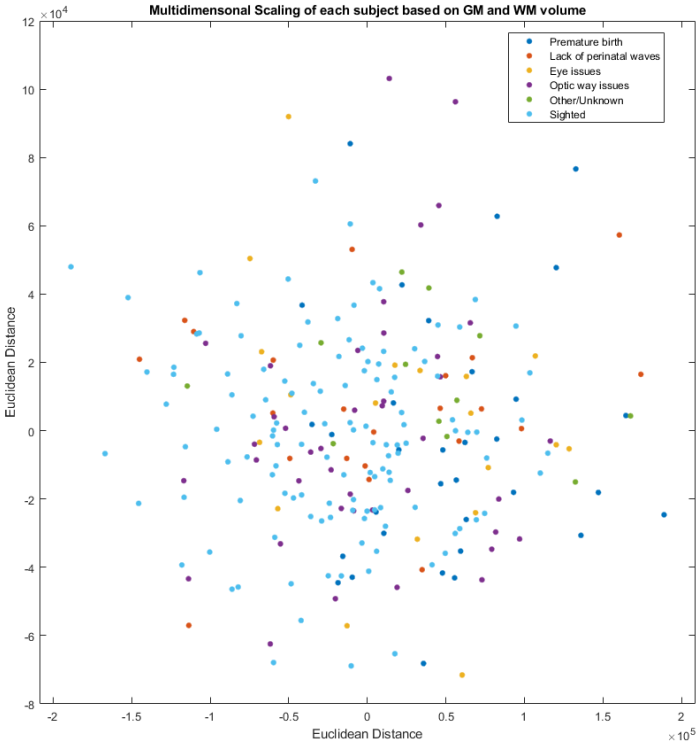


**Figure 9:** Multi-dimensional scaling of all subjects based on gray and white matter volumes. The distribution does not show clear distinction between congenital blind-sighted group or blind subjects with different causes of blindness.

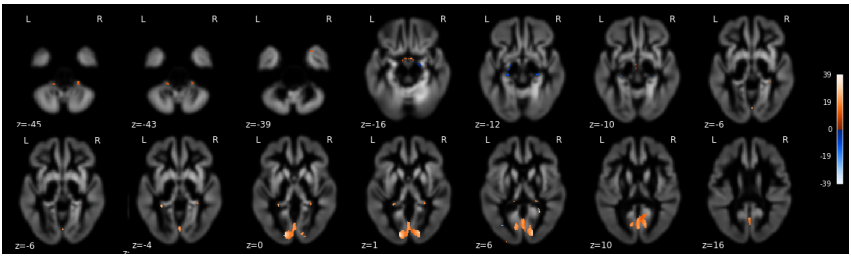


**Figure 10:** Regional grey matter differences between CB and SC. Positive values (warm colors) show the regions with atrophy in CB, negative values (cold colors) show the regions with atrophy in SC ($p<0.05$, corrected for multiple comparisons).

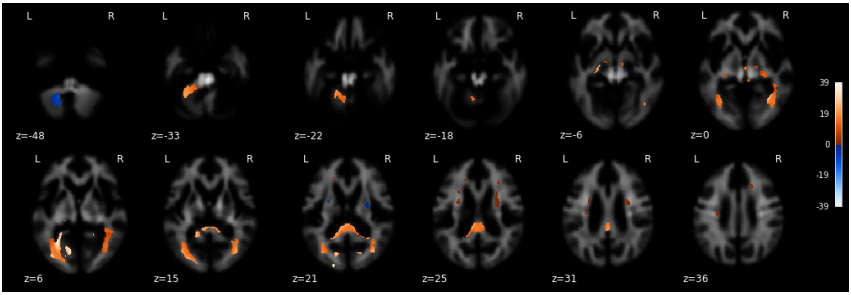


**Figure 11:** Regional white matter differences between CB and SC. Positive values (warm colors) show the regions with atrophy in CB, negative values (cold colors) show the regions with atrophy in SC ($p<0.05$, corrected for multiple comparisons).

| | Tract | Overlap (%) |
|---|---|---|
| **CB>SC** | Pons right | 0.24 |
| | Corticospinal right | 0.17 |
| | Frontostriatal right | 0.12 |
| | Frontoaslant right | 0.08 |
| | Frontal superior longitudinal right | 0.07 |
| | Anterior thalamic projections right | 0.06 |
| | Optic radiations left | 0.03 |
| | Superior longitudinal I left | 0.01 |
| | Corpus callosum | 0.009 |
| | Frontostriatal left | 0.007 |
| | Inferior longitudinal left | 0.002 |
| **SC>CB** | Optic radiations left | 19.44 |
| | Optic radiations right | 15.58 |
| | Inferior longitudinal left | 5.30 |
| | Inferior frontooccipital left | 4.70 |
| | Inferior frontooccipital left | 4.12 |
| | Posterior cingulum left | 3.25 |
| | Inferior longitudinal right | 2.97 |
| | Corpus callosum | 1.60 |
| | Pons right | 1.01 |

**Table 4:** Decomposition of the differences in white matter tracts by Tractotron. The overlap shows the percentage overlap between the significant clusters and the given white matter tract.

| | Size (voxels) | Cluster center(X Y Z) | Atlas Region |
|---|---|---|---|
| **SC>CB** | 1550 | 1 -77 5 | Right cuneus |
| | 53 | 26 -36 1 | Right parahippocampal gyrus |
| | 44 | -26 -36 1 | Left parahippocampal gyrus |
| | 22 | 6 -14 14 | Right Thalamus (Medial Dorsal Nucleus) |
| | 21 | 22 -38 -44 | Right cerebellar Tonsil |
| | 21 | -18 -38 -43 | Left cerebellar tonsil |
| | 20 | -13 -99 22 | Left Cuneus |
| | 15 | 6 2 -15 | Right subcallosal gyrus |
| | 13 | 27 -49 7 | Right parahippocampal gyrus |
| | 9 | 19 -11 -19 | Right ventral DC |
| | 8 | -1 -16 -19 | Left thalamus |
| | 7 | -1 -9 -9 | Left thalamus |
| | 6 | 31 12 -33 | Right superior temporal gyrus |
| | 6 | -3 1 -14 | Left subcallosal gyrus |
| | 5 | 4 -9 12 | Left thalamus (medial dorsal nucleus) |
| **CB>SC** | 34 | -18 -9 -13 | Left parahippocampal gyrus |
| | 21 | 20 -8 -15 | Right parahippocampal gyrus |
| | 5 | 26 -24 -9 | Right parahippocampal gyrus |
| | 5 | -24 -23 -9 | Left parahippocampal gyrus |
| | 5 | 4 -17 -6 | Right thalamus |
| | 3 | 25 -27 -8 | Right parahippocampal gyrus |

**Table 5:** Decomposition of the positive and negative differences in gray matter intensity by Talairach-Tournoux atlas (Talairach, 1988).

### Volume alterations in the hippocampus

Even though a cortical area, the hippocampal volume has been segmented and independently evaluated, since several reports have specifically focused on assessing volumetric alterations in this brain structure sensitive to spatial processing and memory (e.g., Chebat et al., 2007; Leporé, Y. Shi, et al., 2009). Volumetric comparison of overall size, head, body, and tail of hippocampus showed that overall size, both the tails and head and body of the right hippocampus are smaller in CB compared to SC.

### Volume modifications in subcortical volumes

When assessing the subcortical structures (Table 7), congenital blindness was associated with significantly smaller volumes in the right amygdala, both the left and right thalamus, globus pallidus of blind participants. For confirmatory analysis, the data were corrected for total gray matter volume instead of parenchymal volume. The same structures were

| | Difference in cm^3 | Percent decrease | Cohen's D | P-value (corrected) |
|---|---|---|---|---|
| **Left Head** | 100.72 | 8.71 | 0.54 | >0.05 |
| **Left Body** | 143.55 | 7.56 | 0.48 | >0.05 |
| **Left Tail** | 89.16 | 10.46 | 0.58 | **<0.05** |
| **Right Head** | 106.98 | 9.23 | 0.57 | **<0.05** |
| **Right Body** | 164.2 | 8.43 | 0.61 | **<0.05** |
| **Right Tail** | 138.34 | 15.28 | 0.92 | **<0.05** |

**Table 6:** Volumetric difference in segments of hippocampus between congenital blind and sighted sample.

| | **Difference in cm^3** | **Percent decrease** | **Cohen's D** | **P-value (corrected)** |
|---|---|---|---|---|
| **Left Amygdala** | 0.11 | 9.88 | 0.43 | >0.05 |
| **Right Amygdala** | 0.20 | 18.43 | 0.69 | **<0.05** |
| **Left Caudate** | 0.21 | 6.25 | 0.43 | >0.05 |
| **Right Caudate** | 0.21 | 6.12 | 0.41 | >0.05 |
| **Left Hippocampus** | 0.33 | 9.46 | 0.62 | **<0.05** |
| **Right Hippocampus** | 0.40 | 11.33 | 0.83 | **<0.05** |
| **Left Pallidum** | 0.13 | 7.64 | 0.70 | **<0.05** |
| **Right Pallidum** | 0.13 | 7.99 | 0.70 | **<0.05** |
| **Left Putamen** | 0.30 | 6.12 | 0.50 | >0.05 |
| **Right Putamen** | 0.23 | 4.66 | 0.37 | >0.05 |
| **Left Thalamus** | 0.7 | 9.44 | 0.82 | **<0.05** |
| **Right Thalamus** | 0.67 | 9.26 | 0.82 | **<0.05** |
| **Cerebellum** | 4.76 | 3.13 | 0.31 | >0.05 |

**Table 7:** Volumetric difference in subcortical structures between congenital blind and sighted sample.

found significant after the correction.

### Changes in cortical thickness and gyrification

Cortical thickness comparison resulted in two clusters in both hemispheres (Figure 12). The first cluster, lingual gyrus and cuneus, is found to be thicker in CB. Calcarine sulcus, in the middle of this large cluster, did not show any difference. In the second cluster, the entorhinal cortex shows a thinner cortex. The within-ROI correction revealed the same pattern. On a side note, the cluster that shows no significant difference between blind and sighted groups on the calcarine sulcus becomes smaller when the FDR correction is applied, and completely disappears if there is no multiple comparison applied (online supplementary materials ). This gradual

change indicates that the thickness difference in the pericalcarine area extends to calcarine sulcus but does not completely cover the area. The ROI-based analysis (Desikan-Killiany parcellation, Desikan et al., 2006) supported these findings (Table 8). In addition to occipital and entorhinal cortices, this analysis introduced two regions; left middle temporal and left lateral occipital cortices. These two regions did not survive the permutation threshold in the whole-brain analysis but could be seen in the FDR corrected results (Figure 39 ). ROI results on cortex and cortical thickness analyses identify the same regions: occipital and entorhinal cortices. Occipital cortex has smaller volume but thicker in CB, whereas the entorhinal cortex has larger volume but thinner. In general, entorhinal cortices and temporal poles are the thickest regions with the highest variability (Figure 13). However, the inter-individual variability in these regions are not likely a confound for our analysis because they effect both CB and SC groups.

The results of the functional parcellation, HCP-MM1 atlas, indicated the CB has thicker cortex in V1, V2, and V3 of both hemispheres, and left parieto-occipital sulcus, wheras thinner cortex in left perirhinal entorhinal cortex (Table 9). These results are consistent with the results of the whole-brain and the previous ROI analyses, and show that the cortical difference are unique to early visual areas. Percent thickness change among the visual areas show the same pattern: the difference between CB and SC is the highest in the primary visual areas and decreases in the higher visual areas (Figure 14). Lastly, the difference in V1 being lower than the difference in V2 is consistent with the whole-brain analysis, considering the area that show no difference on the calcarine sulcus.

In a subsequent comparison of cortical thickness between CB and SC, mean thickness values derived from 68 ROIs of Desikan Killiany atlas were calculated. Pearson correlation between each region was calculated. This step created a structural connectivity matrix for each group. Difference in the connectivity strength between groups for each node of the matrix was calculated. Significance testing of the difference was completed with the permutation procedure explained in section 3.1.3. The results showed that none of the ROI pairs have different levels of corre-

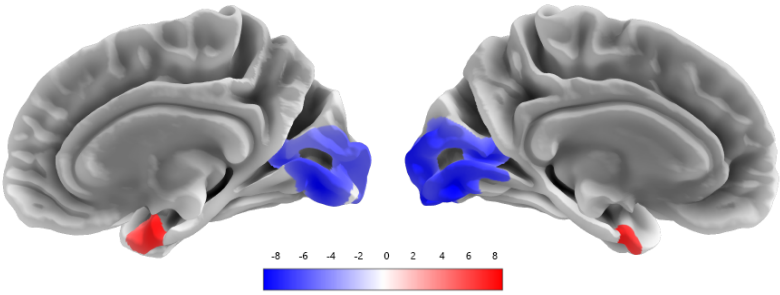


**Figure 12:** Percent cortical thickness difference between CB and SC. Positive values (warm colors) show thinner cortex in SC, negative values (cold colors) show thicker cortex in CB ($p<0.05$, corrected for multiple comparisons)

| ROI | Percent Change |
|---|---|
| Left Cuneus | 4.76 |
| Right Cuneus | 3.88 |
| Left Entorhinal | -5.54 |
| Right Entorhinal | -5.95 |
| Left Lateraloccipital | 2.3 |
| Right Lingual | 4.82 |
| Left Lingual | 3.91 |
| Left Middletemporal | -2.47 |
| Left Pericalcarine | 6.09 |
| Right Pericalcarine | 5.53 |
| Left Temporal Pole | -4.45 |
| Right Temporal Pole | -5.6 |

**Table 8:** Percent thickness difference in the significant ROIs (ROIs derived from Desikan-Killany atlas). Positive values show thickness increase in CB, negative values show thickness increase in SC ($p<0.05$, corrected for multiple comparisons).

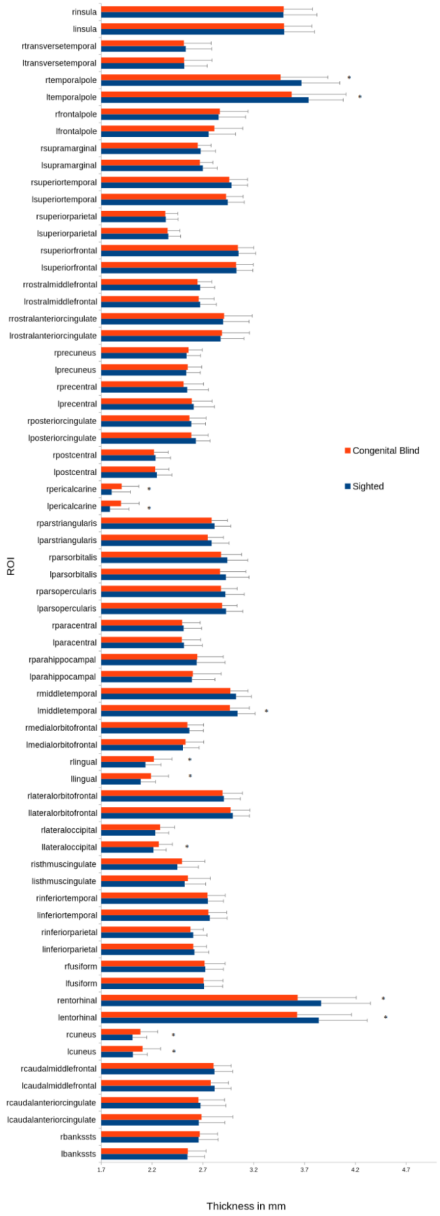


**Figure 13:** Mean thickness of the ROIs across whole brain for both blind and sighted groups. Error bars show the standard deviation of the mean. Asterisk marks the significant differences at $p<0.05$, corrected for multiple comparisons.

| ROI | Percent Change |
|---|---|
| V1 Left | 5.98 |
| V1 Right | 5.18 |
| V2 Left | 6.89 |
| V2 Right | 5.67 |
| V3 Left | 3.03 |
| V3 Right | 3.05 |
| Left Parieto-Occipital | 3.76 |
| Left Perirhinal Entorhinal | -4.57 |

**Table 9:** Percent thickness difference in the significant ROIs (ROIs derived from HCP-MM1 atlas). Positive values show thickness increase in CB, negative values show thickness increase in SC ($p<0.05$, corrected for multiple comparisons).

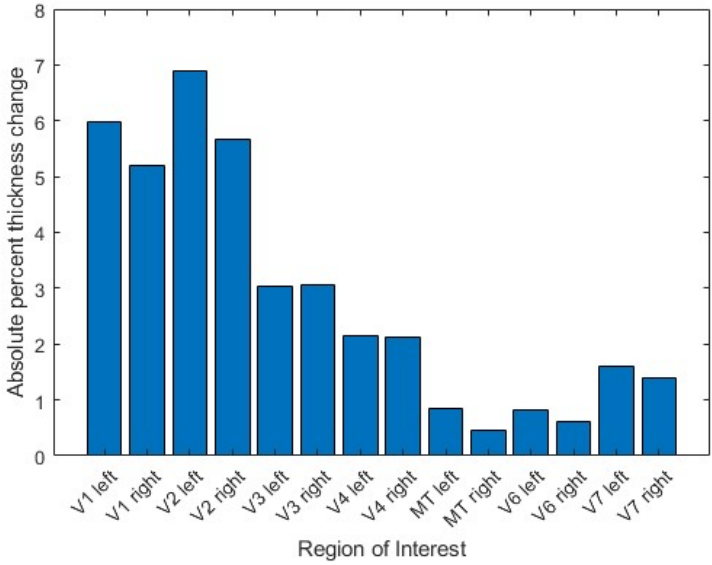


**Figure 14:** Percent cortical thickness difference between CB and SC in visual areas defined by HCP-MM1 atlas. Only the differences in V1, V2, and V3 were significant ($p<0.05$, corrected for multiple comparisons). It can be seen that the difference decreases in the higher visual areas.

lation between groups.

To understand the effect of sample size on the results, the thickness comparison on the whole-brain level was repeated with random subsamples of 17 participants for each group 100 times. Apart from the occipital and entorhinal cortices that were also reported in the original analysis, areas on sensorymotor cortices, middle frontal gyrus, middle cingulate gyrus were identified. The results convey that, even with our strict threshold, if we had a smaller sample size, it was likely (around 10%) to find one of the areas that are shown in the map significant. On the other hand, the lingual gyrus, the most stable area, was found to be significant 33 times out of 100, implying that we could miss it in our results if we had a small dataset (Figure 15).

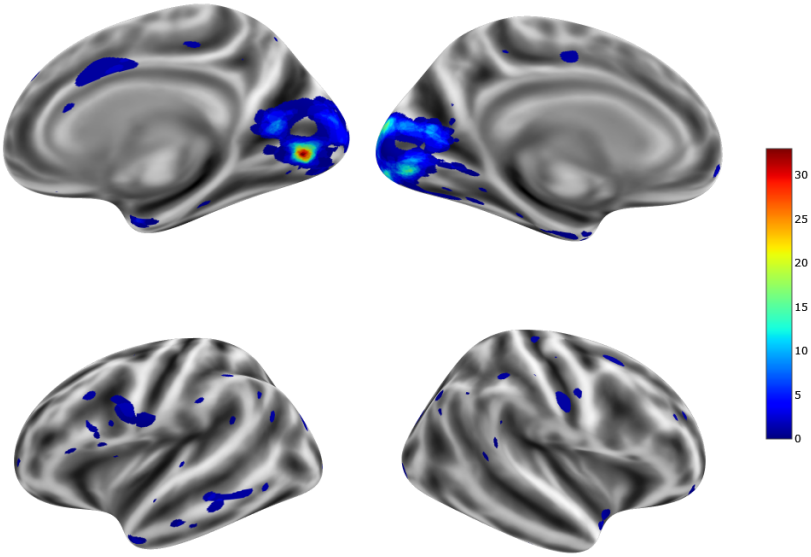


**Figure 15:** Regions identified by comparisons between smaller subsamples. Warmer colors mark the areas that are found significant more times. Even with small sample sizes, the occipital cortex was the most consistent finding.

Analysis of the last surface-based metric, gyrification index, showed

that lingual, cuneus, middle temporal, inferior temporal, medial orbitofrontal and postcentral gyri are less folded in blind group (Figure 16, table). Precuneus and lingual gyrus coincide with regions identified in the analysis in the analysis performed to compare cortical thickness between CB and SC.

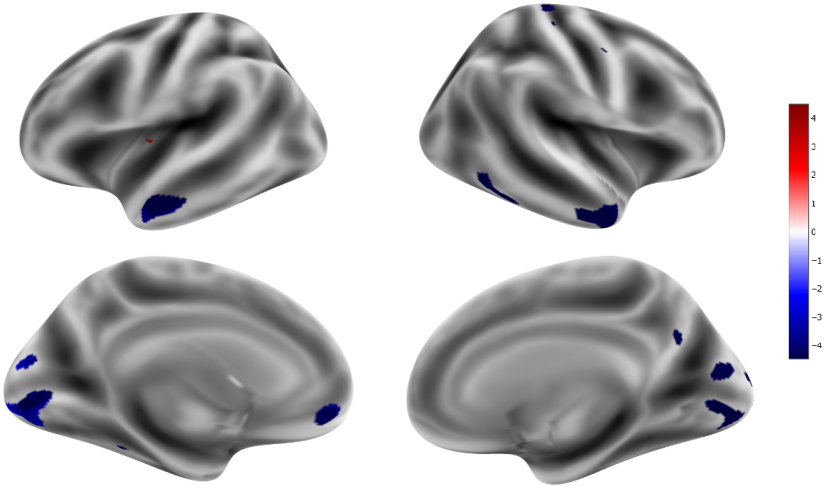


**Figure 16:** Percent gyrification difference between CB and SC. Negative values show more gyrification in CB ($p<0.05$, corrected for multiple comparisons).

### Age related effects

Main linear effects of age were observed for all cortical and subcortical volumes, but no differences in age-related effects were found between the two experimental groups after the permutation correction, consistently with several previous findings suggesting a not significant impact of aging on structural differences (e.g., Pan et al., 2007; H. J. Park et al., 2009). After FDR correction, only in the gyrification index, a small region on the pars triangularis and inferior temporal gyrus were identified (Appendix).

| | Difference in cm^3 | Percent decrease | Cohen's d | P-value (corrected) |
|---|---|---|---|---|
| **Parenchymal** | 58.25 | 5.02 | 0.52 | **<0.05** |
| **Gray Matter** | 20.12 | 3.32 | 0.28 | >0.05 |
| **White Matter** | 38.12 | 6.89 | 0.54 | **<0.05** |

**Table 10:** Difference between parenchyma, GM, and WM volumes between premature born blind sample and blind sample born in term.

### 3.2.2 Within-blind Group Comparisons in Congenitally Blind Group

*Volumetric Comparison*

Parenchymal and white matter volumes resulted to be significantly decreased in RoP after the correction of the individual analyses. The other variables did not result in a significant corrected F-score or p-value for any brain structure. The rest of the tests (other causes, braille, RLP, interaction between braille or RLP with RoP, interaction between age and RoP) among all subcortical structures or significant ones only, corrected with permutation or FDR, did not result in any significant difference.

***VBM***

VBM comparison between RoP and other causes of blindness revealed smaller tissue intensity in the anterior middle temporal gyrus for both tissues when corrected in the whole brain (Figures 17 and 18).

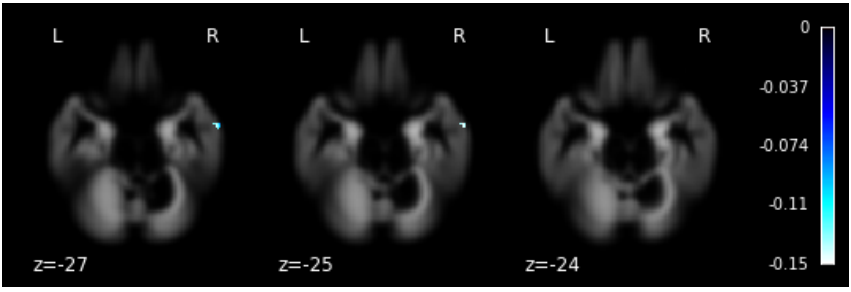


**Figure 17:** Regional grey matter differences between CB and AN-CB. Negative values (cold colors) show the regions with atrophy in AN-CB ($p<0.05$, corrected for multiple comparisons).

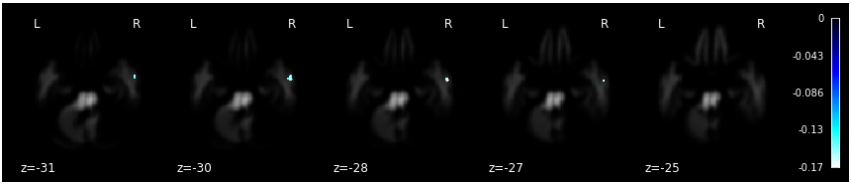


**Figure 18:** Regional white matter differences between CB and AN-CB. Negative values (cold colors) show the regions with atrophy in AN-CB ($p<0.05$, corrected for multiple comparisons).

Similar to the volumetric comparisons, VBM comparison did not indicate any significant differences in the main effect of other causes of blindness (causes related to retinal waves, eye or optic pathway), the main effect of Braille reading, or the main effect of residual light perception. In addition, the interaction between RoP and Braille reading, RLP, age, and interaction between age and Braille, RLP groups were tested. These comparisons are corrected separately both in the whole brain and within the region found in the SC-CB comparison.

***Cortical Thickness***

After multiple comparison correction within the ROI derived from the main analyses (SC-CB), RoP showed significant differences. These are both on the occipital cortex and survive both permutation and FDR corrections (Figure 19, two small regions after permutation correction and pericalcarine area after FDR). These areas indicate a thicker cortex in RoP. None of the results survived the whole-brain correction. The magnitude of difference (less than 1%), may explain why the results did not survive the strict whole-brain threshold. For comparison, the difference between SC and CB in occipital cortex changed between 4% and 8%.

Similar to the results of the other metrics, RLP, Braille reading, and the other causes of blindness did not show any significant results, when corrected at a whole brain or within the significant cluster derived from the main comparison. Additionally, the interaction between RoP, age, Braille reading, and RLP did not return any significant results as well.

The main comparison (SC-CB) was repeated after removing the RoP subjects and their sighted controls from the sample (Figure 20). The re-

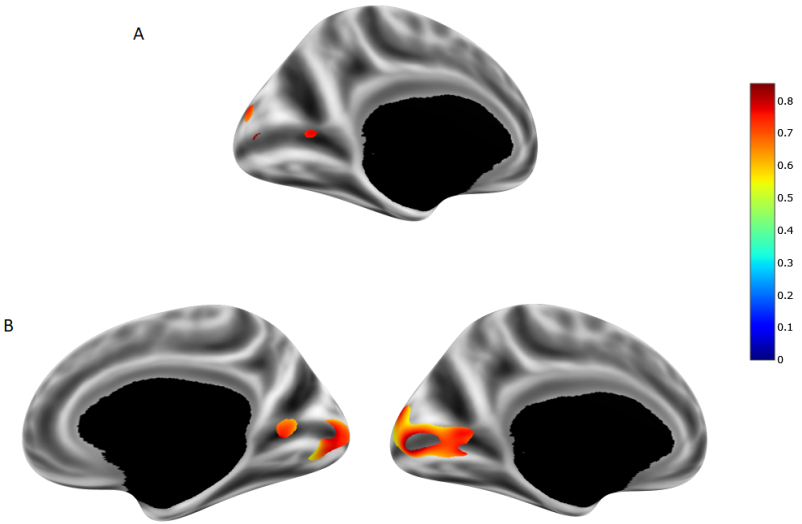


**Figure 19:** Percent thickness change between premature blind sample and blind sample born at term; within the significant cluster aqcuired from the congenital blind-sighted comparison. (A) Results corrected via permutation. (B) Results corrected via FDR. Marked areas show a thicker cortex in premature blind sample.

sults show that CB, without RoP, shows a similar pattern of differences to the previous analysis but at a lower significance. The difference in the cuneus and the calcarine sulcus was almost completely gone.

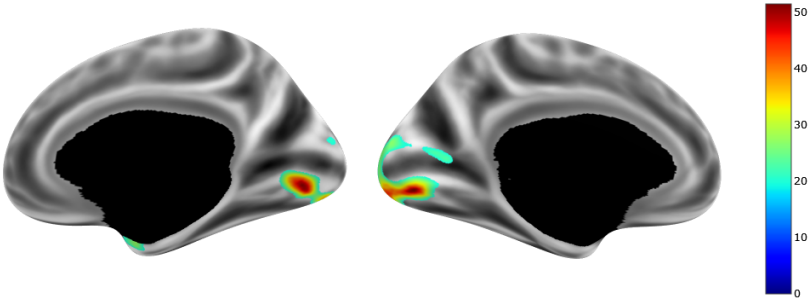


**Figure 20:** Sighted-congenital blind group comparison after removing premature blind sample and their sighted controls. The area is similar to the result of the SC-CB comparison, but it is smaller.

***Gyrification***

RoP subjects were also different from the rest of the CB individuals in terms of gyrification (Figure 21). Their right lingual gyrus, left anterior middle and superior temporal gyrus, and right posterior inferior temporal gyrus was more gyrified than the rest of the blind subjects when corrected in the whole brain. When corrected in the significant cluster found in the main comparison (SC-CB), the results slightly change but reflect the same pattern (Figure 22). Both results are corrected with permutation correction.

Lastly, RLP, Braille reading, and the other causes of blindness did not show significant results, whether corrected in the whole brain or within the significant cluster derived from the main comparison. Additionally, the interaction between RoP, age, Braille reading, and RLP did not return any significant results as well.

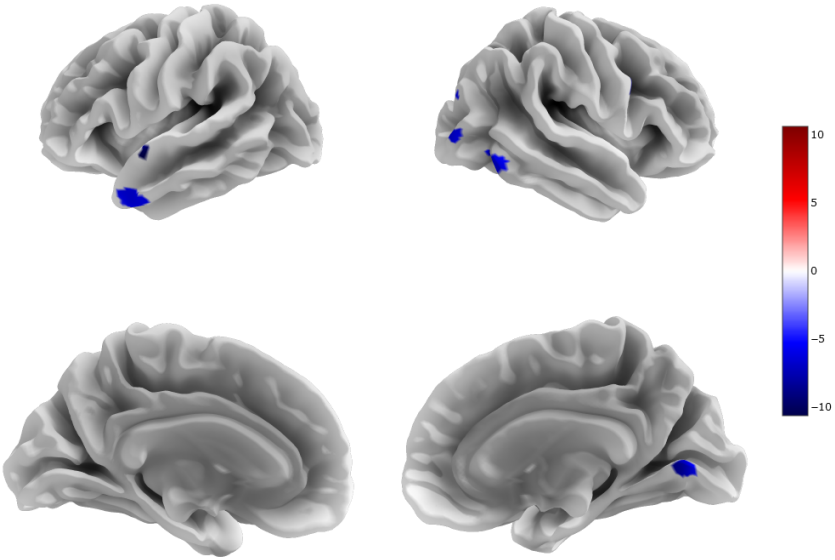


**Figure 21:** Gyrification difference between premature blind sample and blind sample born at term in the whole-brain. Marked areas show increased thickness in premature blind sample. ($p<0.05$, corrected for multiple comparisons).

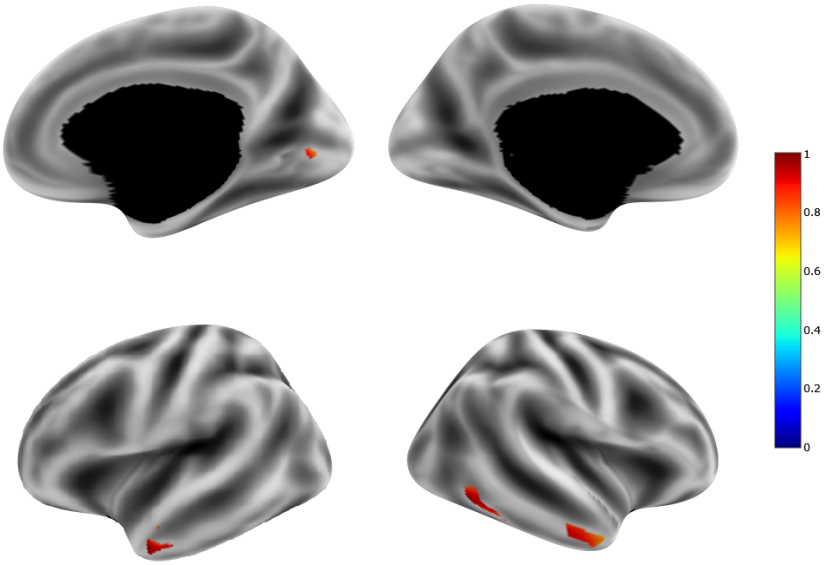


**Figure 22:** Percent gyrification difference between RoP-NRoP within the significant cluster resulted from the SC-CB comparison. The marked areas show increased gyrification in premature blind subjects ($p<0.05$, corrected for multiple comparisons).

## 3.3 Summary of the Findings/Discussion

In this chapter, structural properties of the brain (thickness, gyrification, intensity, overall volume) were compared between blind subjects who lost vision perinatally and sighted controls. The aim was to identify the plastic changes of brain structures, when visual input lacks since birth, and the contribution of the residual effects (such as causes of blindness, residual light perception, and Braille literacy) to these changes.

Overall, lack of vision from birth is associated with alteration in the visual pathway. The cuneus and lingual gyrus of the CB were thicker, smaller and had a higher curvature. This pattern is the most common among the findings in the literature (Noppeney et al., 2005; Pan et al., 2007; Ptito, F. C. G. Schneider, et al., 2008) and supports the experience-dependent plasticity of the visual cortex (Jiang et al., 2009; H. J. Park et al., 2009). As discussed before (Rice and Jr, 2000; Peter R. Huttenlocher, 1990), typical development of the visual cortex starts with a rapid expansion up to 2-3 years of postnatal age and is followed by a synaptic pruning that stabilizes the volume of the visual cortex by removing the unwanted synapses. This work, along with the previous ones, shows that the visual cortex preserves its original postnatal shape (after cortical expansion) in case of lack of vision from birth. Therefore, it can be said that the synaptic pruning - happening within two years of age - is experience-dependent. According to results from sight recovery studies (Aguirre et al., 2016; Feng et al., 2021; Hölig et al., 2022), restored vision does not initialize the pruning process later in life. The thickness and the surface area of the occipital cortex of the sight-recovered subjects was larger than the sighted ones, even if sight is restored in the first years of life. These findings imply that if experience-dependent brain development of visual cortex during a sensitive period is interrupted,the atrophy is not reverted later in the life in case of exposure to vision.

Interestingly, we did not observe any thickness difference on perifoveal area. While early visual areas are found to be thicker in CB, a region on bilateral perifoveal area are the same between two groups. This finding is similar to the results from previous studies (H. J. Park et al.,

2009; Bridge, Cowey, et al., 2009; Anurova, Renier, et al., 2015), but not all. It must be noted that none of the previous studies found such a large area of effect that covers both lingual gyrus and cuneus. Although it is not possible to directly confirm it in this study, in terms of retinotopy, the region that shows no difference between groups corresponds to peripheral vision that comes right after the central vision/fovea (Weaver and Stevens, 2007; Ferreira et al., 2017). There is one study that examined the thickness of V1 in detail. Burge et al. (2016) divided V1 from "most central vision" to "most peripheral" vision. Thickness of 9 ROIs from this dissemination were compared between sighted controls and patients with macular degeneration, who do not have central vision. It was shown that mid-peripheral regions, corresponding to the areas that did not show any difference between SC and CB, were thicker in patients with macular degeneration. However, this difference was observable in the pericalcarine gyrus, banks of calcarine sulcus, but not in the depth of calcarine sulcus, which coincides with our results. Although the sample suffer from central vision loss only, not total blindness, partial visual impairment show similar atrophy patterns with total blindness (Ohno et al., 2015; Machado et al., 2017; Mendola et al., 2005). Results from Burge et al. (2016) show that thickness within V1 can fluctuate and show within-regional differences. The same analysis can be repeated for total blindness in order to see the regional changes in V1 in case of blindness.

Structural changes in visual cortex of CB is not associated with the changes in the other regions of brain. This finding contradicts with results of a very similar study (Voss and Zatorre, 2015), where the authors reported that cuneus of CB has stronger anatomical connectivity with inferior occipital gyrus, and weaker connectivity with frontal and supplementary eye fields, inferior parietal lobule, and precentral gyrus. As much as the inconsistency in the results can be attributed the factors identifed in Chapter 2 (variety in the sample size and characteristics such as blindness onset and pre-/ post-natal factors), in the specific case of connectivity, the discrepancy can be related to the individual variation. Sen et al. (2022) showed that the resting-state functional connectivity patterns of CB has more variability compared to SC, especially for the

visual cortex. If this heterogenity in functional connectivity also persists in structural connectivity, then it is natural to see no differences groups considering the large sample size.

Another common finding across the studies is the volume loss in optic radiation. Current work successfully replicated this result. In the VBM comparison, both right and left optic radiation had smaller volumes. White matter VBM is mainly associated with radial diffusivity, a metric that shows altered myelination (Belke et al., 2015).

These findings indicate that lack of vision from birth affects the structure of the visual pathway in a rather negative way. In case of lack of a sensory modality, brain regions mainly related to vision do not develop as in the typical brain. Structural plasticity does not compensate for those regions in another way, even though the visual cortex start responding to other modality inputs (i.e. so called "cross-modal plasticity"). The source of this change in the function may be the corticocortical connections rather than thalamocortical. This is because according to our results, strong atrophy found on the connections between thalamus and visual cortex, but the structural relationship between cortical regions were intact. Along with the LGN, the nuclei of the thalamus that project to temporal, frontal, and somatosensory cortices were atrophied (Cecchetti et al., 2016; N. H. Reislev et al., 2017), and the blind group did not show any stronger thalamocortical connections compared to the sighted group. Therefore, non-visual information must be delivered to the visual cortex via corticocortical connections. Klinge, Eippert, et al. (2010), for example, found stronger corticocortical functional relationship between primary visual and auditory cortices of blind people, but similar thalamocortical connections. Their reference point in thalamus was MGN, to assess whether MGN relays the auditory information to the visual cortex. Even though this study did not find proof for thalamocrtical pathway to relay cross-modal information on visual cortex, animal studies showed that the thalamus could stimulate the visual cortex through MGN (Sur, Garraghty, and Roe, 1988; Frost et al., 2000). This can be another explanation for non-visual stimuli in the visual cortex. However, no study on humans confirms this process.

Apart from the visual pathway, congenital blindness is also associated with regions that are not involved in the main visual pathway but receive visual feedback. For example, for the first time, this work shows that visual deprivation is related to smaller right amygdala volume. However, the function of the amygdala in blind individuals was explored previously. In their study, Klinge, Röder, and Büchel (2010) showed that CB have stronger amygdala activity in response to negative emotional stimuli, but not to positive stimuli, compared to sighted individuals. This activation was significant for the right amygdala only, implying that there may be a relationship between the excess in the activation and the loss in size. According to visual fear processing hypotheses, the amygdala takes direct input from superior colliculi via pulvinar. This connection was also shown via tract-tracing studies (Silverstein and Ingvar, 2015) for a review on visual fear processing). Therefore, lack of visual input for emotion processing may play a role in the amygdala's size. In terms of lateralization, the right amygdala gives greater response to fear and gaze shift than the left amygdala (Hardee, J. C. Thompson, and Puce, 2008). This finding may be another indicator of the connection between the function and the decrease in the volume.

Globus pallidus is among the structures that showed volume decrease in congenital blind individuals. Like the amygdala, there is no previous research exploring the structure or function of the globus pallidus in blind. Being associated with voluntary movement control (Klaassen et al., 2021), it can be hypothesized that visual cues are essential for developing pallidum and voluntary movement control. This hypothesis is supported by the fact that blind people have poorer posture control than sighted (Perera et al., 2015). Without vision, it may be more challenging to control the movements, and the size of the pallidum must be related to this challenge.

The entorhinal cortex, which is mainly associated with spatial memory, showed cortical thinning in congenital blinds. This is a finding that has been previously shown in some of the cortical thickness studies (H. J. Park et al., 2009; Voss and Zatorre, 2012; Q. Li et al., 2017). CB have superior way-finding skills than sighted (Fortin et al., 2008). This increase in

the performance may be related to the thinning, as cortical thinning is associated with better performance in some tasks (Verbal IQ - Burgaleta et al., 2014; Working memory - Kharitonova et al., 2013). Another possible explanation for cortical thinning is older age (Salat et al., 2004). However, there was no interaction between age and the cortical thickness between the groups. The general trend of thickness decay with older age was the same in both CB and SC. Therefore, the thinning in entorhinal cortices is more likely to be related to its function. The high individual variability in the anatomical features of this region was also reported before (Goncharova et al., 2001; Heinsen et al., 1996). Therefore, our results do not reflect a methodological noise, rather they present a replication of the previous findings.

Both hippocampi were smaller in CB. Following the previous discussion in the literature, we segmented the hippocampus in the anterior-posterior direction and compared the head, tail, and body segments of blind subjects with sighted. Posterior parts of both hippocampi and the body and tail of the right hippocampus were the smaller regions. The left hippocampus's head and body did not result in significant differences. It can be speculated that the posterior hippocampus is related to visual memory since it is consistently smaller in CB. The London taxi driver study (E. A. Maguire, Woollett, and Spiers, 2006) can be shown as supporting evidence for this hypothesis. In that study, it was shown that the posterior hippocampus of the taxi drivers is larger than controls. Since our study shows the opposite (smaller posterior hippocampus vs. controls), it can be argued that visuo-spatial memory is associated with the size of the posterior hippocampus.

The anterior part of hippocampus, likewise, suffers from volume loss. This part directly takes input from the entorhinal cortex and is often associated with spatial memory (Strange et al., 2014). Thinning on the entorhinal cortex may be associated with the smaller head of the hippocampus. Additionally, the reason why the right hippocampus suffers more from the volume loss can be the lateralization of the function. The right hippocampus responds to allocentric representation rather than egocentric (Iglói et al., 2010). Previous research shows that EB/CB utilize ego-

centric navigation strategies, and visual experience enhances allocentric navigation (Iglói et al., 2010; Iachini, Ruggiero, and Ruotolo, 2014). Therefore, it can be argued that the the volume difference in right hippocampus related to this lateralization of function.

In this work, for the first time, the gyrification difference between CB and SC was tested. The visual cortex, along with the anterior medial and inferior temporal gyrus, were more gyrified. The difference in the visual cortex can be attributed to the disruption of the typical development due to the lack of visual input. The anterior middle temporal gyrus, on the other hand, is mostly associated with semantic tasks (Davey et al., 2016; Visser et al., 2012). However, there is another function related to the anterior middle temporal gyrus (aMTG). Some studies report that aMTG plays a role in recognizing familiar faces (Borghesani et al., 2019; Gobbini and Haxby, 2007). In this context, the excess of gyrification can be justified since there is no visual input to feed this region.

From a general perspective, it can be seen that some cortical or subcortical regions that take part in visual processing or receive visual feedback are atrophied (e.g., hippocampus, entorhinal, anterior medial temporal), but some are not (e.g., parahippocampal gyrus, rest of the higher-order visual pathways -dorsal and ventral-). It can be inferred that those intact regions do not suffer from a lack of vision from birth. What keeps them intact may be their multi (or supra) modality. They may not rely on vision as much as the atrophied regions to follow typical development.

There has been an ongoing discussion on how premature birth affects the research on blindness. The number of RoP included in the samples of the previous research is relatively high, as in our dataset. Previous evidence shows that premature birth affects brain structure and this effect is mainly seen in the white matter and the subcortical structures (Boardman et al., 2006; B. S. Peterson, Vohr, Staib, Cannistraci, A. Dolberg, et al., 2000). To differentiate the general effect of premature birth from the effect of blindness on the brain structure, blind subjects who lost their sight due to premature birth were treated differently from the rest of the blind subjects. Our analyses show that RoP, compared to the rest of the blind subjects, have smaller total white matter volume, smaller and more

gyrified anterior middle gyrus, thicker and more gyrified visual cortex. In order to show that the effects on these regions are not due to RoP only, the comparison between blind and sighted subjects was repeated after removing the RoP from the sample. The result was the same, except it was weaker. Therefore, it can be argued that the regions mentioned above are more susceptible to atrophy in case of blindness acquired due to preterm birth. In their study, Wan et al. (2013), states that after removing the RoP subjects from the blind sample, the volume decreases found on middle temporal gyri disappear as in our study. However, they add that volume decreases in frontal gyri, caudate nucleus, and thalamus disappear. These regions are not found to be related to RoP in our study. Ptito, F. C. G. Schneider, et al. (2008), on the other hand, showed that RoP in their sample do not affect the whole-brain comparison. They are only associated with smaller gray and white matter volume than other blind subjects. Our results confirm them and add that RoP subjects indeed affect the results.

Considering that the thicker visual cortex is related to the interrupted synaptic pruning, the thicker and more gyrified visual cortex of RoP subjects imply that the synaptogenesis produces a larger mass in case of premature birth. Even though synaptogenesis starts in the fetus (Fox, Leavitt, and Warhol, 1999), the visual cortex expands dramatically only after birth (Peter R Huttenlocher and Dabholkar, 1997). Therefore, the thickness and gyrification difference must be due to the overexpansion of the visual cortex after premature birth. The analysis of the RoP sample can be enhanced in the future if the gestational age of the subjects is known and if a control sample born prematurely but not blind is available.

The rest of the causes of blindness were categorized according to the following features: causes related to lack of perinatal waves (anophthalmia/microphthalmia), causes related to eye issues (glaucoma, cataracts), causes related to retinal or optic-pathway issues (optic nerve atrophy, Leber's amaurosis, retinoblastoma, retinal dysplasia). These causes do not differ in terms of the morphological changes they cause. They can be investigated under the general term of "congenital blindness." The location of the atrophy (eye or optic nerve) or whether the subject received

spontaneous prenatal retinal activity does not affect the brain structure per se. Even though prenatal spontaneous retinal activity is known to contribute to the development system (Butts and Rokhsar, 2001), it may not affect the brain morphometry macro level, but only on the cellular level. This lack of difference is in line with previous studies, which the surface area of V1 (Andelin et al., 2019) and splenium of corpus callosum (Bock et al., 2013) are not affected by the lack of prenatal waves, compared to early acquired blindness.

Another topic that has been discussed in blindness research is residual light perception. Previously, it had been shown that white matter integrity is more preserved in the blind individuals that can perceive residual light (Shimony et al., 2006; Zhou et al., 2019). In the current study, RLP was not associated with changes in brain structure. One explanation for the lack of difference can be that the studies that found a difference caused by RLP were DTI studies, a more sensitive method for assessing white matter integrity. Likewise, Pan et al. (2007), using only the VBM metric derived from T1 MRI scans, did not find any effect. Another alternative can be that the lack of difference reflects the truth, and the partial visual loss studies support this explanation. Individuals that are partly blind still show the same patterns of atrophy in the brain (Mendola et al., 2005; Ohno et al., 2015; Machado et al., 2017). Therefore, the visual pathway reshapes itself in the same way regardless of the residual light perception.

Unlike Matuszewski et al. (2021), and Bola et al. (2017), who found changes in white matter (measured via FA) in sighted after Braille training, our study shows that Braille literacy is not related to any change in the brain structure. To our knowledge, this work is the first one to assess the structural correlates of Braille reading in blind individuals. The lack of effect indicates that functional plasticity related to the Braille reading (Sadato et al., 1998; Gizewski, Timmann, and Forsting, 2004) cannot be attributed to any structural reorganization in the brain.

In conclusion, the structural differences in the brain of the CB reflect an interrupted neurodevelopment of the visual system, rather than complete reshaping. The visual cortex and optic radiations give a snapshot

of their version around the time of birth, and their development is interrupted due to the lack of external input: An intense synaptic density in the occipital cortex that reach its peak between 8 and 24 postnatal months (Peter R. Huttenlocher, 1990), blood and glucose consumption level is similar to the same period (Chugani, Phelps, and Mazziotta, 1987), white matter connections are present but their volume is yet to be myelinated and to increase their volume to adult level (Fine and J.-M. Park, 2018).

# Chapter 4

# Structural Changes in the Late Blind Brain

## 4.1 Methods

### 4.1.1 Data Collection and Contributing Sites

The data collection procedure was described in section 3.1. Among the 10 research groups that contributed to the project, five included 3D structural T1 MRI scans of the late blind individuals (blindness onset - BO $>$ 0 year of age) and their sighted controls. Although non-congenital blind subjects are categorized as "early blind, adolescent blind, late blind depending on their blindness onset in some studies, we wanted to use "late blindness" term for all subjects whose blindness onset is not 0. This is because in the following analysis, we make the statistical analyses for identifying the effect of blindness onset and time spent as blind, therefore we wanted to keep our "noncongenital blind" sample homogenous. Those research groups are Université Catholique de Louvain -Belgium, Massachusetts Eye and Ear Infirmary, Harvard Medical School - the USA, IMT School for Advanced Studies Lucca and University of Turin – Italy, Brainnetome Center and Beijing Normal University – China. In total, 153 late blind participants (LB) and 226 sighted controls (SC) were available

in the dataset. Detailed information on the samples can be seen in online supplementary table.

Across different laboratories, LB MRI data were acquired using 1.5, 3T, or 4T scanners, T1/3D-TFE/MPRAGE sequences, 3/4 B0 strength, TR changing between 2000-8100, TE changing between 2.19-4.38

### 4.1.2 MRI dataset and Samples

The research groups gathered 153 LB and their SC T1 images for the study. After data processing and a quality check procedure (see below), 115 LB (BO>0 years of age), 32.55 ± 9.91years old, 34 female, 1 hermaphrodite) and 115 SC (30.51 ± 9.1 years old, 39 female) were used to create two samples that were balanced in terms of age, gender and scanning site (online supplementary material). Apart from 5 left-handed (2 LB), one ambidextrous LB, and 11 not reported, all participants were right-handed. Mean BO was 13.6 ± 9.2, and mean time spent as blind (TSAB) was 18.96 ± 10.87. All sighted and blind subjects received a medical interview or examination to exclude any disorder affecting brain function and metabolism other than blindness in the blind group. All participants provided written consent before the MRI examinations according to the approved protocols of each contributing site. 36 of the SC were also selected for the SC group of the congenital blind analyses. This selection procedure was blind to the ID of the participant. The only aim was to create a balanced age, gender, and site distribution between blind and sighted groups. Since the total SC sample is almost twice as big as SC and LB groups separately, some SC happened to be selected for both samples.

### 4.1.3 Data Preprocessing and Hypothesis Testing

The same data preprocessing and hypothesis testing procedures explained in chapter 3.1 were used.

### 4.1.4 Comparisons Between Late Blind and Sighted Group

Procedures that are explained in chapter 3.1 were followed. A volumetric comparison of total tissue and subcortical volumes, VBM, cortical thickness, and gyrification metrics were used to compare the LB and SC groups.

### 4.1.5 Within-blind Group Comparisons in Late Blind Group

Volumetric comparison of total tissue and subcortical volumes, VBM, cortical thickness, and gyrification metrics were selected to make further investigations within the LB group. After cleaning the data from age, gender, site, and parenchymal volume (not included in the surface-based analyses), residuals of the blind sample were used in additional within-group comparisons to investigate the extent to which distinct causes of blindness, residual light perception (RLP), common postnatal experiences (i.e., Braille reading), or time spent as blind might have influenced the main effect of the congenital lack of vision on morphometric measures.

To explain the contribution of the selected variables on the differences between groups, the LB sample was further examined by considering potentially important factors. These factors are causes of blindness, blindness onset and time spent as blind, residual light perception, and Braille literacy.

Categorization of the causes of the blindness was done as described in Chapter 3. Three subjects were labeled with the causes of blindness related to lack of perinatal waves, 38 subjects were labeled with causes related to eye issues, 58 subjects were labeled with causes related to retinal or optic pathway issues. Since the number of subjects in the first group was too small, they were removed from the further analyses, and only the second and third groups were compared.

Similar to the uneven distribution of the Braille literacy within the CB sample, the number of Braille literate LB (n=95, 94 with a known onset, mean age of onset= 15.7 ± 7.98) was much higher than the number of Braille illiterate (n=17). 16 Braille readers out of 95 learned the alphabet before their BO. Average Braille literate years before losing sight: 8.26

± 10.09. 5 of them had retinopathy, 3 retinitis pigmentosa, 3 cataracts, 2 glaucoma, 1 optic nerve atrophy/dystrophy/damage, 1 eyeball dysplasia. Braille onset of one participant was coded as bigger than their age at scan time. That participant is removed from further analyses. In addition, two subjects marked as "not Braille literate anymore" were excluded because of possible confoundings. At the end, LB were divided into three groups as Braille illiterate (n=17), Braille literate before losing sight (n=15), and Braille literate after losing sight (n=76). The difference between the three groups was tested with a one-way ANOVA.

The number of LB who can perceive residual light perception (n=56) and who cannot (n=58) was close to each other. These two groups were directly compared with a linear regression model where the regressor was a categorical variable indicating the group (RLP or not RLP).

One of the main interests of this thesis is the effect of blindness onset (BO) and time spent as blind (TSAB) on brain anatomy. Having the same BO, atrophy in the subjects with different TSAB can have different magnitudes. Likewise, the brains of two subjects with the same TSAB can be different because of earlier/later BO. Clarifying the effect of these two parameters will help us see the critical point of neurodevelopment and the regular progress of plasticity.

Naturally, BO and TSAB are highly correlated (spearman rho=-0.63, $p<0.05$), and it is impossible to include them in a classic linear regression model due to collinearity. Therefore, the two parameters are reduced to one by using the following formula: *(BO-TSAB)/Age*

This formula (from now on will be referred to as blindness index ( BI) gives a value between -1 and 1. Lower BI indicates later BO and shorter TSAB, and higher BI indicates earlier BO and longer TSAB (Figure 23). This measure is not correlated with age (Pearson's r=0.09, p=0.28, Spearman's rho=0.14, p=0.1). The Spearman correlation between BO was 0.2 (p=0.02), and between TSAB and age was 0.52 ($p<0.01$).

After cleaning the data from age, gender, site (and parenchymal volume for volumetric and the VBM analyses), the residuals of the late blind sample were explained with BI. Subjects who learned the Braille alphabet before losing sight (n=15) were not included in this analysis. These sub-

jects may have experienced partial visual impairment long before they completely lose sight. As it was shown that partial visual impairment also affects the visual pathways (Ohno et al., 2015; Machado et al., 2017; Mendola et al., 2005), BO of those subjects may not reflect the real onset of atrophy and confound the BI analysis. After removing the subjects mentioned above, the number of participants in the sample was down to 100 from 113. This analysis aims to see if the variance in the relevant structural measure can be explained with the timing of the BO and the duration of the TSAB. Significance testing of this relationship was done via the permutation procedure explained above (to sum up: random shuffling of the BI values, repeating the analysis 10,000 times). If there is any significant relationship, a second step was applied to clarify whether it is sourced from BO or TSAB.

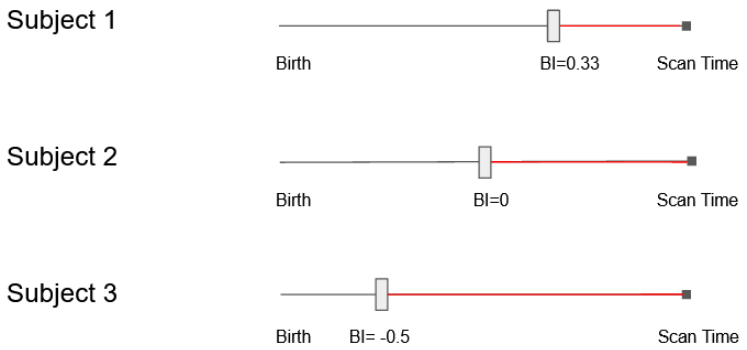


**Figure 23:** Graphical representation of the blindness index (BI). Positive BI indicates that the participant spent more than half of their lifespan as blind, indicating late blindness onset and short time spent as blind. Negative BI, on the other hand, indicates early blindness onset and long time spent as blindness.

After finding the areas related to BI, the second aim was to identify if the relationship is sourced from BO or TSAB. In order to do so, first, the contribution of each subject to the whole model was calculated via a stepwise regression model. The procedure is as follows: Mean values of

the clusters identified by the BI regression was calculated. This step was done to avoid the computational load of doing the same calculations for each vertex/voxel found. The acquired series was explained with BI as explained above. The F-score of this model was saved. Then, the same test was repeated with excluding one subject each time. The difference between the original F-score and the newly calculated one after removing a subject was calculated in each iteration. The idea was to see if there is a critical BI value where the strength of the model decreases significantly.

In addition to BI, BO, and TSAB were also used to explain the variance within the LB in separate models. This step is applied as a sanity check. In theory, both TSAB and BO should pick up similar regions with each other and BI.

Another attempt to clarify the effects of BO and TSAB was implemented via identifying subsamples whose BO or TSAB is above the critical period for GM and WM development. Participants whose BO is later than these thresholds should have had regular neurodevelopment. Therefore, the variance among them can be explained with TSAB only. Likewise, participants whose TSAB is longer than decades could be used to explore the effect of BO. Therefore, 24 subjects, whose BO is later than 19, were used to explain the variance in structural measures with TSAB. Similarly, another 24 subjects whose TSAB is longer than 27 years were used to explore the effects of BO.

## 4.2 Results

### 4.2.1 Sighted vs. Late Blind Groups

#### Demographics

There were no significant age (two-way t-test, t=1.694, p=.987, Cohen's d=.002) or gender-related ($X^2$ =0.44, p=.091) differences between groups.

#### Quantitative comparison of brain volumes

When assessing the differences in the overall brain parenchymal volume, GM and WM were significantly decreased in LB subjects compared to

| | Difference in $cm^3$ | Percent decrease | Cohen's d | P-value (corrected) |
|---|---|---|---|---|
| **Parenchymal** | 82.16 | 6.65 | 0.70 | **<0.05** |
| **Gray Matter** | 41.5 | 6.65 | 0.66 | **<0.05** |
| **White Matter** | 40.65 | 6.82 | 0.61 | **<0.05** |

**Table 11:** Volumetric difference in total volumes of the tissues between LB and SC.

| | Difference in $cm^3$ | Percent decrease | Cohen's D | P-value (corrected) |
|---|---|---|---|---|
| **Left Amygdala** | 0.05 | 4.23 | 0.22 | >0.05 |
| **Right Amygdala** | 0.15 | 12.26 | 0.59 | >0.05* |
| **Left Caudate** | 0.25 | 7.18 | 0.50 | >0.05 |
| **Right Caudate** | 0.23 | 6.62 | 0.47 | >0.05 |
| **Left Hippocampus** | 0.15 | 4.10 | 0.30 | >0.05 |
| **Right Hippocampus** | 0.22 | 5.80 | 0.45 | >0.05 |
| **Left Pallidum** | 0.16 | 9.30 | 0.84 | **<0.05*** |
| **Right Pallidum** | 0.15 | 8.76 | 0.78 | **<0.05*** |
| **Left Putamen** | 0.31 | 6.05 | 0.49 | >0.05 |
| **Right Putamen** | 0.26 | 5.09 | 0.41 | >0.05 |
| **Left Thalamus** | 0.62 | 8.05 | 0.79 | >0.05* |
| **Right Thalamus** | 0.56 | 7.41 | 0.74 | >0.05 |
| **Cerebellum** | 7.79 | 5.13 | 0.47 | >0.05 |

**Table 12:** Volumetric difference in subcortical structures between LB and SC. *: Significant when corrected with FDR.

SC (differences in $cm^3$ were 82.16±168.84, 41.5±88.87, and 40.65±94.82, respectively, Table 11). Percent volume losses related to blindness since birth ranged around 6.7% (specifically, 6.65%, Cohen's d=.70 for parenchymal volume; 6.65%, d=.66 for GM; 6.82%, d=.61 for WM).

When assessing the subcortical structures (Table 12), late blindness was associated with significantly smaller volumes in the left (0.16±0.3 $cm^3$, 9.3%, d=0.84) and right globus pallidus (0.15±0.3 $cm^3$, 8.76%, d=0.78) of the late blind participants. The left thalamus and right amygdala were also significant when corrected with FDR.

### Voxel-based Morphometry

VBM results showed a significant volume decrease in the WM of the optic radiations and the GM of the early visual cortex (Figures 25, 24). When corrected with FDR (instead of permutation correction, figures 48, 49),

the results were the same, suggesting that the rest of the brain is prone to structural plasticity changes in case of acquired blindness.

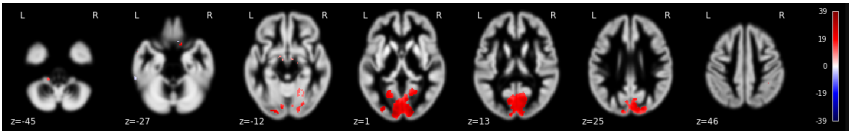


**Figure 24:** Regional grey matter differences between LB and SC. Positive values (warm colors) show the regions with atrophy in LB ($p<0.05$, corrected for multiple comparisons).

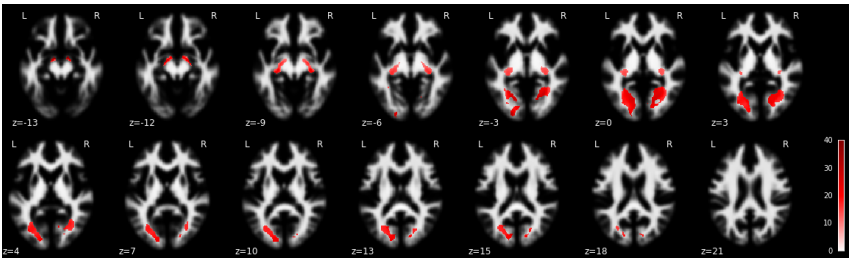


**Figure 25:** Regional white matter differences between LB and SC. Positive values (warm colors) show the regions with atrophy in LB ($p<0.05$, corrected for multiple comparisons).

### Cortical Thickness and Gyrification

Late blindness was associated with the increased thickness of the cuneus (Figure 26. Similar to VBM results, the FDR corrected results gave almost the same difference maps (Figure 50).

Gyrification showed a difference in the occipital cortex as well (Figure 27). This effect covers the lingual gyrus and right cuneus.

There was no significant interaction between sight and age in terms of any structural measure tested here. Age has the same effect on both sighted and late blind groups.

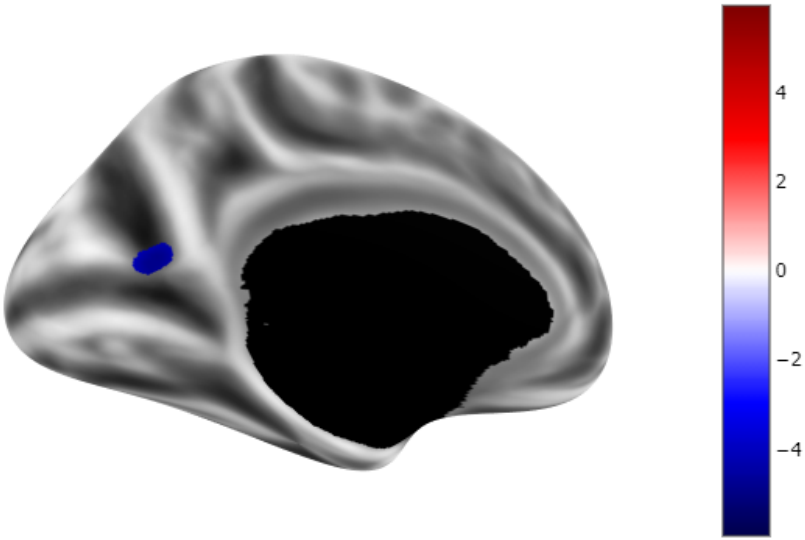


**Figure 26:** Percent cortical thickness difference between LB and SC. Negative values (cold colors) show thicker cortex in LB ($p<0.05$, corrected for multiple comparisons)

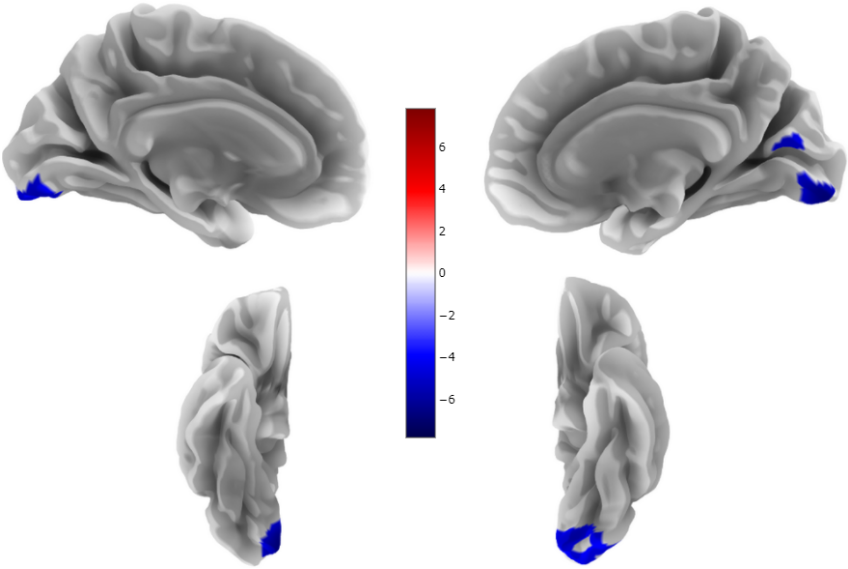


**Figure 27:** Percent gyrification difference between LB and SC. Negative values (cold colors) show increased gyrification in LB ($p<0.05$, corrected for multiple comparisons).

### 4.2.2 Within-blind Group Comparisons in Late Blind Group

BI, corrected via permutation in the whole-brain level, is related to thickness in cuneus and lingual gyrus area (Figure 28). As BI increases, thickness increases in the region revealed by BI. In other words, as BO gets earlier and TSAB gets longer, thickness increases. The stepwise regression approach was applied to the mean thickness from the area identified by BI, in order to see if there is a critical BI value after which the explanatory power of the model spikes or drops. As shown in the Figure 30, the distribution of the changes in the strength of the model is not consistent and does not give a hint for a critical value for BI, after which the strength of model drops or increases. Instead, the strength of the model changes dramatically when the participants who spent a high or low percentage of their life as blind are excluded, however, there is no indication of which side (low BI or high BI) is more dominant.

The separate models for BO and TSAB, on the other hand, show a difference in the results. When corrected within the whole brain via permutation, BO was found to be associated with an area on the lingual gyrus (Figure 33), whereas TSAB had no significant association on the brain. This difference in the results were more evident in the unthresholded maps. Correlates of TSAB was more spread and uniform, whereas correlates BO was more concentrated on the visual cortex (Figure 29). In addition, F-stat of the models was much stronger in the BO map (max. F-stat = 31.63) compared to BO map (max F-stat: 13.63). It can be said that, although they are collinear, BO is more decisive in terms of structural plasticity after visual loss, compared to TSAB. This statement can be further supported by the fact that BO related region is involved in the area that is found by the SC-CB comparison, but not SC-LB comparison (Figure 31).

The relationship between BO and the thickness was clarified in the subsequent analysis. LB group was divided into 6 based on their BO: BO$<$3 (n=13), 2$<$BO$<$7 (n=12), 6$<$BO$<$11 (n=23), 10$<$BO$<$15 (n=17), 14$<$BO$<$19 (n=25), 20$<$BO (the rest of the LB, n=10). These six groups, plus the sighted controls, were used to explain the variance in the mean thick-

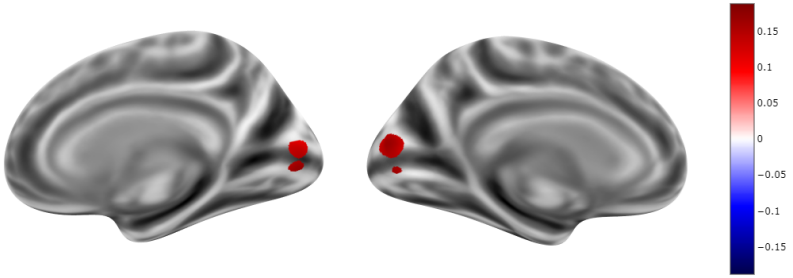


**Figure 28:** Correlates of BI with cortical thickness. Higher blindness index (meaning earlier blindness onset and longer time spent as blind)is associated with increased cortical thickness on lingual gyrus and precuneus ($p<0.05$, corrected for multiple comparisons).

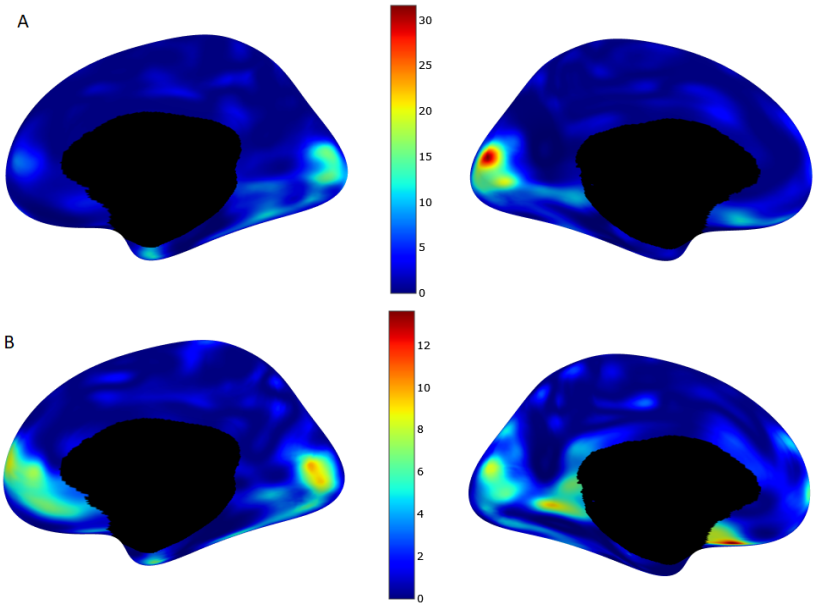


**Figure 29:** Unthresholded F-stat maps of the relationship between cortical thickness and BO (A) TSAB (B). Effect of BO is visible the visual cortex, whereas effect of TSAB on the same region is also found but its F-stat is much weaker.

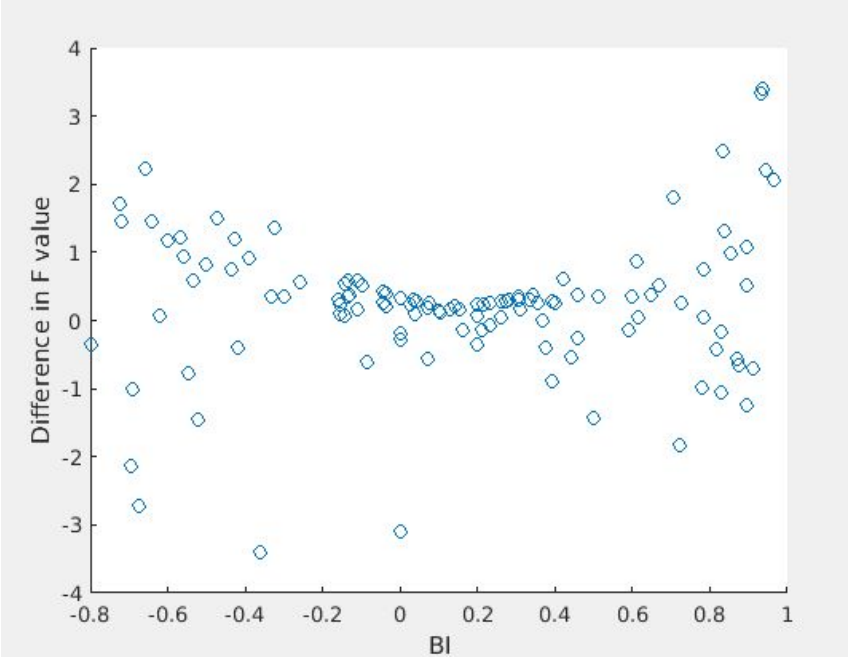


**Figure 30:** Distribution of the change in the model strength after removing one participant from the model that explains mean thickness in lingual gyrus and cunus with BI. A sinusoidal shape was expected to identify a critical BI value, however, the resulting distribution is not suitable for fitting such a model.

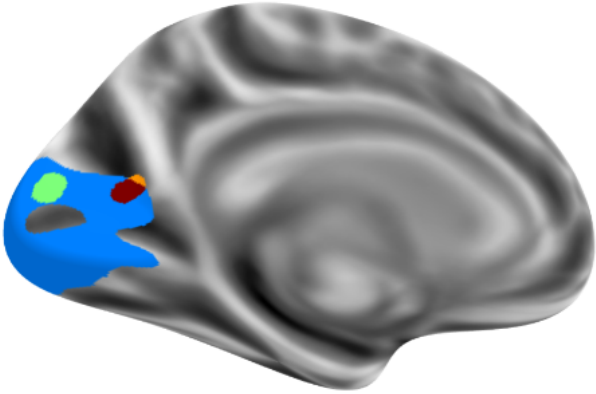

**Figure 31:** Clusters identifited by the BI (green), and SC-LB (orange), SC-CB (blue) and the overlap of SC-CB and SC-LB (red). It can be seen that the region identified by BI is a subregion of the cluster identified by SC-CB.

ness in the BI-relevant regions (Figure 32). The model was significant ($p<0.0001$, $F=5.55$). The BO<3 group has significantly higher values than all LB with BO>6 and higher than the sighted group (post-hoc correction between groups was done with the Bonferroni method at $p=0.05$). In addition, the 2<BO<7 group was significantly higher than the 19<BO group.

Apart from cortical thickness, GM intensity was the only other measure that showed a significant relationship with BI (Figure 34). A region on the left lingual gyrus showed a positive relationship between BI and GM intensity. The stepwise approach resulted in a graph that is similar to the one generated by cortical thickness data, therefore individual models of BO and TSAB were taken into consideration. Separate analyses of BO and TSAB did not reveal any significant pattern when corrected with FDR or permutation in the whole brain, but both revealed large areas on the occipital cortex when corrected with FDR only within the significant cluster identified by the main (SC-LB) analysis. However, the region identified by BI does not correspond to neither the SC-CB, nor the

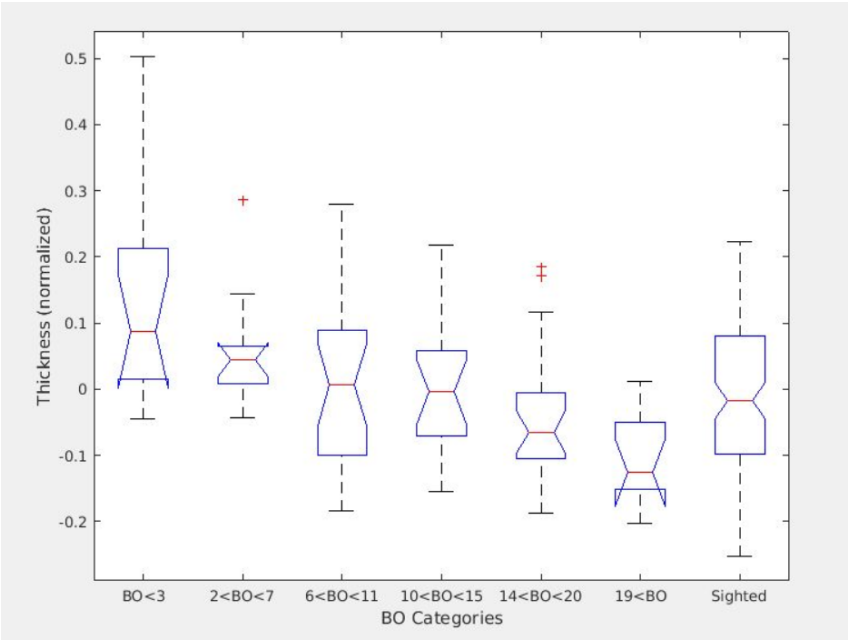


**Figure 32:** Mean thickness of the BI-related region explained by different BOs and sighted controls. The BO<3 group has significantly higher values than all LBs with BO>6 and higher than the sighted group (post-hoc correction between groups was done with the Bonferroni method at p=0.05). In addition, the 2<BO<7 group was significantly higher than the 19<BO group.

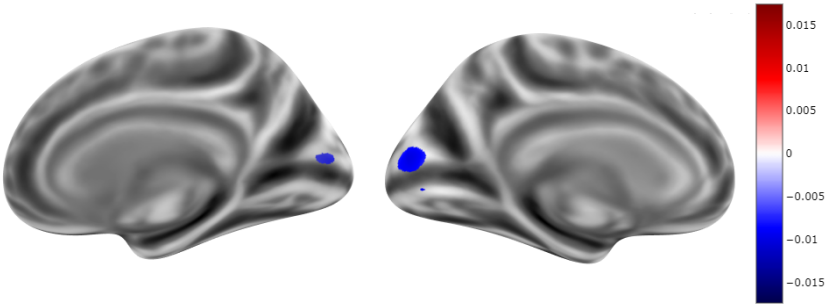


**Figure 33:** Correlates of BO with cortical thickness. Earlier blindness onset is associated with increased cortical thickness on lingual gyrus and precuneus ($p<0.05$, corrected for multiple comparisons).

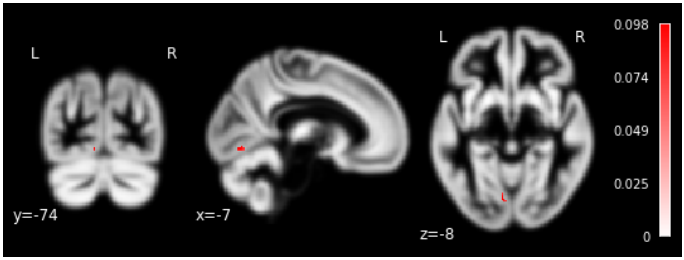


**Figure 34:** Correlates of BI with GM intensity. Higher blindness index (meaning earlier blindness onset and longer time spent as blind)is associated with increased GM intensity on lingual gyrus ($p<0.05$, corrected for multiple comparisons).

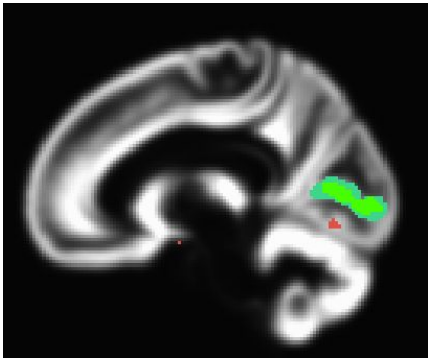

**Figure 35:** Clusters identifited by the BI (red), and SC-LB (light green) and the overlap of SC-LB and SC-CB (dark green). It can be seen that correlates of BI forms a different cluster than the other analyses.

SC-LB cluster (Figure 35. Taken both findings into consideration, it can be said that although there is an effect of onset of losing sight or time spent as blind in the early visual cortex, the peak of this effect is found in a region that is on a different part of the visual cortex. Specifically, The six BO categories explained above were used to explain the mean intensity in the BI-related region (Figure 36). The model was significant ($p<0.0001$, $F=11.62$). BO<3 group had significantly higher intensity than all the LB with BO>6, 14<BO group had lower intensity than all the LB with BO<11. SC have significant difference with BOs higer than 14 (post-hoc correction between groups was done with the Bonferroni method at $p=0.05$. Although SC group has higher GM intensity compared to both CB and LB groups in calcarine area, the BI-related region on the ventral visual cortex has a different trend. SC has higher intensity compared to BO>14 groups, and the LB with earlier onset has higher intensity compared to LB with late onset.

Analyses of high BO and high TSAB groups did not reveal any significant pattern. These groups consisted of BO values higher than 19 and TSAB groups larger than 27. The aim was to reduce the collinearity between the two variables by eliminating the hypothetically insignificant values for both regressors. However, these subsets of groups were still

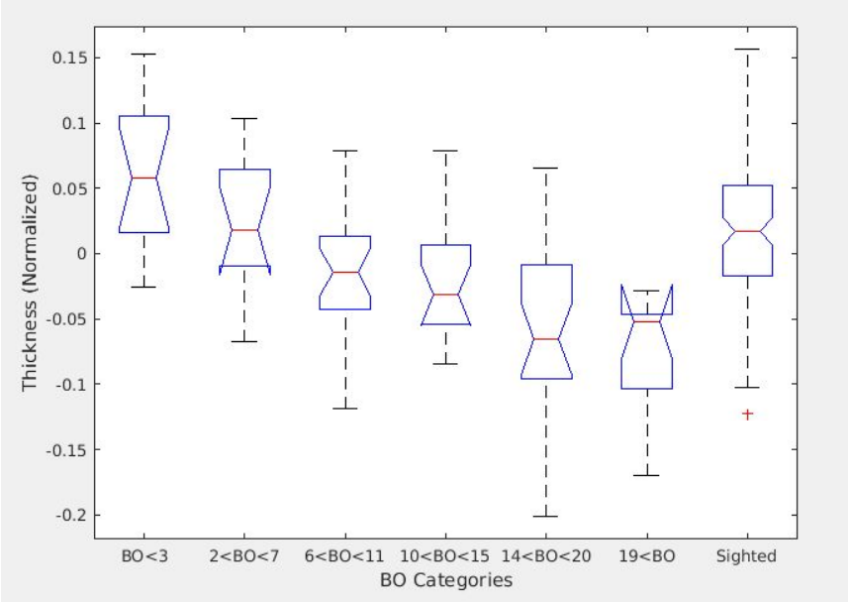


**Figure 36:** The BI-related region's mean GM intensity is explained by different BOs and sighted controls. BO<3 group had significantly higher intensity than all the LBs with BO>6, 14<BO group had lower intensity than all the LBs with BO<11. The only significant difference of SC was with the 14<BO group (post-hoc correction between groups was done with the Bonferroni method at p=0.05).

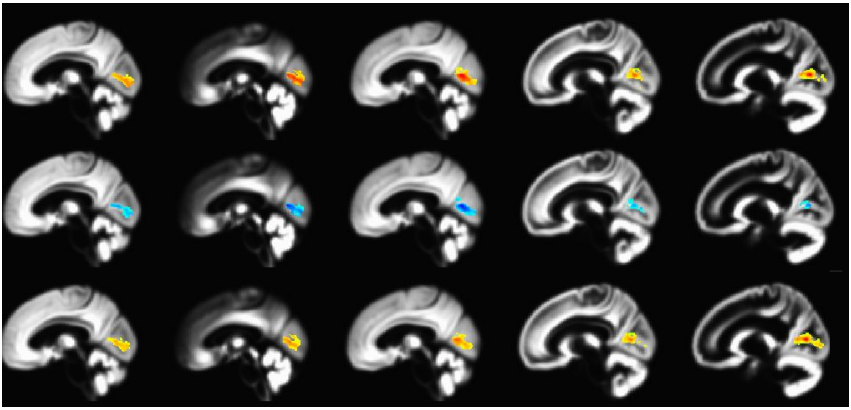

**Figure 37:** Correlates of BI (top row), BO (middle row), and TSAB (bottom row) when corrected with FDR within the significant cluster of main (SC-LB) comparison. Warm colors show positivie relationship, wheras cold colors show negative relationship.

not related to any of the structural measures, and the correlation between BO and TSAB in the high BO group was -0.2 (pearson r, p=0.32), and in the high TSAB group was -0.04 (pearson r , p=0.8).

Braille literacy was found to be relevant to only one brain structure. Braille readers who learned the alphabet after losing sight have smaller cerebellum than the Braille illiterate group (Figure 38) (4.2 $cm^3$, 2.08%, d=0.25). This was confirmed via a further post-hoc test (Tukey's honest significant difference criterion, $p<0.05$).

Like the Braille reading, RLP was associated with only one brain structure. Right pallidum is smaller in non-RLP group compared to RLP group (0.07 $cm^3$, 4.03%, d=0.39).

Lastly, there was no difference between the causes of the blindness in any of the metrics. These results are the same whether corrected with permutation, FDR, in the whole brain or the significant clusters derived from the main (SC-LB) analyses.

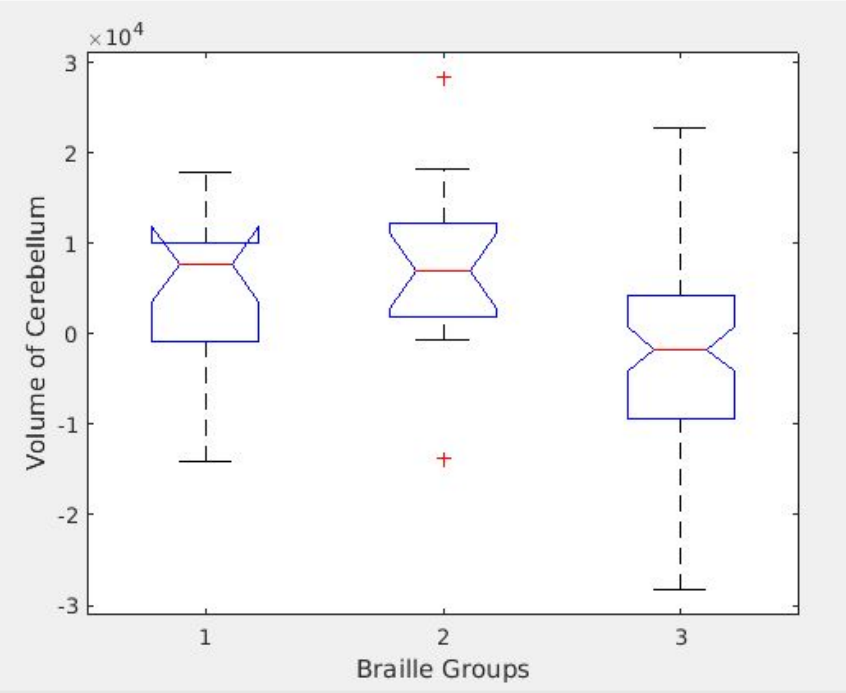


**Figure 38:** Mean cerebellum volume between different Braille groups. The difference between first (Braille illiterate) and third (Braille learned after the loss of vision) was significant after post-hoc correction.

## 4.3 Summary of the Findings/Discussion

In this chapter, structural properties of the brain (thickness, gyrification, intensity, overall volume) were compared between blind subjects who lost vision after birth and sighted controls. The aim was to identify the neuroplastic changes in the brain structure when visual perception is lost later in life; and the contribution of the residual effects (such as causes of blindness, residual light perception and Braille literacy, blindness duration/onset of blindness) to these changes.

Acquired blindness is related to smaller total brain volume, volume reductions on the optic radiations, and more curved, smaller, occipital cortex. Smaller white and gray matter volume in the visual pathway (via VBM analysis) has been reported previously (Voss, Pike, and Zatorre, 2014). However, the rest of the findings are inconsistent with the previous literature. This is partly because there is no consensus on the effect of acquired blindness in brain structure, which is one of the motivations of this study. For example, cortical thickness in LB shows different patterns: No difference was found on the visual cortex (Jiang et al., 2009; Q. Li et al., 2017), or the visual cortex was thinner in the LB (H. J. Park et al., 2009; Voss and Zatorre, 2012). This work suggests that the previous results that show a thinning in LB are due to chance, and there is no difference between the thickness of the occipital cortex between SC and LB subjects. Similarly, other areas reported in the previous research (somatomotor areas, parahippocampal gyrus, superior temporal gyrus...) are not found in this work. On the other hand, VBM results look consistent with previous research, although only one study uses the distinction between CB and LB for VBM studies as it was used for thickness studies (Voss, Pike, and Zatorre, 2014). In that study, it was shown that gray matter volume on the occipital cortex is smaller in the LB group, as we did. Lastly, similar to VBM results, the gyrification comparison also showed the same pattern: more gyrification on the occipital cortex in LB. To our knowledge, this is the first study that explores the gyrification difference between blind and sighted groups.

Overall, the lack of significant results except for the visual pathway

and the effect of blindness onset on the visual cortex suggest that functional cross-modal plasticity on the cortex (Ricciardi, Bonino, et al., 2014 for a review) does not have a structural basis. This is because the only difference between LB and SC is on the visual pathway, which can be attributed to the onset of blindness. Blind subjects with the earliest onset show the characteristics of the CB (thicker visual cortex), and this effect decays as the onset of blindness increases, and brain development is more complete. The only exception to this hypothesis can be the increased gyrification in LB. Since there is no association between this metric and the blindness onset, and the late-onset subjects acquire the blindness after the visual cortex takes its adult-like shape, one could argue that there should be no difference between LB and SC, like the cortical thickness. However, we see increased gyrification, similar to the results of CB. It is not very likely that the subjects did not go through the typical development steps that shape the brain. Therefore, there is a chance that the visual cortex becomes more gyrified after losing sight, and this change in structure can be attributed to the cross-modal plasticity of the visual cortex.

One of the main aims of this thesis was to identify the relationship between time spent as blind, age onset of blindness, and the morphometric changes in the brain due to blindness. Our analyses showed that the onset of blindness, but not the time spent as blind, is correlated with the occipital cortex's cortical thickness and volumetric measures. The earlier onset of blindness is associated with more atrophy, similar to CB. This finding suggests that the atrophy of the visual cortex is due to the interrupted neurodevelopment rather than compensatory plasticity that occurs in the case of loss of vision. Previous research, where they only observed the onset of blindness, also found the same trend (Q. Li et al., 2017; Anurova, Carlson, and Rauschecker, 2019). Cortical thickness and the surface area differences in the visual cortex decreased as the onset of blindness increased. A novel finding of this study is that the region on the lingual gyrus, whose gray matter intensity changes with blindness onset, forms a different cluster than the one found after comparing sighted and blind population, which covers pericalcarine area. Still,

when looked into the pericalcarine area only, rather than the whole brain, and corrected with a less strict threshold, the a meaningful relationship between GM volume and BO was seen. It can be said that although blindness gradually affects the gray matter volume of the early visual areas, this effect peaks in higher areas in the ventral pathway. This finding shows similarity with the one that Pan et al., 2007 reported. They found that blindness duration is related to small localized regions, rather than the whole visual cortex. Although they conducted the analysis with TSAB, their sample was all EB/CB whose BO was earlier than 6 years. This sample characteristic is in accordance with our finding, the earlier the BO is, the the stronger the association with GM.

Globus pallidus was the only subcortical structure that showed a volume decrease in LB. It was even smaller in the blind subjects who could not perceive residual light. As discussed in the previous chapter, globus pallidus is related to voluntary movements, and visual cues may be necessary to regulate them (Klaassen et al., 2021). Smaller pallidus in blind subjects who cannot perceive light also support this statement, as residual light perception may still be helpful to guide the movements.

Blind subjects who learned the Braille alphabet after vision loss had smaller cerebellar volume than the blind subjects that are not Braille literate. Even though some studies have shown the functional association between the Braille reading and cerebellum (Sadato, 2005; Gizewski, Timmann, and Forsting, 2004), no studies have shown the structural relationship between them.

Lastly, the causes of blindness were not related to any structural change within the LB. Whether they are sourced from an issue in the eye, retina, or optic pathway, they are always associated with a similar brain structure.

In summary, structural plasticity shows different patterns depending on the time of loss of sight. If the sight is lost roughly before the visual cortex completes its development, the typical neurodevelopment will be interrupted, and the visual cortex will stay thicker. However, if the sight is lost much later in life, regardless of how much time spent as blind, the effect of blindness on the brain will be the same: smaller optic radiations,

more curved and smaller visual cortex, and smaller pallidum. Whether the LB are Braille literate or can perceive light or not affects only a limited number of structures (pallidum and cerebellum).

# Chapter 5

# Conclusions

The main aim of this thesis was to identify the structural changes in the brain in the case of blindness. Even though there have been several studies on this topic, due to the inconsistency among the results and the heterogeneity in sample characteristics of the previous research, a study with a large and uniform sample to allow a more detailed and reliable investigation was necessary. For my thesis, thanks to the contribution of the researchers from different parts of the world, we managed to create such a dataset that may answer the open questions in the field. It was the largest MRI dataset consisting of congenital and late blind samples up-to-date.

In chapter 2, a literature search was conducted to summarize the current state of the literature and to identify the potential variable that could confound the previous research. Atrophy on the visual pathways was consistently reported across studies. However, some findings on the whole brain (temporal gyrus, corpus callosum, sensorimotor areas, caudate, hippocampus) were differently reported and open to discussion. A coordinate-based meta-analysis supported the controversy of the results. Among all the regions reported in the studies, only the occipital cortex and the LGN survived the analysis. This heterogeneity among the results was attributed to a number of factors such as small sample sizes, different causes of blindness dominating each study, different blindness

onset and time spent as blind, residual light perception, and post-natal experience with Braille reading.

Considering the issues identified in chapter 2, structural features (total volume, VBM intensity, thickness, gyrification) of the blind and sighted participants were compared in chapters 3 and 4. The results suggest that the onset of vision loss is important for the structural plasticity of the brain. If vision is lost perinatally, typical development of the visual cortex is interrupted and cannot progress due to lack of sensory input. In addition, regions or structures not directly related to the visual pathway are also affected (i.e., entorhinal cortex and middle temporal gyrus, hippocampus, amygdala). Late blindness, on the other hand, especially when vision is lost after adulthood, has a much narrower area of effect, mostly restricted to optic radiations and early visual cortex. This effect has no relationship with how much time the person spends as blind.

This work brought new insights into controversial topics in blindness research. First, blind subjects born prematurely show a different brain structure than the rest of the blind subjects; they have smaller total white matter volume, smaller and more gyrified anterior middle gyrus, thicker and more gyrified visual cortex. In order to create a homogeneous sample and generate reliable results, it is suggested that they should be excluded or at least accounted for in further research. The rest of the causes of blindness have no specific effects on the brain structure. Second, residual light perception and Braille reading are essential in the case of late blindness only. These two factors effected the brain structure of late blind subjects, but not congenital blinds. Lastly, a larger sample size helps reducing the false positives. This study showed that smaller subsamples of the dataset resulted in significant regions that are also reported in the previous research.

Naturally, current work has some limitations. To start with, DTI scans would have been useful to examine the white matter tracts in detail. In the current dataset, only T1 MRI images were available. Although appropriate for gray matter-related metrics, T1 MRI images are not sufficient for a reliable white matter examination. Another shortcoming is the sensitivity of the supplementary information (i.e., metadata). Since

the loss of sight in the first years of life is critical, it would be more accurate to conduct this study based on the postnatal month (or day, ideally) on which the subjects lost their sight. Similarly, more information could be derived on premature born blind subjects if their gestational age was known.

Apart from misrecording the information, well-categorized but missing information was a challenge for this study. For example, subjects who lost their sight most recently in this dataset had been blind for four years already. This duration is too long for observing the temporal changes in the brain. This lack of data makes it impossible to track the temporal plasticity change right after losing sight. Ideally, the availability of subjects who lost their sight within the year or two before the MRI scan can significantly contribute to this study. The perfect case would be to have the data from the sight recovery and the blindfolding, or longitudinal studies.

To conclude, this work gathered the largest anatomical dataset of blind subjects thanks to different research groups from all over the world to investigate the structural plasticity in the case of blindness and address the controversial issues. This project highlights the importance of collaboration between research groups and data-sharing to accelerate scientific progress. Hopefully, this project will be the first of many consortiums in this field of research.

# Appendix A

# Supplementary Figures

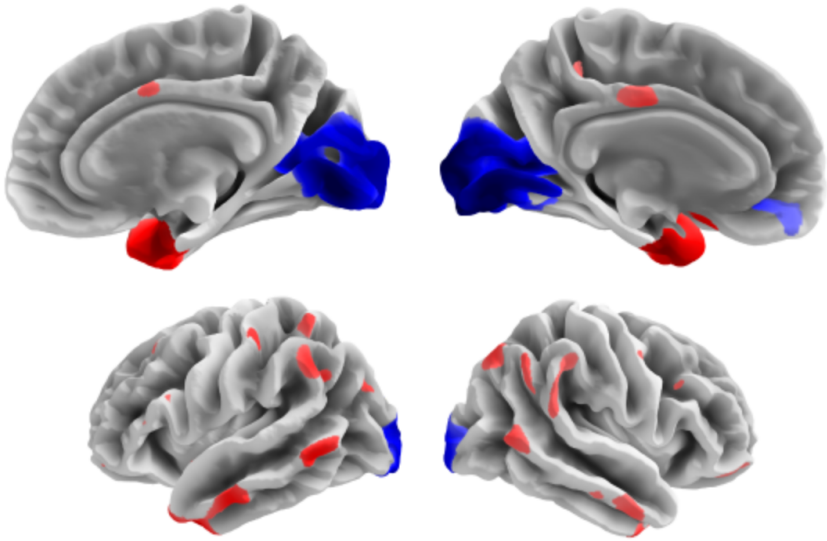

**Figure 39:** Percent thickness decrease in CB compared to SC (corrected with FDR at 0.05).

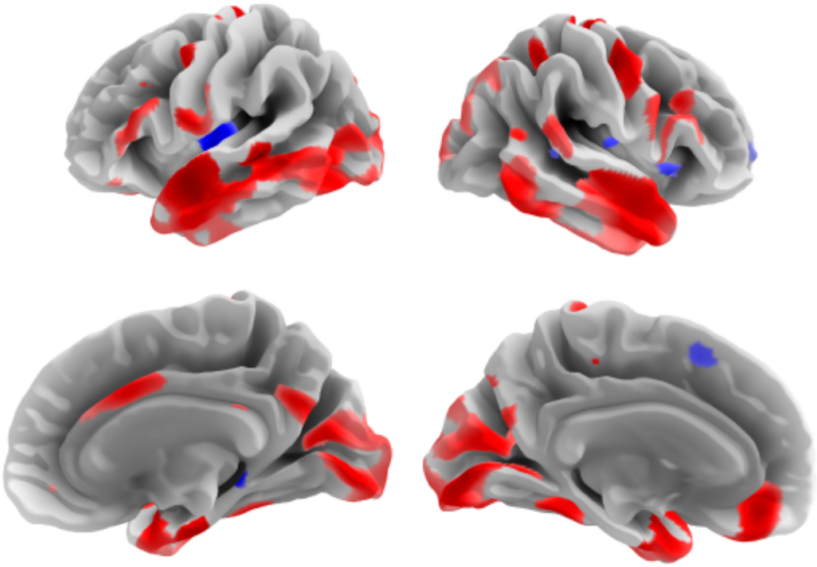

**Figure 40:** Percent gyrification increase in CB compared to SC (corrected with FDR at 0.05)

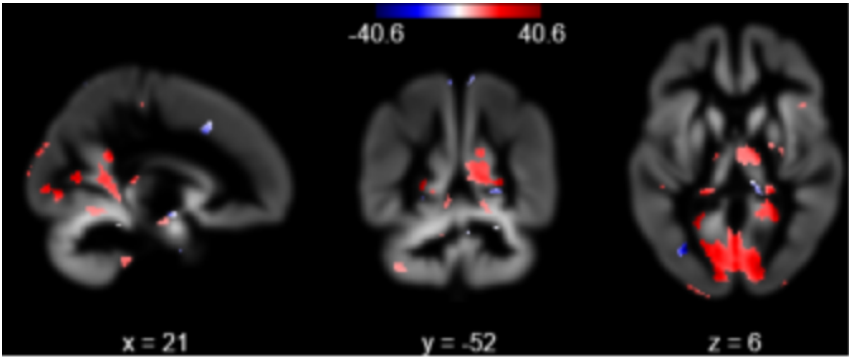


**Figure 41:** Percent GM intensity decrease in CB compared to SC (corrected with FDR at 0.05)

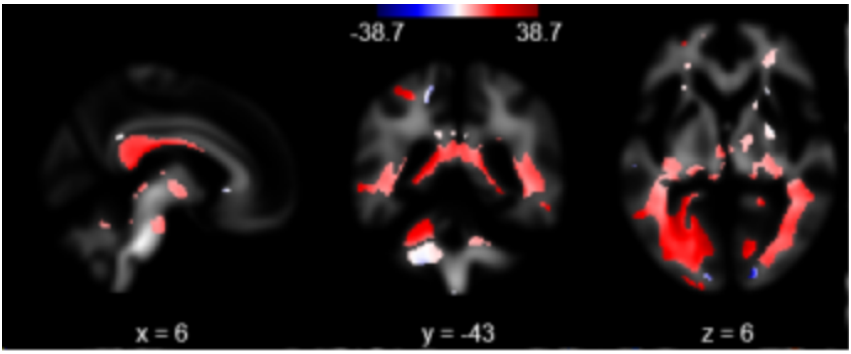


**Figure 42:** Percent WM intensity decrease in CB compared to SC (corrected with FDR at 0.05)

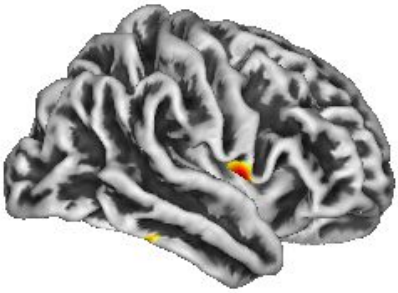

**Figure 43:** Regions showing an interaction between age and blindness in gyrification (corrected with FDR at 0.05)

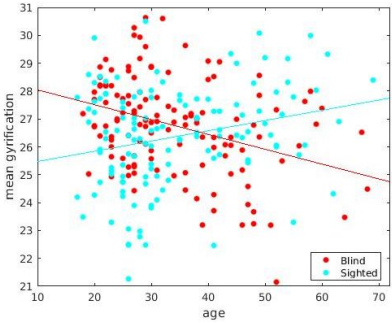


**Figure 44:** Scatter plot of the age and mean gyrification of the ROIs shown in the figure above.

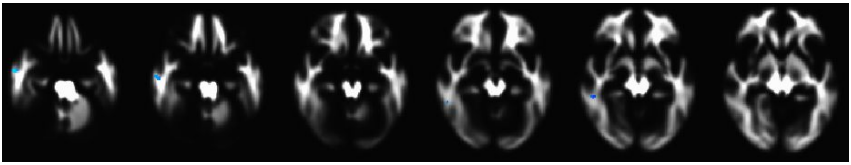

**Figure 45:** Intensity loss in WM of RoP compared to NRoP in CB (corrected with FDR).

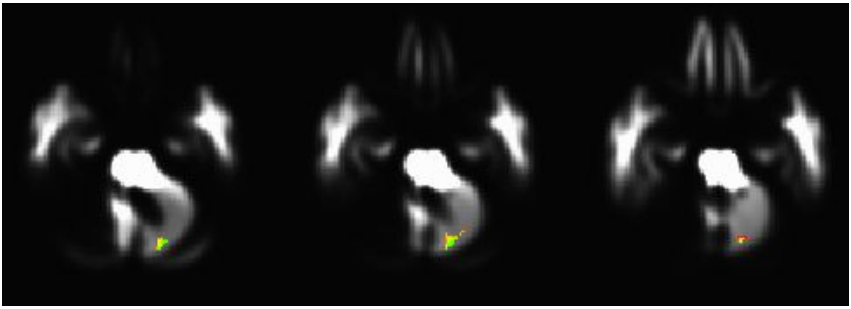

**Figure 46:** Region that shows an interaction between age and RoP on cerebellum white matter in CB (corrected with FDR)

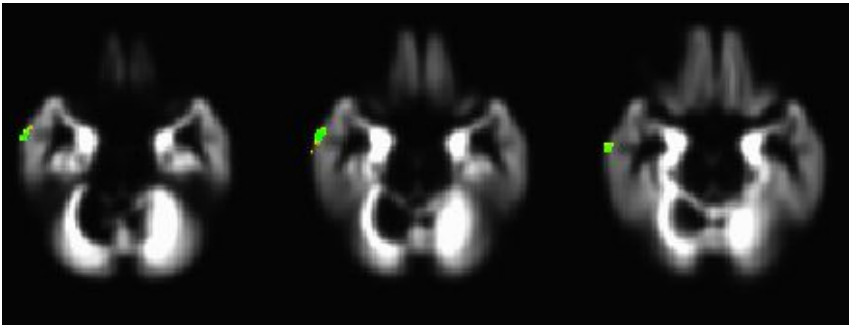

**Figure 47:** Intensity loss in GM of RoP compared to NRoP in CB (corrected with FDR).

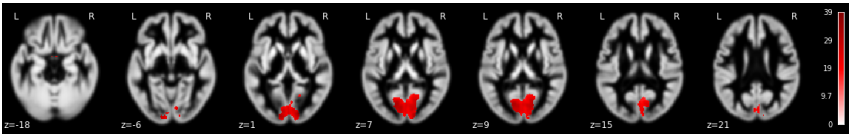


**Figure 48:** Percent GM intensity decrease in LB (FDR corrected)

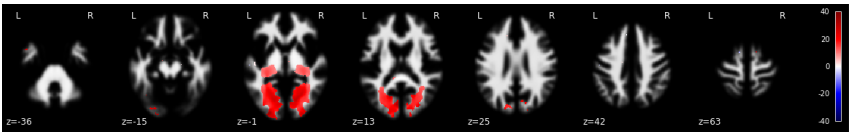


**Figure 49:** Percent WM intensity decrease in LB (FDR corrected)

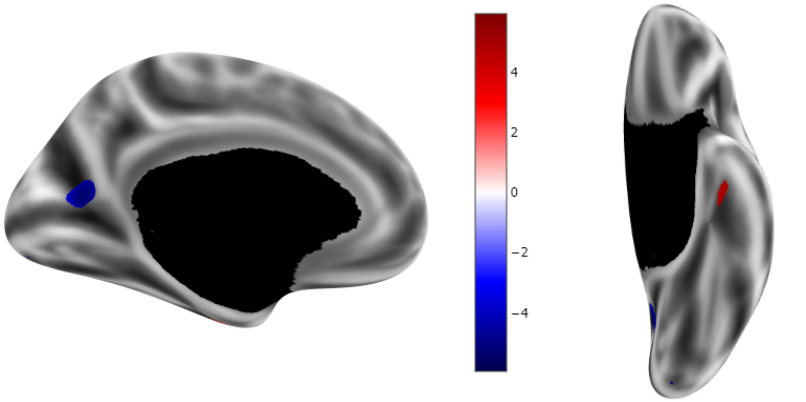


**Figure 50:** Percent thickness in LB (both left hemisphere, side and bottom view - nothing on the right hemisphere, FDR corrected)

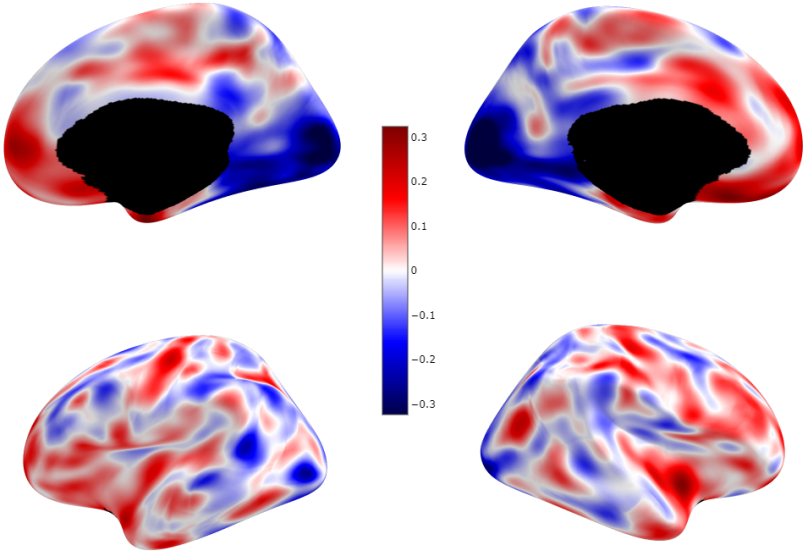


**Figure 51:** Pearson correlation between BO and cortical thickness at whole-brain level.

# Bibliography


Aguirre, Geoffrey K et al. (Nov. 2016). "Patterns of individual variation in visual pathway structure and function in the sighted and blind". In: *PLoS One* 11.

Alexander, Andrew L et al. (2007). "Diffusion tensor imaging of the brain". In: *Neurotherapeutics* 4.3, pp. 316–329.

Amedi, Amir et al. (2010). "Cortical activity during tactile exploration of objects in blind and sighted humans". In: *Restorative neurology and neuroscience* 28.2, pp. 143–156.

Andelin, Adrian K et al. (Sept. 2019). "The Effect of Onset Age of Visual Deprivation on Visual Cortex Surface Area Across-Species". In: *Cereb. Cortex* 29, pp. 4321–4333.

Ankeeta, A et al. (2021). "Evaluation of Memory and Language Network in Children and Adolescents with Visual Impairment: A Combined Functional Connectivity and Voxel-based Morphometry Study". In: *Neuroophthalmology* 45, pp. 147–161.

Anurova, Irina, Synnöve Carlson, and Josef P Rauschecker (2019). "Overlapping Anatomical Networks Convey Cross-Modal Suppression in the Sighted and Coactivation of "Visual" and Auditory Cortex in the Blind". In: *Cerebral Cortex*. ISSN: 1047-3211. DOI: 10.1093/cercor/bhz021.

Anurova, Irina, Laurent A Renier, et al. (Aug. 2015). "Relationship between Cortical Thickness and Functional Activation in the Early Blind". In: *Cereb. Cortex* 25, pp. 2035–2048.

Ashburner, John (2010). "VBM tutorial". In: *Tech. repWellcome Trust Centre for Neuroimaging, London, UK*.

Ashtari, Manzar et al. (2015). "Plasticity of the human visual system after retinal gene therapy in patients with Leber's congenital amaurosis". In: *Science translational medicine* 7.296, 296ra110–296ra110.

Atilgan, Hicret, Olivier Collignon, and Uri Hasson (July 2017). "Structural neuroplasticity of the superior temporal plane in early and late blindness". In: *Brain Lang.* 170, pp. 71–81.

Avants, Brian B, Nick Tustison, and Gang Song (2011). "Advanced Normalization Tools (ANTS) Brian B. Avants, Nick Tustison and Gang Song". In: pp. 1–35. URL: www.picsl.upenn.edu/ANTS..

Baliyan, Vinit et al. (2016). "Diffusion weighted imaging: technique and applications". In: *World journal of radiology* 8.9, p. 785.

Barcella, Valeria et al. (Dec. 2010). "Evidence for retrochiasmatic tissue loss in Leber's hereditary optic neuropathy". In: *Hum. Brain Mapp.* 31, pp. 1900–1906.

Basser, Peter J, James Mattiello, and Denis LeBihan (1994). "MR diffusion tensor spectroscopy and imaging". In: *Biophysical journal* 66.1, pp. 259–267.

Bauer, Corinna M, Zaira Cattaneo, and Lotfi B Merabet (Mar. 2018). "Early blindness is associated with increased volume of the uncinate fasciculus". In: *Eur. J. Neurosci.* 47, pp. 427–432.

Bauer, Corinna M, Gabriella V Hirsch, et al. (Mar. 2017). "Multimodal MR-imaging reveals large-scale structural and functional connectivity changes in profound early blindness". en. In: *PLoS One* 12.3, e0173064.

Belke, Marcus et al. (2015). "DTI and VBM reveal white matter changes without associated gray matter changes in patients with idiopathic restless legs syndrome". In: *Brain and behavior* 5.9, e00327.

Boardman, James P et al. (2006). "Abnormal deep grey matter development following preterm birth detected using deformation-based morphometry". In: *Neuroimage* 32, pp. 70–78.

Bock, Andrew S et al. (Nov. 2013). "Visual callosal topography in the absence of retinal input". In: *Neuroimage* 81, pp. 325–334.

Bola, Łukasz et al. (Dec. 2017). "Structural reorganization of the early visual cortex following Braille training in sighted adults". In: *Sci. Rep.* 7.

Borghesani, Valentina et al. (2019). ""Looks familiar, but I do not know who she is": The role of the anterior right temporal lobe in famous face recognition". In: *Cortex* 115, pp. 72–85.

Bourne, Rupert et al. (2021). "Trends in prevalence of blindness and distance and near vision impairment over 30 years: an analysis for the Global Burden of Disease Study". In: *The Lancet Global Health* 9.2, e130–e143.

Breitenseher, M et al. (1998). "Morphological dissociation between visual pathways and cortex: MRI of visually-deprived patients with congenital peripheral blindness". In: *Neuroradiology* 40.7, pp. 424–427.

Bridge, Holly, Gaelle S L Coullon, et al. (2021). "The Effect of Congenital and Acquired Bilateral Anophthalmia on Brain Structure". In: *Neuroophthalmology* 45, pp. 75–86.

Bridge, Holly, Alan Cowey, et al. (2009). "Imaging studies in congenital anophthalmia reveal preservation of brain architecture in 'visual' cortex". In: *Brain* 132, pp. 3467–3480.

Brown, M A and R C Semelka (2011). *MRI: basic principles and applications*. John Wiley & Sons.

Büchel, Christian et al. (1998). *Different activation patterns in the visual cortex of late and congenitally blind subjects*.

Burgaleta, Miguel et al. (2014). "Cognitive ability changes and dynamics of cortical thickness development in healthy children and adolescents". In: *Neuroimage* 84, pp. 810–819.

Burge, Wesley K et al. (2016). "Cortical thickness in human V1 associated with central vision loss". In: *Scientific reports* 6.1, pp. 1–10.

Burton, H et al. (2002). "Adaptive changes in early and late blind: a FMRI study of verb generation to heard nouns". In: *Journal of neurophysiology*.

Butts, Daniel A and Daniel S Rokhsar (2001). "The information content of spontaneous retinal waves". In: *Journal of Neuroscience* 21.3, pp. 961–973.

Carp, Joshua (2012). "On the plurality of (methodological) worlds: Estimating the analytic flexibility of fmri experiments". In: *Front. Neurosci.*

Cavaliere, Carlo et al. (Jan. 2020). "Organization of the commissural fiber system in congenital and late-onset blindness". In: *NeuroImage: Clinical* 25.

Cecchetti, Luca et al. (Apr. 2016). "Congenital blindness affects diencephalic but not mesencephalic structures in the human brain". In: *Brain Struct. Funct.* 221, pp. 1465–1480.

Chebat, Daniel Robert et al. (2007). "Alterations in right posterior hippocampus in early blind individuals". In: *NeuroReport* 18.4, pp. 329–333. ISSN: 09594965. DOI: 10.1097/WNR.0b013e32802b70f8.

Chen, Wei W et al. (Jan. 2013). "Structural brain abnormalities in patients with primary open-angle glaucoma: A study with 3T MR imaging". In: *Invest. Ophthalmol. Vis. Sci.* 54, pp. 545–554.

Chugani, Harry T, Michael E Phelps, and John C Mazziotta (1987). "Positron emission tomography study of human brain functional development". In: *Annals of neurology* 22.4, pp. 487–497.

Clancy, Barbara, Richard B Darlington, and Barbara L Finlay (2001). "Translating developmental time across mammalian species". In: *Neuroscience* 105.1, pp. 7–17.

Collignon, Olivier et al. (2011). "Functional specialization for auditory–spatial processing in the occipital cortex of congenitally blind humans". In: *Proceedings of the National Academy of Sciences* 108.11, pp. 4435–4440.

Cox, Robert W (1996). "AFNI: software for analysis and visualization of functional magnetic resonance neuroimages". In: *Computers and Biomedical research* 29.3, pp. 162–173.

Dahnke, Robert, Rachel Aine Yotter, and Christian Gaser (2013). "Cortical thickness and central surface estimation". In: *Neuroimage* 65, pp. 336–348.

Davey, James et al. (2016). "Exploring the role of the posterior middle temporal gyrus in semantic cognition: Integration of anterior temporal lobe with executive processes". In: *Neuroimage* 137, pp. 165–177.

De Volder, A G et al. (Mar. 1997). "Brain energy metabolism in early blind subjects: neural activity in the visual cortex". en. In: *Brain Res.* 750.1-2, pp. 235–244.

Desikan, Rahul S et al. (2006). "An automated labeling system for subdividing the human cerebral cortex on MRI scans into gyral based regions of interest". In: *Neuroimage* 31.3, pp. 968–980.

Dietrich, Susanne et al. (Apr. 2015). "Experience-related structural changes of degenerated occipital white matter in late-blind humans - a diffusion tensor imaging study". en. In: *PLoS One* 10.4, e0122863.

Duffy, Kevin R., Kathryn M. Murphy, and David G. Jones (1998). "Analysis of the postnatal growth of visual cortex". In: *Visual Neuroscience* 15.5, pp. 831–839. ISSN: 0952-5238. DOI: 10.1017/s0952523898155049.

Eickhoff, Simon B, Danilo Bzdok, et al. (Feb. 2012). "Activation likelihood estimation meta-analysis revisited". In: *Neuroimage* 59, pp. 2349–2361.

Eickhoff, Simon B, Angela R Laird, et al. (Sept. 2009). "Coordinate-based activation likelihood estimation meta-analysis of neuroimaging data: a random-effects approach based on empirical estimates of spatial uncertainty". en. In: *Hum. Brain Mapp.* 30.9, pp. 2907–2926.

Eickhoff, Simon B, Thomas E Nichols, et al. (Aug. 2016). "Behavior, sensitivity, and power of activation likelihood estimation characterized by massive empirical simulation". In: *Neuroimage* 137, pp. 70–85.

Feng, Yixuan et al. (2021). “Brief postnatal visual deprivation triggers long-lasting interactive structural and functional reorganization of the human cortex”. In: *Frontiers in Medicine* 8.

Ferreira, Sónia et al. (2017). “Primary visual cortical remapping in patients with inherited peripheral retinal degeneration”. In: *NeuroImage: Clinical* 13, pp. 428–438.

Fine, Ione and Ji-Min Park (2018). “Blindness and human brain plasticity”. In: *Annual review of vision science* 4, pp. 337–356.

Fortin, Madeleine et al. (Nov. 2008). “Wayfinding in the blind: Larger hippocampal volume and supranormal spatial navigation”. In: *Brain* 131, pp. 2995–3005.

Foulon, Chris et al. (2018). “Advanced lesion symptom mapping analyses and implementation as BCBtoolkit”. In: *Gigascience* 7.3, giy004.

Fox, Nathan A, Lewis A Leavitt, and John G Warhol (1999). *The role of early experience in infant development*. Citeseer.

Frick, Kevin D et al. (2015). “The global burden of potential productivity loss from uncorrected presbyopia”. In: *Ophthalmology* 122.8, pp. 1706–1710.

Friedman, David S et al. (2004). “Racial variations in causes of vision loss in nursing homes: The Salisbury Eye Evaluation in Nursing Home Groups (SEEING) Study”. In: *Archives of Ophthalmology* 122.7, pp. 1019–1024.

Frost, Douglas O et al. (2000). “Surgically created neural pathways mediate visual pattern discrimination”. In: *Proceedings of the National Academy of Sciences* 97.20, pp. 11068–11073.

Gagnon, Léa et al. (2012). “Activation of the hippocampal complex during tactile maze solving in congenitally blind subjects”. In: *Neuropsychologia* 50.7, pp. 1663–1671.

Gaser, Christian, Robert Dahnke, et al. (2016). “CAT-a computational anatomy toolbox for the analysis of structural MRI data”. In: *Hbm* 2016, pp. 336–348.

Geuter, Stephan et al. (2018). “Effect Size and Power in fMRI Group Analysis”. In: *bioRxiv*.

Gizewski, Elke R, Dagmar Timmann, and Michael Forsting (2004). “Specific cerebellar activation during Braille reading in blind subjects”. In: *Human brain mapping* 22.3, pp. 229–235.

Glasser, Matthew F et al. (2016). “A multi-modal parcellation of human cerebral cortex”. In: *Nature* 536.7615, pp. 171–178.

Gobbini, M Ida and James V Haxby (2007). “Neural systems for recognition of familiar faces”. In: *Neuropsychologia* 45.1, pp. 32–41.

Goncharova, II et al. (2001). "MRI of human entorhinal cortex: a reliable protocol for volumetric measurement". In: *Neurobiology of aging* 22.5, pp. 737–745.

Goto, Masami et al. (2022). "Advantages of Using Both Voxel-and Surface-based Morphometry in Cortical Morphology Analysis: A Review of Various Applications". In: *Magnetic Resonance in Medical Sciences*, rev–2021.

Guerreiro, Maria J S et al. (Dec. 2015). "Increased visual cortical thickness in sight-recovery individuals". In: *Hum. Brain Mapp.* 36, pp. 5265–5274.

Hardee, Jillian E, James C Thompson, and Aina Puce (2008). "The left amygdala knows fear: laterality in the amygdala response to fearful eyes". In: *Social cognitive and affective neuroscience* 3.1, pp. 47–54.

Hasler, Holly M, Timothy T Brown, and Natacha Akshoomoff (2020). "Variations in brain morphometry among healthy preschoolers born preterm". In: *Early human development* 140, p. 104929.

Hasson, Uri et al. (Mar. 2016). "Congenital blindness is associated with large-scale reorganization of anatomical networks". In: *Neuroimage* 128, pp. 362–372.

Heinsen, H et al. (1996). "Variability in the human entorhinal region may confound neuropsychiatric diagnoses". In: *Cells Tissues Organs* 157.3, pp. 226–237.

Hirsch, Gabriella V, Corinna M Bauer, and Lotfi B Merabet (2015). "Using structural and functional brain imaging to uncover how the brain adapts to blindness". In: *Annals of neuroscience and psychology* 2.

Hölig, Cordula et al. (2022). "Sight restoration in congenitally blind humans does not restore visual brain structure". In: *Cerebral Cortex*.

Hou, Fen et al. (2017). "Reduction of Interhemispheric Functional Brain Connectivity in Early Blindness: A Resting-State fMRI Study". In: *Biomed Res. Int.* 2017.

Huettel, S.A., A.W. Song, and G. McCarthy (2009). *Functional Magnetic Resonance Imaging*. Oxford University Press, Incorporated. ISBN: 9780878932863. URL: https://books.google.com.tr/books?id=BNhMPgAACAAJ.

Huttenlocher, Peter R and Arun S Dabholkar (1997). "Regional differences in synaptogenesis in human cerebral cortex". In: *Journal of comparative Neurology* 387.2, pp. 167–178.

Huttenlocher, Peter R. (1990). "Morphometric study of human cerebral cortex development". In: *Neuropsychologia* 28.6, pp. 517–527. DOI: 10.1016/0028-3932(90)90031-I.

Iachini, Tina, Gennaro Ruggiero, and Francesco Ruotolo (2014). "Does blindness affect egocentric and allocentric frames of reference in small and large scale spaces?" In: *Behavioural brain research* 273, pp. 73–81.

Iglói, Kinga et al. (2010). "Lateralized human hippocampal activity predicts navigation based on sequence or place memory". In: *Proceedings of the National Academy of Sciences* 107.32, pp. 14466–14471.

Inuggi, Alberto et al. (Aug. 2020). "Multisystemic Increment of Cortical Thickness in Congenital Blind Children". In: *Cerebral Cortex Communications* 1.

Ioannidis, John PA et al. (2014). "Publication and other reporting biases in cognitive sciences: detection, prevalence, and prevention". In: *Trends in cognitive sciences* 18.5, pp. 235–241.

Jenkinson, M et al. (2012). "Fsl". In: *Neuroimage* 62.2, pp. 782–790. ISSN: 1053-8119. DOI: 10.1016/j.neuroimage.2011.09.015.

Jiang, Jiefeng et al. (Feb. 2009). "Thick visual cortex in the early blind". In: *Journal of Neuroscience* 29, pp. 2205–2211.

Johnson, W Evan, Cheng Li, and Ariel Rabinovic (2007). "Adjusting batch effects in microarray expression data using empirical Bayes methods". In: *Biostatistics* 8.1, pp. 118–127.

Kestenberg, Judith S (1979). *Insights from the Blind. Comparative Studies of Blind and Sighted Children. By Selma Fraiberg, with the collaboration of Louis Fraiberg. New York: Basic Books, Inc., 1977. 297 pp.*

Kharitonova, Maria et al. (2013). "Cortical gray-matter thinning is associated with age-related improvements on executive function tasks". In: *Dev. Cogn. Neurosci.* 6, pp. 61–71.

Klaassen, Arndt-Lukas et al. (2021). "Ventral pallidum regulates the default mode network, controlling transitions between internally and externally guided behavior". In: *Proceedings of the National Academy of Sciences* 118.36.

Klinge, Corinna, Falk Eippert, et al. (2010). "Corticocortical connections mediate primary visual cortex responses to auditory stimulation in the blind". In: *Journal of Neuroscience* 30.38, pp. 12798–12805.

Klinge, Corinna, Brigitte Röder, and Christian Büchel (2010). "Increased amygdala activation to emotional auditory stimuli in the blind". In: *Brain* 133.6, pp. 1729–1736.

Kosif, Rengin, Bünyamin Sahin, and Safiye Gürel (Mar. 2013). "Comparación del volumen cerebelar entre individuos sanos y con ceguera bilateral congénita". In: *Int. J. Morphol.* 31, pp. 239–245.

Lao, Yi et al. (Dec. 2015). "A study of brain white matter plasticity in early blinds using tract-based spatial statistics and tract statistical analysis". In: *Neuroreport* 26, pp. 1151–1154.
Lazzouni, Latifa and Franco Lepore (June 2014). "Compensatory plasticity: Time matters". In: *Front. Hum. Neurosci.* 8.
Leporé, Natasha, Yonggang Shi, et al. (July 2009). *Pattern of hippocampal shape and volume differences in blind subjects*.
Leporé, Natasha, Patrice Voss, et al. (Jan. 2010). *Brain structure changes visualized in early- and late-onset blind subjects*.
Lerch, Jason P et al. (July 2006). "Mapping anatomical correlations across cerebral cortex (MACACC) using cortical thickness from MRI". In: *Neuroimage* 31, pp. 993–1003.
Li, Jiajia et al. (2013). "Age of onset of blindness affects brain anatomical networks constructed using diffusion tensor tractography". In: *Cerebral Cortex* 23.3, pp. 542–551.
Li, Qiaojun et al. (Aug. 2017). "Cortical thickness development of human primary visual cortex related to the age of blindness onset". In: *Brain Imaging Behav.* 11, pp. 1029–1036.
Luders, Eileen et al. (2006). "A curvature-based approach to estimate local gyrification on the cortical surface". In: *Neuroimage* 29.4, pp. 1224–1230.
Machado, Ana Rita et al. (Dec. 2017). *Structure-function correlations in Retinitis Pigmentosa patients with partially preserved vision: A voxel-based morphometry study*.
Maguire, Eleanor A, Katherine Woollett, and Hugo J Spiers (2006). "London taxi drivers and bus drivers: a structural MRI and neuropsychological analysis". In: *Hippocampus* 16.12, pp. 1091–1101.
Maller, Jerome J et al. (Nov. 2016). "Brain morphometry in blind and sighted subjects". In: *J. Clin. Neurosci.* 33, pp. 89–95.
Marek, Scott et al. (2022). "Reproducible brain-wide association studies require thousands of individuals". In: *Nature* 603.7902, pp. 654–660.
Matuszewski, Jacek et al. (Feb. 2021). "Brain plasticity dynamics during tactile Braille learning in sighted subjects: Multi-contrast MRI approach". In: *Neuroimage* 227.
Mendola, Janine D et al. (June 2005). "Voxel-based analysis of MRI detects abnormal visual cortex in children and adults with amblyopia". In: *Hum. Brain Mapp.* 25, pp. 222–236.
Mitchell, Paul, Phillip Hayes, and Jie Jin Wang (1997). "Visual impairment in nursing home residents: the Blue Mountains Eye Study". In: *Medical Journal of Australia* 166.2, pp. 73–76.

Mitelman, Serge A et al. (Oct. 2005). "Cortical intercorrelations of frontal area volumes in schizophrenia". In: *Neuroimage* 27, pp. 753–770.

Modi, Shilpi et al. (Oct. 2012). "Effect of visual experience on structural organization of the human brain: A voxel based morphometric study using DARTEL". In: *Eur. J. Radiol.* 81, pp. 2811–2819.

Müller, Veronika I et al. (Jan. 2018). "Ten simple rules for neuroimaging meta-analysis". In: *Neurosci. Biobehav. Rev.* 84, pp. 151–161.

Naidoo, Kovin S et al. (2019). "Potential lost productivity resulting from the global burden of myopia: systematic review, meta-analysis, and modeling". In: *Ophthalmology* 126.3, pp. 338–346.

Nichols, Thomas and Satoru Hayasaka (2003). "Controlling the family-wise error rate in functional neuroimaging: a comparative review". In: *Statistical methods in medical research* 12.5, pp. 419–446.

Noppeney, Uta et al. (July 2005). "Early visual deprivation induces structural plasticity in gray and white matter [1]". In: *Curr. Biol.* 15.

Ohno, Naonori et al. (2015). "Alteration of the optic radiations using diffusion-tensor MRI in patients with retinitis pigmentosa". In: *British Journal of Ophthalmology* 99.8, pp. 1051–1054.

Pan, Wen Ju et al. (Aug. 2007). "Progressive atrophy in the optic pathway and visual cortex of early blind Chinese adults: A voxel-based morphometry magnetic resonance imaging study". In: *Neuroimage* 37, pp. 212–220.

Park, Hae Jeong et al. (Aug. 2009). "Morphological alterations in the congenital blind based on the analysis of cortical thickness and surface area". In: *Neuroimage* 47, pp. 98–106.

Paus, T et al. (Mar. 1999). "Structural maturation of neural pathways in children and adolescents: in vivo study". en. In: *Science* 283.5409, pp. 1908–1911.

Perera, Chandrasan et al. (2015). "The Eye Phone Study: reliability and accuracy of assessing Snellen visual acuity using smartphone technology". In: *Eye* 29.7, pp. 888–894.

Peterson, Bradley S, Betty Vohr, Lawrence H Staib, Christopher J Cannistraci, Aaron Dolberg, et al. (2000). "Regional brain volume abnormalities and long-term cognitive outcome in preterm infants". In: *Jama* 284.15, pp. 1939–1947.

Peterson, Bradley S, Betty Vohr, Lawrence H Staib, Christopher J Cannistraci, Ba Aaron Dolberg, et al. (n.d.). *Regional Brain Volume Abnormalities and Long-term Cognitive Outcome in Preterm Infants*.

Peterson, Candida C, James L Peterson, and Julie Webb (2000). "Factors influencing the development of a theory of mind in blind children". In: *British Journal of Developmental Psychology* 18.3, pp. 431–447.

Ptito, Maurice, Samuel Paré, et al. (2021). "A quantitative analysis of the retinofugal projections in congenital and late-onset blindness". In: *NeuroImage: Clinical* 32, p. 102809.

Ptito, Maurice, Fabien C G Schneider, et al. (May 2008). "Alterations of the visual pathways in congenital blindness". In: *Exp. Brain Res.* 187, pp. 41–49.

Qin, Wen et al. (Jan. 2013). "The Development of Visual Areas Depends Differently on Visual Experience". In: *PLoS One* 8.

Reich, Michael et al. (2006). "GenePattern 2.0". In: *Nature genetics* 38.5, pp. 500–501.

Reislev, N H et al. (2017). "Thalamocortical Connectivity and Microstructural Changes in Congenital and Late Blindness". In: *Neural Plast.* 2017.

Reislev, Nina L et al. (July 2016). "Blindness alters the microstructure of the ventral but not the dorsal visual stream". In: *Brain Struct. Funct.* 221, pp. 2891–2903.

Reislev, Nina Linde et al. (2016). "Simultaneous Assessment of White Matter Changes in Microstructure and Connectedness in the Blind Brain". In: *Neural Plast.* 2016.

Ricciardi, Emiliano, Daniela Bonino, et al. (Mar. 2014). "Mind the blind brain to understand the sighted one! Is there a supramodal cortical functional architecture?" In: *Neurosci. Biobehav. Rev.* 41, pp. 64–77.

Ricciardi, Emiliano, Davide Bottari, et al. (2020). "The sensory-deprived brain as a unique tool to understand brain development and function". In: *Neurosci. Biobehav. Rev* 108, pp. 78–82.

Rice, Deborah and Stan Barone Jr (2000). "Critical Periods of Vulnerability for the Developing Nervous System: Evidence from Humans and Animal Models". In: 108.June.

Roeder, Brigitte et al. (2002). "Speech processing activates visual cortex in congenitally blind humans". In: *European Journal of Neuroscience* 16.5, pp. 930–936.

Rojkova, K et al. (2016). "Atlasing the frontal lobe connections and their variability due to age and education: a spherical deconvolution tractography study". In: *Brain Structure and Function* 221.3, pp. 1751–1766.

Sadato, Norihiro (2005). "How the blind "see" Braille: lessons from functional magnetic resonance imaging". In: *The Neuroscientist* 11.6, pp. 577–582.

Sadato, Norihiro et al. (1998). "Neural networks for Braille reading by the blind." In: *Brain: a journal of neurology* 121.7, pp. 1213–1229.
Salat, David H et al. (July 2004). "Thinning of the cerebral cortex in aging". In: *Cereb. Cortex* 14, pp. 721–730.
Salimi-Khorshidi, Gholamreza et al. (Apr. 2009). *Meta-analysis of neuroimaging data: A comparison of image-based and coordinate-based pooling of studies*.
Schaer, Marie et al. (2012). "How to measure cortical folding from MR images: a step-by-step tutorial to compute local gyrification index". In: *JoVE (Journal of Visualized Experiments)* 59, e3417.
Schoth, F et al. (May 2006). "Diffusion tensor imaging in acquired blind humans". In: *Neurosci. Lett.* 398, pp. 178–182.
Seiger, Rene et al. (2018). "Cortical thickness estimations of FreeSurfer and the CAT12 toolbox in patients with Alzheimer's disease and healthy controls". In: *Journal of Neuroimaging* 28.5, pp. 515–523.
Sen, Sriparna et al. (2022). "The role of visual experience in individual differences of brain connectivity". In: *Journal of Neuroscience*.
Shi, Jie et al. (July 2015). "Impact of Early and Late Visual Deprivation on the Structure of the Corpus Callosum: A Study Combining Thickness Profile with Surface Tensor-Based Morphometry". In: *Neuroinformatics* 13, pp. 321–336.
Shimony, J S et al. (Nov. 2006). "Diffusion tensor imaging reveals white matter reorganization in early blind humans". In: *Cereb. Cortex* 16, pp. 1653–1661.
Shu, Ni, Jun Li, et al. (Jan. 2009). "Abnormal diffusion of cerebral white matter in early blindness". In: *Hum. Brain Mapp.* 30, pp. 220–227.
Shu, Ni, Yong Liu, et al. (Sept. 2009). "Altered anatomical network in early blindness revealed by diffusion tensor tractography". In: *PLoS One* 4.
Silverstein, David N and Martin Ingvar (2015). "A multi-pathway hypothesis for human visual fear signaling". In: *Frontiers in systems neuroscience* 9, p. 101.
Siu, Caitlin R and Kathryn M Murphy (2018). "The development of human visual cortex and clinical implications". In: *Eye and brain* 10, p. 25.
Squeglia, Lindsay M et al. (2013). "Early adolescent cortical thinning is related to better neuropsychological performance". In: *J. Int. Neuropsychol. Soc.* 19, pp. 962–970.
Strange, Bryan A et al. (2014). "Functional organization of the hippocampal longitudinal axis". In: *Nature Reviews Neuroscience* 15.10, pp. 655–669.

Sur, Mriganka, Preston E Garraghty, and Anna W Roe (1988). "Experimentally induced visual projections into auditory thalamus and cortex". In: *Science* 242.4884, pp. 1437–1441.

Talairach, Jean (1988). "Co-planar stereotaxic atlas of the human brain-3-dimensional proportional system". In: *An approach to cerebral imaging*.

Thompson, Deanne K et al. (May 2008). "Neonate hippocampal volumes: Prematurity, perinatal predictors, and 2-year outcome". In: *Ann. Neurol.* 63, pp. 642–651.

Tobin, Michael J (1998). "Is blindness a handicap?" In: *British Journal of Special Education* 25.3, pp. 107–113.

Tomaiuolo, Francesco et al. (Sept. 2014). "Morphometric changes of the corpus callosum in congenital blindness". In: *PLoS One* 9.

Tovée, Martin J. (2008). "The organisation of the visual system". In: *An Introduction to the Visual System*. 2nd ed. Cambridge University Press, pp. 62–77. DOI: 10.1017/CBO9780511801556.004.

Tregillus, Katherine E M and Lora T Likova (Jan. 2020). "Differences in the major fiber-tracts of people with congenital and acquired blindness". In: vol. 2020. Society for Imaging Science and Technology.

Turkeltaub, Peter E et al. (2002). "Meta-analysis of the functional neuroanatomy of single-word reading: Method and validation". In: *Neuroimage* 16, pp. 765–780.

Uhl, F et al. (1993). *Increased regional cerebral blood flow in inferior occipital cortex and cerebellum of early blind humans*. Tech. rep., pp. 162–164.

Veraart, C et al. (Feb. 1990). "Glucose utilization in human visual cortex is abnormally elevated in blindness of early onset but decreased in blindness of late onset". en. In: *Brain Res.* 510.1, pp. 115–121.

Visser, Maya et al. (2012). "Both the middle temporal gyrus and the ventral anterior temporal area are crucial for multimodal semantic processing: distortion-corrected fMRI evidence for a double gradient of information convergence in the temporal lobes". In: *Journal of Cognitive Neuroscience* 24.8, pp. 1766–1778.

Voss, Patrice (2019). "Brain (re) organization following visual loss". In: *Wiley Interdisciplinary Reviews: Cognitive Science* 10.1, e1468.

Voss, Patrice, Bruce G Pike, and Robert J Zatorre (2014). "Evidence for both compensatory plastic and disuse atrophy-related neuroanatomical changes in the blind". In: *Brain* 137, pp. 1224–1240.

Voss, Patrice and Robert J Zatorre (Nov. 2012). "Occipital cortical thickness predicts performance on pitch and musical tasks in blind individuals". In: *Cereb. Cortex* 22, pp. 2455–2465.

— (Mar. 2015). "Early visual deprivation changes cortical anatomical covariance in dorsal-stream structures". In: *Neuroimage* 108, pp. 194–202.

Wan, Catherine Y et al. (2013). "The influence of preterm birth on structural alterations of the vision-deprived brain". In: *Cortex* 49, pp. 1100–1109.

Wanet-Defalque, M C et al. (Apr. 1988). "High metabolic activity in the visual cortex of early blind human subjects". en. In: *Brain Res.* 446.2, pp. 369–373.

Wang, Dawei et al. (2013). "Altered white matter integrity in the congenital and late blind people". In: *Neural Plast.* 2013.

Weaver, Kurt E and Alexander A Stevens (2007). "Attention and sensory interactions within the occipital cortex in the early blind: an fMRI study". In: *Journal of cognitive neuroscience* 19.2, pp. 315–330.

WHO (2004). *ICD-10 : international statistical classification of diseases and related health problems : tenth revision*.

— (2019). *World report on vision*. World Health Organization, 160 p.

Workman, Alan D. et al. (2013). "Modeling Transformations of Neurodevelopmental Sequences across Mammalian Species". In: *Journal of Neuroscience* 33.17, pp. 7368–7383. ISSN: 0270-6474. DOI: 10.1523/JNEUROSCI.5746-12.2013. eprint: https://www.jneurosci.org/content/33/17/7368.full.pdf. URL: https://www.jneurosci.org/content/33/17/7368.

Yang, Chunlan et al. (Jan. 2014). "Anatomic Differences in Early Blindness: A Deformation-Based Morphometry MRI Study". In: *J. Neuroimaging* 24, pp. 68–73.

Yarkoni, Tal (2009). "Big Correlations in Little Studies: Inflated fMRI Correlations Reflect Low Statistical Power—Commentary on Vul et al. (2009)". In: *Perspect. Psychol. Sci.* 4, pp. 294–298.

Yu, Chunshui et al. (June 2007). "Plasticity of the corticospinal tract in early blindness revealed by quantitative analysis of fractional anisotropy based on diffusion tensor tractography". In: *Neuroimage* 36, pp. 411–417.

Zhou, Zhifeng et al. (2019). "Alterations of the Brain Microstructure and Corresponding Functional Connectivity in Early-Blind Adolescents". In: *Neural Plast.* 2019.

Zikou, A K et al. (Jan. 2012). "Voxel-based morphometry and diffusion tensor imaging of the optic pathway in primary open-angle glaucoma: A preliminary study". In: *AJNR Am. J. Neuroradiol.* 33, pp. 128–134.